2012

Key Factors Influencing the Structure and Electrochemical Performances of LiFePO4 via sol-gel Synthesis

Chuang Guan
Wright State University

Key factors Influencing the Structure and Electrochemical Performances of $LiFePO_4$/C via Sol-Gel Synthesis

A thesis submitted in partial fulfillment
of the requirements for the degree of
Master of Science in Engineering

By

Chuang Guan

B.S., Dalian Jiaotong University, 2009

2012

Wright State University

Wright State University

SCHOOL OF GRADUATE STUDIES

March 16, 2012

I HEREBY RECOMMEND THAT THE THESIS PREPARED UNDER MY SUPERVISION BY Chuang Guan ENTITLED Key Factors Influencing the Structure and Electrochemical Performance of LiFePO4/C via Sol-Gel Synthesis BE ACCEPTED IN PARTIAL FULFILLMENT OF THE REQUIREMENTS FOR THE DEGREE OF Master of Science in Engineering.

Hong Huang, Ph.D.
Thesis Director

George Huang, Ph.D.
Chair, Department of Mechanical
and Materials Engineering

Committee on
Final Examination

Hong Huang, Ph.D.

Bor Z. Jang, Ph.D

H. Daniel Young, Ph.D.

Andrew T.Hsu, Ph.D.,
Dean, School of Graduate Studies

Abstract

Guan, Chuang., M.S.Egr., Department of Mechanical and Materials Engineering, Wright State University, 2012. Key Factors Influencing the Structure and Electrochemical Performance of $LiFePO_4$/C via Sol-Gel Synthesis.

Olivine structured $LiFePO_4$ is a promising cathode material for the next generation of lithium ion batteries for its low cost, environmental benign, good cycling performance and safety, etc. However, its intrinsic poor electrical conductivity and diffusion capability of lithium ion greatly hinder its application in the high power recharge battery. In this research, a cost-effective sol-gel method was used to synthesize carbon coated $LiFePO_4$ ($LiFePO_4$/C) materials. The influences of the synthesis parameters, including the species of iron source, lithium content, chelating agents and carbon sources, PH value of the sol, and sintering conditions etc., on the structure and electrochemical properties of the $LiFePO_4$/C were investigated by means of X-ray diffraction (XRD), Scanning electron microscope (SEM), galvanostatic charge-discharge and electrochemical impedance spectroscopy.

Nanocrystalline $LiFePO_4$/C materials with spherical particles of less than 500nm and appropriate amount of carbon coating are successfully obtained after optimizing the synthesis parameters. Maximum capacity of 152mAh/g was achieved at 0.2C rate, in addition to long cycle life (over 150 cycles) and good discharge rate capability (120mAh/g at the 2C rate). Further, the impact of stability of complexing compounds on the electrochemical properties, carbon contents and the mircrostructure of the $LiFePO_4$ products were discussed based on the coordination chemistry principle.

Key words: Lithium ion batteries, Cathode, LiFePO4, Sol-Gel method, Complexing agents, Electrochemical performance

TABLE OF CONTENTS

List of Figures

List of Tables

ACKNOWLEDGEMENTS

I would like to give my biggest thanks to my advisor Dr. Hong Huang for her patience in helping me develop my thesis and guiding my research. I also want to thank Dr. Bor Z. Jang and Dr. H. Daniel Young for being my graduate committee members. I thank my parents for supporting me during my studies and my friend Jason Thompson for helping me with my English.

Chapter 1 Introduction

1.1 Introduction

Science and technology, along with the progress of the society, develop at an unexpected fast speed, resulting in the dilemma of increasing energy demand and environment protection. Therefore, high efficient, clean, economical and safe energy systems are currently under extensive development. For instance, electric vehicles, medical equipments, military equipments, and space technology requires power systems with features like high energy, safety, long life, maintenance-free and so on. The demand for energy also provides a strong driving force for the development of electrochemical power technology. Many high performance electrochemical powers have been developed in the past several decades. Lithium-ion battery attracts much attention due to its advantages in terms of high energy density, recharge ability, long cycle life, etc. At present, most portable devices like mobile phones, laptops, and digital cameras are powered by Li-ion batteries[1-2].

The earliest study of lithium secondary batteries began in the oil crisis period of 1960s~1970s[3]. At that time research was mainly concentrated on studying the lithium batteries made up of lithium metal anode and lithium compound cathode. However, when such a battery is charged, the deposition of lithium on the surface Li anode leads to uneven distribution of surface potential, resulting in the formation of dendrites. The dendrites have two disadvantages: 1) the breaking of dendrites will cause the lithium irreversible and 2) dendrites can penetrate the separator membrane causing short circuit of the cell, which will lead to an explosion hazard. Because of above problems, Exxon's Li/TiS_2 system[4] failed to achieve the commercialization.

In 1990 Sony Corporation announced the product of lithium - ion secondary battery, which eliminated metallic lithium anode, and succeeded in the commercialization[5]. The battery is made up of 1) $LiCoO_2$ cathode material which can reversibly intercalate/extract Li ions material at the potentials of 3.7-4.2V; 2) graphitic carbon anode which is also a reversible intercalate/extract Li ions with no formation of metallic lithium in the potential range of 0.05-0.3V; and 3) $LiPF_6$+EC+DEC electrolyte which is comparable with the two novel electrodes and stable in the high voltage range. Ever since, along with the progress of scientific research on electrode and electrolyte materials, lithium-ion secondary battery have advanced rapidly and achieved extensive applications in various fields.

1.2 Lithium ion battery structure, principle and characteristics

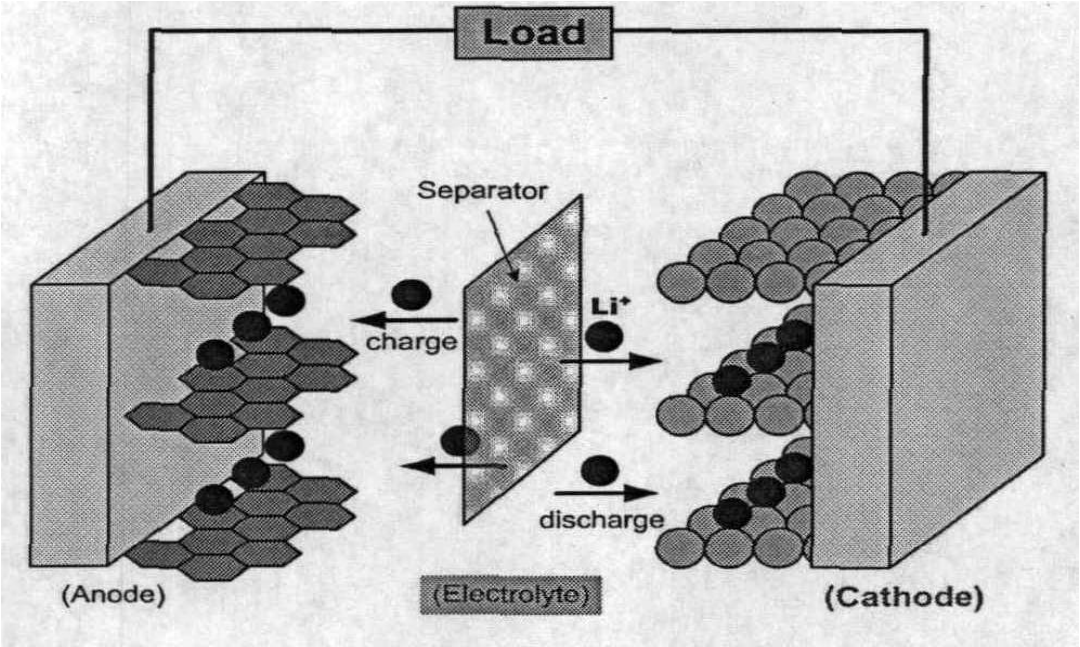

Fig. 1 Working principle of a typical lithium-ion battery

Fig.1 illustrates the working principle of a typical lithium-ion battery. When the battery is charging, lithium ions extract from the cathode lattice of cathode material, penetrate through the

electrolyte and separator, intercalate into the anode material. The discharge period is the inverse process of the charge process. During the whole charge and discharge process, lithium ions travel between the cathode and anode materials. This charge and discharge process is similar to a rocking chair[11], so the lithium ion batteries also known as a rocking chair battery, which was constantly used at the early 1990s. Because lithium ion battery only involves lithium ions instead of lithium metal during charge and discharge processes, fundamentally solves the circulation and safety issues due to the deposition of lithium dendrites.

A lithium-ion battery consists of a cathode and an anode separated by a lithium-ion conducting electrolyte soaked in a macro porous polymer separator. The cathode materials are generally high redox potential transition metal oxides or phosphides. Typical cathode materials include layer-structured $LiMO_2$, spinel-structured LiM_2O_4, and olivine-structured $LiMPO_4$, where M = Fe, Co, Ni, Mn and other transition metals[6-8]. Anode materials, in most cases, are carbon-based materials which can store large amount of lithium at low redox potentials vs. Li/Li+, such as graphite, coke, carbon microspheres etc. Tin and silicon –based metals can also serve as the anode. Lithium-ion battery electrolytes are generally lithium salt (mostly are fluorine-containing organic lithium salt) like $LiClO_4$, $LiPF_6$, $LiBF_4$, $LiAsF_6$, $LiCF_3SO_3$ dissolved in appropriate organic solvent combination, e.g. propylene carbonate (PC), ethylene carbonate (EC), dimethyl carbonate (DMC), diethyl carbonate (DEC) etc[9-10]. The electrochemical reaction of lithium-ion battery can be expressed as follows, in which M represents the transition metal atom, X represents anionic groups.

$$\text{Cathode reaction: } Li_{1-x}M_yX_z \underset{discharge}{\overset{charge}{\Longleftrightarrow}} Li_{1-x-\delta}M_yX_z + \delta Li^+ + \delta e$$

$$\text{Anode reaction: } Li_xC_n + \delta Li^+ + \delta e \underset{discharge}{\overset{charge}{\Leftrightarrow}} Li_{x+\delta}C_n$$

$$\text{Overall reaction: } Li_{1-x}M_yX_z + Li_xC_n \underset{discharge}{\overset{charge}{\Leftrightarrow}} Li_{1-x-\delta}M_yX_z + Li_{x+\delta}C_n$$

1.3 Cathode Materials in Lithium ion battery

An ideal insertion cathodic material, as a core component of the lithium-ion battery, should have the following properties[12-13]:

(1) The metal ion M^{n+} should have a high redox potential in the compound $Li_xM_yX_z$ in order to obtain a high voltage output from the battery;

(2) The structure should allow a large number of lithium ions reversible intercalation and extraction to obtain a high specific capacity and hence, high battery capacity;

(3) Lithium ions should have high diffusion coefficient upon entering into or leaving out of the matrix structure of materials in order to obtain high rate capability and hence, high power density;

(4) Materials should have both good electronic and lithium-ion conductivities. This will minimize potential polarization and rendering small voltage drop at high discharge current densities;

(5) The material matrix structure should maintains stable during repeatedly charge and discharge processes to ensure good cycle ability;

(6) Material should be stable in the whole range of applied voltages and not react with electrolyte to obtain long cycle life, shelf life and good safety;

(7) The raw materials used to obtain the final cathode products should be abundant, low-cost, and environment friendly for mass production and commercialization.

At present, layer-structured $LiMO_2$, spinel-structured LiM_2O_4, and olivine-structured $LiMPO_4$, where M = Fe, Co, Ni, Mn , have been developed and are the most common cathode materials used in Li-ion batteries, because they satisfy most of the above requirements. Some of them have one or two shortcomings which can be improved through doping with other elements or surface modification.

1.3.1 Lithium cobalt oxide and Lithium nickel oxide

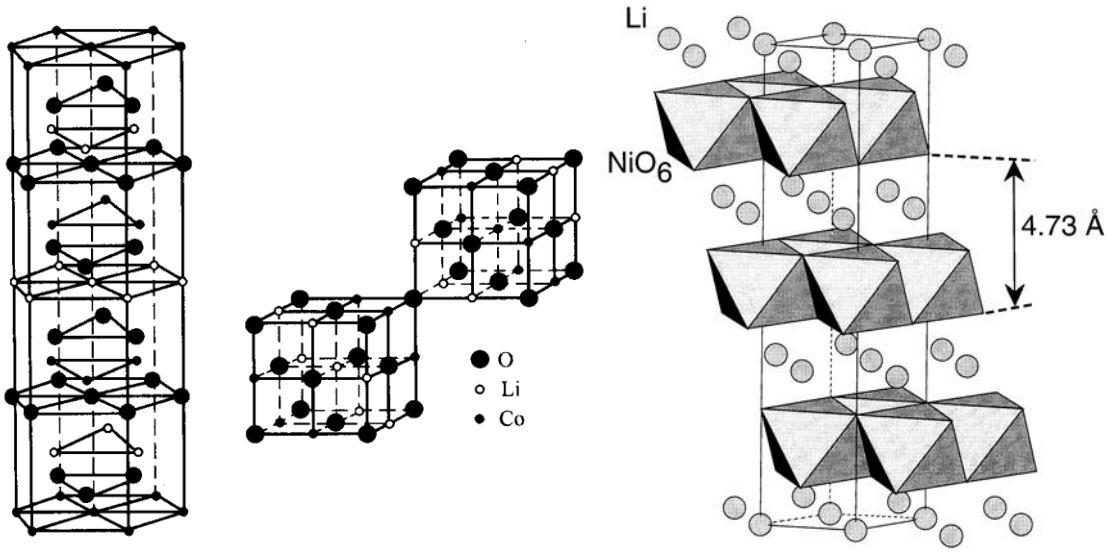

(a) (b)

Fig. 2 Schematics of the layered-structured (a) $LiCoO_2$ (b) $LiNiO_2$

In 1980, Mizushima[4] developed layer-structured $LiCoO_2$ and reported its performance as the cathode material for lithium ion secondary batteries. It has the α-$NaFeO_2$ structure, suitable for intercalation and extraction of lithium ions. The crystal structure of $LiCoO_2$ is schematically illustrated in Fig. 2 (a). If all Li ions could be extracted from the structure, the

maximum specific capacity would be 274mAh/g. However, the practical reversible capacity is only 50~60% of the theoretical value, i.e. around 140mAh/g. When more lithium ions are extracted from the host structure, the material experiences a series phase transformation leading to capacity degradation. Because of its simple production process and stable electrochemical performance, $LiCoO_2$ is a major cathode material in commercialized lithium ion batteries.

However, $LiCoO_2$ is not an ideal cathode for Li-ion batteries. It has been discovered that active structure will gradually change after many times of contraction and expansion resulting in increase of the resistance and decrease of the capacity. In addition, after overcharge $LiCoO_2$ can transform into CoO_2 which has a strong catalytic activity on electrolyte oxidation. CoO_2 decomposition yields oxygen at low temperature (240^oC) when a large amount of heat[14] will be released simultaneously causing high safety risk. On the other hand, cobalt is one kind of strategic resources but the global reserves are very limited. Besides it is expensive, cobalt is also toxic and not environmentally friendly.

$LiNiO_2$ also has layered structure like $LiCoO_2$ (see figure 2 b). Compare to $LiCoO_2$, $LiNiO_2$ has following advantages: (1) lower operating voltage than $LiCoO_2$; (2) higher capacity than $LiCoO_2$ with a practical specific capacity up to 220mAh/g[15]; (3) better cycle life than $LiCoO_2$; (4) more resources reserves in the nature; and (5) low cost and environment friendly.

Unfortunately, it is technically challenge to synthesize the stoichiometric $LiNiO_2$ product. Lithium volatilization[16] results the loss during the high temperature synthesis process. The bivalent nickel precursors are hard to be completely oxidized into trivalent nickel. $LiNiO_2$ easily experiences phase transition and decomposes at high synthesis temperatures. The processing difficulties seriously impact the electrochemical performance of this material.

Cobalt and nickel are the adjacent elements in the period table. They have similar configurations of extra-nuclear electrons and they both belong to α-$NaFeO_2$ structured materials[17]. Therefore, they can be mixed at any proportion. To benefit from advantages and overcome the disadvantages of each material, a series of layered $LiCo_xNi_{1-x}O_2$ materials have been studied. It was found that $LiCo_xNi_{1-x}O_2$ can effectively improve the preparation conditions, reduce costs, and increase electrochemical performances.

1.3.2 Lithium manganese oxide

Compared with $LiNiO_2$ and $LiCoO_2$, lithium manganese oxides have advantages because manganese resources are low-cost, abundant, non-toxic and so on. Existing lithium manganese oxides include $LiMnO_2$ series mainly use the 3V lithium ion batteries, $Li_2Mn_4O_9$, $Li_4Mn_5O_{12}$ and spinel series $Li_{1+x}Mn_2O_4$ ($0<<x<<0.1$). The cubic spinel $LiMn_2O_4$ is the currently under extensive investigations for the 4V lithium-ion batteries.

The spinel structure $LiMn_2O_4$ belongs to space grouping Fd3m[18]. There are 8 lithium atoms, 16 manganese atoms and 32 oxygen atoms altogether 56 atoms in one unit cell (Fig. 3 left). In the unit cell, the oxygen atoms form a face-centered cubic structure. Li ions occupy the LiO_4 tetrahedral centers, i.e. 8a sites, and Mn ions occupy the MnO_6 octahedral centers, i.e. 16d sites. The rest of the octahedral centers, i.e. 16c are holes. During charge-discharge process, Li^+ ions diffuse between 8a and 16c sites, which is a good diffusion channel (Fig.3 right).

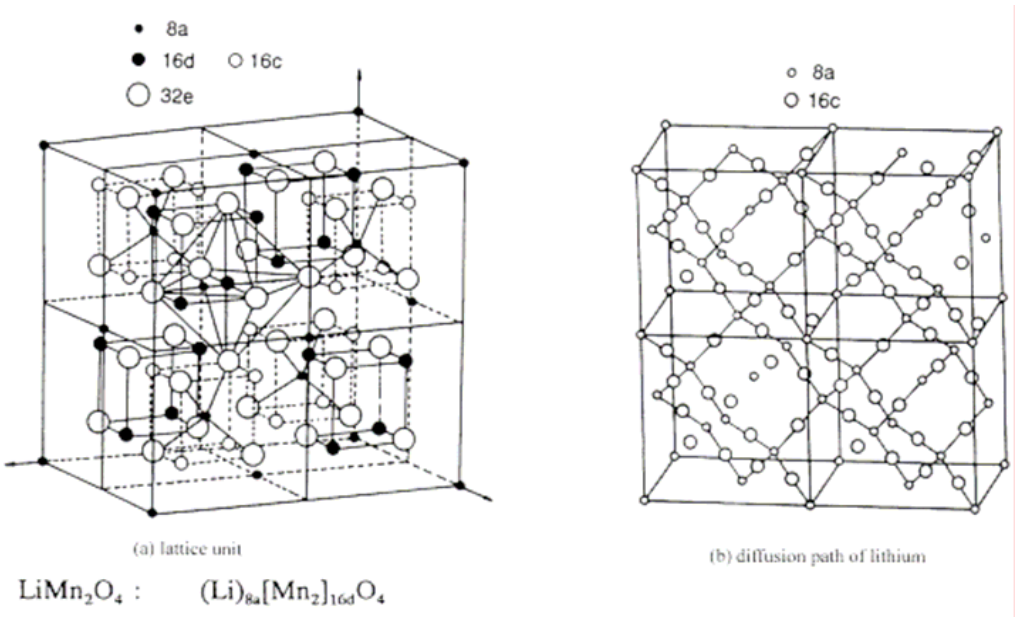

Fig. 3 Structure of spinel $LiMn_2O_4$ unit cell (left) and diffusion path of Li+ ions (right)

The theoretical lithium storage specific capacity of $LiMn_2O_4$ is 148mAh/g. However, during charge and discharge, Jahn-teller effect will occur when Mn^{4+}/Mn^{3+} conversion, causing significant volume change. Furthermore, it was found that at high battery operating temperatures, e.g. 55°C, Mn^{3+} ions have the disproportionation effect and Mn^{2+} ions are easy to dissolve in the electrolyte. These disadvantageous impacts led to poor cycle performance, particularly at high temperatures[19]. Current researches are focused on the surface modification and doping with other elements such as Co, Ni, Al, Cr, Fe, Zn, B, Cd, Sn, and so on. Elements like Ni, Cr, Cu, Fe, Co, La, Sm improved the cycle performance, while elements like Li, Al, B, Ga improved the capacity[20-22].

1.3.3 Lithium iron phosphate

Recently, it was found that a series of polyanionic compounds[23-27] can be used as the cathode materials for lithium ion batteries. This polyanionic compounds contain tetrahedral or octahedral anions as the constructure units $(XO_m)^{n-}$ (X=P, S, As, Si, Mo and W[24]). The olivine

structure polyanionic materials, particularly $LiFePO_4$, have attract much attention. Table 1 compares $LiFePO_4$ with the other three common cathode materials.

Table 1 Comparison of the Four Common Cathode Materials Used in Li-ion Batteries

material	capacity(mAh/g)	reversible range x	potential(V)	toxicity	price
$LiCoO_2$	140	0.5	3.7	very strong	expensive
$LiNiO_2$	220	0.7	3.5	strong	expensive
$LiMn_2O_4$	148	1.0	4.0	little	cheap
$LiFePO_4$	170	1.0	3.5	none	very cheap

1.3.3.1 Structure of $LiFePO_4$

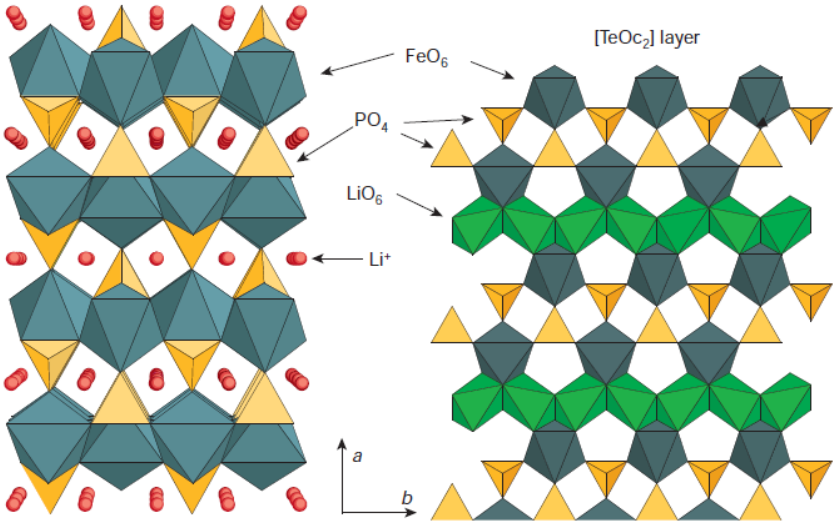

Fig. 4 Illustration of the crystal structure of $LiFePO_4$

$LiFePO_4$ is olivine structure[24], orthorhombic (D_{2h}^{16}, Pmnb). Its crystal structure shows in Fig.4. The lattice parameters of LiFePO4 are: a=0.6008nm, b=1.0334nm, c=0.4693nm; the unit cell volume is 0.291392nm^3. In $LiFePO_4$, the oxygen atoms are arranged in a slightly distorted hexagonal close packing manner, P atoms occupy tetrahedral sites to form PO_4 tetrahedron[28]; Li and Fe atoms are filled in the gap of the oxygen octahedral. Li atoms occupy

common edge octahedral M1(100) sites, Fe atoms occupy common angle octahedral M2(010) sites, respectively to form the LiO_6 octahedron and FeO_6 octahedron. The alternately arranged LiO_6 octahedral, FeO_6 octahedral and PO_4 tetrahedron form the layered scaffold structure. The adjacent FeO_6 octahedrons by sharing oxygen atoms as common vertexes to form FeO_6 layers on the bc plane. Among the FeO_6 layers, adjacent LiO_6 octahedrons use two oxygen atoms along the same edge to form a chain on the b direction. One PO_4 tetrahedron and one FeO_6 octahedron share two oxygen atoms along the same edge.

1.3.3.2 Electrochemical properties of $LiFePO_4$

The charge-discharge mechanism of $LiFePO_4$ is different from the other traditional cathode materials like $LiCoO_2$ and $LiNiO_2$. During charge and discharge, there are two phases, i.e. $LiFePO_4$ and $FePO_4$, involve in the electrochemical reactions. Upon charging, Li^+ ions are extracted from $LiFePO_4$. At the same time, the Fe^{2+} ions in the structure lose electrons and are oxidized to Fe^{3+} accompanied by the formation of $FePO_4$ phase. When all lithium ions are extracted from the host structure, all LiFePO4 transforms into $FePO_4$. Upon discharge, reverse process takes place. Li^+ ions are inserted into $FePO_4$, structure. Meanwhile Fe^{3+} ions gain electrons and are reduced to Fe^{2+} . Therefore, the $LiFePO_4$ overall charge-discharge reaction is a two phase transformation reaction. The Li^+ ions intercalation/extraction occur at the $LiFePO_4/FePO_4$ interface. Therefore, the material has very flat charge-discharge curves and stable potentials, it is very suitable for used as electrode material. The charge and discharge reactions show as follows[29]:

Charge reaction: $LiFePO_4 - x\,Li^+ - xe^- = xFePO_4 + (1-x)LiFePO_4$

Discharge reaction: $FePO_4 + xLi^+ + xe^- = xLiFePO_4 + (1-x)FePO_4$

The theoretical specific capacity of $LiFePO_4$ is 170mAh/g, electrode potential relative to lithium is 3.4V and theoretical energy density is 550wh/Kg. $LiFePO_4$ has a very good cycle performance, that is mainly because the structural similarity of $LiFePO_4$ and $FePO_4$. The product after charge ($FePO_4$) has very similar structure to $LiFePO_4$. They both have space grouping of Pmnb. Table 2 shows lattice parameters[24] of $LiFePO_4$ and $FePO_4$. We can tell from the table, after $LiFePO_4$ transforms to $FePO_4$, a and b axis slightly become shorter, c axis slightly becomes longer. The volume difference is just 6.81%, so the difference is very small. Moreover, this volume difference is just being counteracted by the volume change of the carbon anode material during charge-discharge process. The structural similarity of $LiFePO_4$ and $FePO_4$ still keep stable at high temperature around 400^oC. Therefore, $LiFePO_4$ is stable, not easy to occur deformation or broken and has a good cycle performance[30-31], especially high temperature cycle performance in comparison with $LiMn_2O_4$. Moreover, the cathode alternative is very safe when it is used in Li-ion batteries.

Table 2 Lattice Parameters Comparison of $LiFePO_4$ and $FePO_4$

	$LiFePO_4$	**$FePO_4$**	**Difference**
Space grouping	Pnmb	Pnmb	-
a(nm)	0.6008	0.5792	-3.6%
b(nm)	1.0334	0.9821	-4.9%
c(nm)	0.4363	0.4788	+2.0%
V(nm^3)	0.291392	0.272357	-6.81%

1.3.3.3 Intrinsic Problems of the Olivine Structure

In $LiFePO_4$, the FeO_6 octahedrons share the same vertexes but are separated by the PO_4^{3-} tetrahedrons. Therefore, it is unable for the FeO_6 octahedrons to form the continuous octahedron

network like the structure of FeO_6 octahedrons share same edges. This feature will dramatically reduce the electronic conductivity[23]. It is an intrinsic n-type semiconductor. However, because of the large band gap of 3.7eV calculated by the First Principle[32], intrinsic $LiFePO_4$ has a very poor electronic conductivity at room temperature, which means its poor electrochemical performance at high current loading. Meanwhile, because the oxygen atoms are arranged in the hexagonal close packing order, they only can provide limited channels for Li^+ ions. Therefore, the Li^+ ions migration rate is very small at room temperature[33-34].

Padhi [24]. first reported the $LiFePO_4$ for potential application in Li-ion battery. At room temperature and low current density, there were only 0.6mol Li^+ ions[35] (equivalent to 110mAh/g) participated in the intercalation/extraction reaction per mole $LiFePO_4$. Padhi pointed out that the $LiFePO_4$ charge-discharge process was a Li^+ ion diffusion control process. The specific capacity would sharply decrease with the increase of the current density; if the current density was further reduced, the specific capacity would increase to the original value. Later Takahashi et al[36]. studied the influence of current density on the discharge capacity at different temperatures. At 20^oC, the discharge capacity decreased with the increase of the current density. The discharge capacity also increased along with the increase of the temperature. The higher the operating temperature, the greater the diffusion rate. This research supports the Li^+ ion diffusion control theory.

1.4 Improvement of $LiFePO_4$ for Li-ion batteries application

As stated previously, $LiFePO_4$ are advantageous in the aspects of safety, environment friendliness, non-toxicity, good cycle life, high specific capacity, low-cost and so on. But it has intrinsic poor electric conductivity and limited Li ion diffusion rate, which is not suitable for high-current discharge/charge. In order to improve its overall performances, especially for its

utilization in hybrid electric vehicles and other large Li-ion batteries applications, extensive studies towards improving the electrochemical performances have been conducted. The efforts on improving $LiFePO_4$ can be divided into two aspects, i.e. increase of electronic conductivity and improve Li-ion diffusion rate. The research strategies include doping with aliovalent metal ions, coating with conductive layer, and advance synthesis approach to achieve $LiFePO_4$ nanopowders.

1.4.1 The influence of metal doping on the performance of $LiFePO_4$

Croce et al[37]. used sol-gel method to synthesize $LiFePO_4$. During the synthesis process, they added 1 % Cu or Ag powder as nuclei to reduce the particle size of the product. According to the authors, the addition of metal powder had no affect to the $LiFePO_4$ structure but increased the capacity by 25mAh/g. Chung et al[38]. used high valence metal ions (Nb^{5+}, Mg^{2+}, Al^{3+}, Ti^{4+}, W^{6+}, Zr^{4+}) alkoxides as dopant to synthesize $LiFePO_4$. The conductivity of the synthesized $LiFePO_4$ increased by 8 orders of magnitude and the conductivity at room temperature was reported to be $4.1x10^{-2}$S/cm. Meanwhile, they reported that the activation energy of the $LiFePO_4$ without doping is 500meV, while doped $LiFePO_4$ just had 60-80meV of activation energy. The author believed that the ratio of Fe^{3+}/Fe^{2+} would change during the charge-discharge process, causing the electronic conducting characteristic changing between p-type and n-type. The conductivity of either pure Fe^{3+} or pure Fe^{2+} was very poor, but doping resulted in the formation of Fe^{3+}/Fe^{2+} mixed valence state. This effectively increased the conductivity of $LiFePO_4$. Later, more researchers have studied the influences of a small amount of metal ion doping on the structure, conductivity and high current discharge performance of $LiFePO_4$. The results of XRD patterns showed that the Mg doping could reduce the binding energy of Li-O bond, thus to increased the ions migration rate and diffusion rate. Mg doping also increased electronic

conductivity which was attributed to the improved specific capacity. Shi et al[39]. calculated based on the First Principle and found that the Cr^{3+} ions incorporated in $LiFePO_4$ structure could reduce the activation energy and increase the electronic conductivity.

From a different point of view, Herle et al[40]. pointed out that that the improvement due to the doping was related with the formation of phosphide impurities during the synthesis process. Followed in this direction, researchers studied the influence of the phosphide impurities[41,42] on the electrochemical performance of non-doped $LiFePO_4$. It was believed that the phosphide impurities did improve the $LiFePO_4$ kinetic performance. For instance, Rho et al[43]. used sol-gel method and sintered the precursor under inert gas for different times to obtain the $LiFePO_4$/C powder with different content of phosphides. They found appropriate content of Fe_2P improved the high rate performance of $LiFePO_4$.

In short, it is no doubt that cation doping can improve the $LiFePO_4$ high rate performance. However, the mechanistic understanding on the improvement resulting from metal ion doping is still unclear. Some researchers considered that the doping increased the electric conductivity of olivine structure, while others believed that the improvement is caused by the existence of phosphide impurities during processing[44-45]. Whittingham et al[46]. summarized several issues need to be clarified, just name a few here: 1) whether the doped ions enter the $LiFePO_4$ crystal lattice; 2) whether the doping increases the electronic or ionic conductivity; 3) how the doping process improve the electrochemical performance; 4) where are the doped ions located, Li site or Fe site; and 5) how to accurate control these two kinds of dopings if the performance difference is caused by Li site and Fe site doping, and so on so forth.

1.4.2 The influence of surface carbon coating on the performance of $LiFePO_4$

Beside the effort of increasing electronic conductivity of the $LiFePO_4$ host, surface carbon coating can also increase electronic conductivity and hence significantly improved the electrochemical performance of $LiFePO_4$. In 1999, Ravet et al[46]. first studied the carbon surface coating of $LiFePO_4$. They explored two different approaches to add the carbon into the $LiFePO_4$ product. One approach was to mix the $LiFePO_4$ powder with sugar solution followed by sintering at 700^oC. The other approach was to mix the precursor with carbon and sintered at 700^oC. The carbon content in the $LiFePO_4$ synthesized by the latter method was 1 wt%. The carbon additives increased the discharge capacity to 160mAh/g under 1C rate at 80^oC. Afterwards, systematical studies on the synthesis methods of $LiFePO_4$/C have been performed including the carbon source types, total amount of the carbon adding to the precursor and the structure of the added carbon and so on.

In 2001, Ravet et al[47]. used $LiFePO_4$ mix with the organic carbon solution to obtain the carbon-containing precursor. Three different kind of carbon sources, which were sucrose, cellulose acetate and poly-aromatic compounds, were studied and compared with $LiFePO_4$ without carbon coating. The cyclic voltammetry testing results showed that the sample with carbon coated had obviously sharper redox peaks than the sample without carbon coating (see Fig.5). The observance indicated that the $LiFePO_4$ with carbon coated had a better kinetic property. The $LiFePO_4$/C materials coated with different carbon sources also showed different electrochemical performance. Among them, the $LiFePO_4$/C coated with poly-aromatic had a relative better performance. The reversible capacity was 83% of the theoretical value. After 10 charge/discharge cycles, the capacity loss was only 1%.

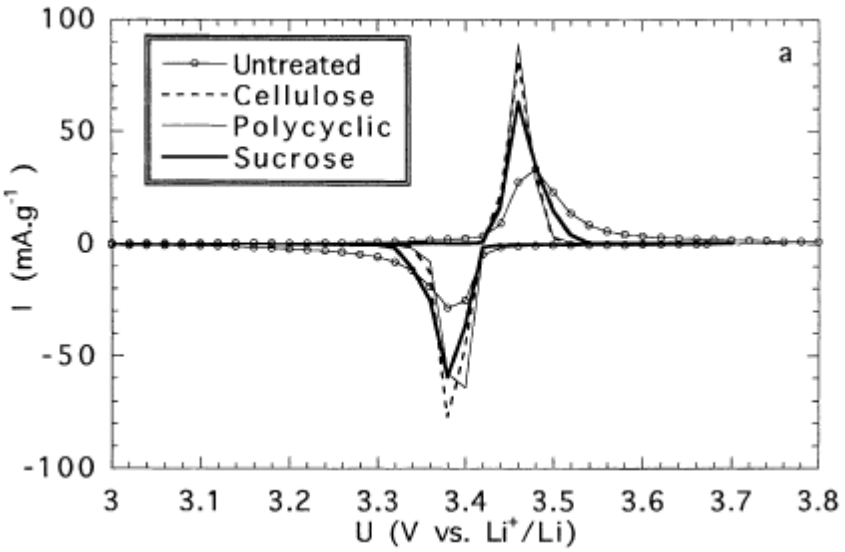

Fig. 5 Tenth voltammetric scans (evolution of discharge capacity upon cycling)

The surface carbon coating not only increases the electronic conductivity of the product but also effectively inhibits the growth of $LiFePO_4$ particles. Gaberscek et al[48]. studied the particle sizes of $LiFePO_4$, synthesized by different research groups and its the relationship with the electrochemical performance. They ascribed improvement by carbon coating to the inhabitance of the $LiFePO_4$ particle growth.

Up to date, it is well accepted that the carbon coating improves the kinetic performance in two aspects. On one hand, the coated carbon increase the electrical contact between the particles. on the other hand, the coated carbon inhibit the growth of the $LiFePO_4$ resulting nanoparticle product. $LiFePO_4$ with small particles shortens the Li^+ diffusion path thus the diffusion rate becomes greater. It is worth to note that carbon coating seriously reduced the material's tap density and hence volumetric energy density[49]. How to get the uniformly distributed and small particle size of $LiFePO_4$ with the minimum content of carbon is the key of the surface carbon coating research for $LiFePO_4$.

1.4.3 The influence of particle size refinement on the performance of $LiFePO_4$

Gaberscek et al[48]. proposed that the small particle size is more important than the carbon coating. They believed that when the particle size is small enough, the electrochemical reactions will become the rate control step. When the particle is very small (less than 70nm); the rate performance of $LiFePO_4$ will be electrochemical reaction control instead of diffusion control, according to Allen. Experimentally, Xia et al[50]. used solid-state method synthesized non-carbon $LiFePO_4$ with high specific surface area ($24.1 m^2/g$). It was reported that the discharge capacity at 5C rate was 115mAh/g. It can be seen, from the experimental results, that the particle size also has a significant impact on the electrochemical performance of $LiFePO_4$. As long as the $LiFePO_4$ has small (nano-level)[51] particle size, whether carbon coated or not, its rate performance will be superior to the bulk $LiFePO_4$.

1.5 Objective and Scope of This Master Thesis Research

Olivine $LiFePO_4$ has advantageous of low cost, environment friendly, safety, high electrochemical performance and so on, so it attracts much attention recent years. However, improvement $LiFePO_4$ electronic conductivity and Li ions diffusion coefficient is the challenge and key problem in technology of whether $LiFePO_4$ can be applied to large-scale industrial production. Previous research provided a rough guidance of high-performance $LiFePO_4$ cathode applicable for Li-ion batteries. Nanoparticles of LiFePO4 coated with a thin layer of carbon, i.e. $LiFePO_4$/C nanocomposite, will facilitate rapid electronic conduction and ionic diffusion.

This thesis consider improve the electrochemical performance of $LiFePO_4$ as the core of research, and the objective of this research is to synthesize $LiFePO_4$ with nanoparticle size, high capacity, long cycle life and good kinetic performance. This thesis use sol-gel method synthesized carbon coated $LiFePO_4$ cathode material, systematically study the main techniques

and their parameters during the synthesis process, including the influence of species of carbon and iron source, carbon content, sintering temperature etc. on the $LiFePO_4$/C morphology and structure; test and analyze the electrochemical performances of corresponding materials, in order to grasp the key factors that impact the electrochemical performance of $LiFePO_4$, reveal the improvement mechanism of $LiFePO_4$ kinetic performance, provide experimental evidence and theoretical principle for future research. The main research content is as follows:

(1) Use citric acid as complexing agent and carbon source to synthesize carbon coated LiFePO4/C, study the influence of sintering temperature on the electrochemical performance of LiFePO4, and get the optimized sintering temperature. Study the influence of non-stoichiometric lithium content on the electrochemical performance of $LiFePO_4$, optimized the synthesis technics and parameters of $LiFePO_4$/C with the best lithium content and then further study the influence of different content of citric acid on the electrochemical performance of $LiFePO_4$ under this synthesis condition. Optimize the synthesis technics and parameters of $LiFePO_4$ with the best carbon content.

(2) Use ethylene glycol (EG) as complexing agent and carbon source, use $FeCl_2.4H_2O$ and $FeC_2O_4.2H_2O$ as iron source respectively and add different content of EG to synthesize $LiFePO_4$/C, study the influence of iron source and the content of EG on structure and electrochemical performance, optimize the synthesis technics and parameters of $LiFePO_4$ with the best iron source and carbon content; further study the influence of PH value on the structure and electrochemical performance under this condition. In order to grasp the relationships among synthesis technics, structure and electrochemical performance.

(3) Based on the first and second part of the search, optimal screening the iron source, carbon source and the content of carbon source, use citric acid plus EG two compound complexing agents system to synthesize $LiFePO_4$/C, study the influence of compound complexing agents system on the electrochemical performance of $LiFePO_4$/C. Further do the de-agglomeration pretreatment on dry gel, study the influence of pretreatment on the structure and electrochemical performance of $LiFePO_4$/C. Optimize the synthesis technics and parameters of $LiFePO_4$/C.

(4) Compare the influences of different complxing agents on the performances of the LiFePO4 according the coordination chemistry theory. Find a effective basis for the choice of complexing agent in the sol-gel method, thereby reduce the blind experiments to try different complexing agents.

Chapter 2:Review of Various Methods of Synthesizing $LiFePO_4$

The amount of $LiFePO_4$ in the nature, i.e. triphylite, is not abundant. In addition, electrochemical performance of lithium reversible storage in the nature triphylite, is rather poor due to the existence of the impurities[47], intrinsic low electronic conductivity and large particle size .Most $LiFePO_4$used in research and development for Li-ion batteries are synthetic. There are various synthetic methods developed in the past twenty years. This chapter will briefly review the synthesis methods correlated with electrochemical performance assessment. Sol-gel approach, due to its low cost processing, easy for mass production, flexible for doping and surface modification will be the emphasized in relation with this thesis research.

2.1 Solid-State Method

Solid-state method generally comprises of three-step processing including two sections of heating processing. The raw materials in a certain proportion are firstly well-mixed and fully grinded. Afterwards, the first sintering takes place in the temperature range of 300-350^oC for 5 hours under protection gas like H_2 or Ar followed by cooling to the room temperature. After grinded again, the pre-sintered powders are subjected to second-time sintering at higher temperatures in the range of 600-800^oC for 20-36 hours under the inert environment. The two-step sintering can ensure the materials to well mixed and fully react.

Padhi et al[23]. firstly reported $LiFePO_4$, synthesized by the solid-state reaction. The precursors used are Fe_2O_3, $NH_4H_2PO_4$ and Li_2CO_3. The first heating temperature is in the range of 200-300^oC and the second high sintering temperature was 850^oC. Its electrochemical performances were examined at constant current density of 0.05mA/cm^{-2}. A flat plateau about 3.5V (vs.Li^+/Li) was exhibited in the discharge/charge profile with a specific lithium reversible

capacity of 100-110mAh/g. Yamada et al[52]. used $Fe(CH_3CO_2)_2$, $NH_4H_2PO_4$ and Li_2CO_3 as raw materials to synthesize $LiFePO_4$. The raw materials were dispersed and well-stirred in acetone. After evaporation of the acetone, the obtained precipitates were sintered in the temperature range 400-800^oC under the N_2environment. The inert atmosphere can protect the Fe^{2+}ions in the precursor from being oxidized to Fe^{3+}, which is crucial to achieve the desired $LiFePO_4$products. Anderson et al[53]. used $LiCO_3$, $FeC_2O_4.2H_2O$ and $(NH_4)_2HPO_4$ as raw materials under Ar protection to sinter $LiFePO_4$. It was found that the capacity could reach 120mAh/g and with good cycle performance.

Herstedt et al[54]. used $Fe_3(PO_4)_2.8H_2O$ and $LiPO_4$ as raw material mixed with polypropylene to prepare the carbon-coated $LiFePO_4$.The content of carbon was 0.56wt%, the electric conductivity was $2x10^{-5}$S/cm. There were only two main raw materials in this synthesis route, which makes it easier to mix homogeneously. Further, the formation of corrosive substances like $NH_3$was avoided in the sintering process due to the elimination of $(NH_4)_2HPO_4$. However, the preparation for pure $Fe_3(PO4)_2.8H_2O$ precursor is quite difficult for this approach.

Solid-state synthesis requires simple equipments and processes. It is easy to control the synthesis conditions and hence, suitable for industrial production. However, it has the shortcomings in terms of controlling quality of the products. The resulting products have irregular morphology with large particle size and wide range of particle size distribution and usually contains non-uniform phase. Therefore, the electrochemical performances are usually very poor.

2.2 Mechanochemical Method

Mechanochemical method is also called high-energy ball-milling method. The basic principle is to use the energy generated by the high-speed revolving beads to promote the reaction between raw materials. On the one hand, it can cause the particle breakage through the mechanical force, increasing the contact area of reactants. On the other hand, it also can produce a variety of lattice defects, dislocations, atomic vacancies and lattice distortion, etc. It will increase the surface activity of the new resultant, reduce the surface free energy, and promote chemical reactions at low temperatures[55-57]. Apparently, this approach is advantageous over simple solid state reaction. For instance, S.Franger et al[58]. synthesized $LiFePO_4$ used $Fe_3(PO_4)_2$ and Li_3PO_4 as raw materials. Those raw materials were high energy ball-milled for 24h before heat treatment. The specific discharge capacity of synthesized material reached 150mAh/g. Shin et al. synthesized the nano-carbon coated $LiFePO_4$ particles. After mechanical ball-milling, again a good electrochemical performance (150mAh/g at 0.05C) was achieved.

Because the reactants are mixed evenly and break in to fine particles in the ball-milling process, the products usually have high activity. The heat treatment temperature of high-energy ball-milling method is lower than the solid-state method and the sintering time is shorter. Mechannochemical method is one kind of energy-saving and high-efficient material processing technologies.

2.3 Microwave Sintering Method

Microwave is a kind of electromagnetic wave in the frequency range of 0.3-300GHz. The microwave heating occurs as the electromagnetic energy was absorbed by the objects. Since it is an internal energy penetration process, samples can be heated evenly and quickly in a short time. Microwave synthesis has advantages including short reaction time (3-10min), low energy

consumption, high synthetic efficiency, uniform particles etc. Higuchi et al[59]. used microwave heating synthesis method quickly and easily prepared $LiFePO_4$ with good electrochemical performance. They used Li_2CO_3, $NH_4H_2PO_4$ and $Fe(CH_3COO)_3$ as raw materials. Those raw materials were mixed with the addition of ethanol. After dried at 60°C, the precursors were then sintered for 5-20min in the microwave oven. The initial discharge capacity synthesized by this method reached 125mAh/g. Park et al[60]. used co-precipitation method to prepare the precursor. The synthesized precursors were then placed into a beaker with carbon black. $LiFePO_4$ was synthesized in an industrial microwave oven under gas protection. At C/10 discharge rate, the initial discharge capacity achieved 151mAh/g.

The microwave sintering uses microwave energy absorbed directly by the material, therefore, it requires short sintering time and low sintering temperature. It can control the phase structure of the powder by adjusting the microwave power, so it is easily applied to industrial production. However, the microwave heating is excessively quickly. The rapid crystal growth causes the product of enormous agglomerations, which will have negative impacts on electrochemical performance of the products.

2.4 Hydro-thermal Method

Hydro-thermal method uses a high pressure autoclave as the reactor. By heating the reactor to create a high temperature and high pressure reaction environment in which generally insoluble reactants can be dissolved. Oxygen solubility in the hydrothermal system is very small; therefore, the hydrothermal synthesis doesn't need the inert gas protection. Yang et al[61]. used $FeSO_4$, H_3PO_4 and LiOH as raw materials with the molar ratio of 1.0:1.0:3.0. The raw materials were mixed and reacted in the high pressure autoclave at the temperature of 120°C for 5 hours. The as-synthesized precursors were filtered and air-dried for two hours. At $0.14mA/cm^{-2}$, the capacity of

the obtained $LiFePO_4$ reached 100mAh/g. According to the authors, this synthetic route may result in 2/3 of the lithium waste. Franger et al[58]. used $Fe_3(PO_4)_2.5H_2O$ and Li_3PO_4 as raw materials. After mixed in distilled water, the raw materials were put into the high pressure autoclave under argon protection. After heated at 220°C and 2.4MPa for 1h, the $LiFePO_4$ powders were obtained. The powder was filtered, vacuum dried, and heat- treated with carbon black additives under the protective atmosphere. At 55^oC, the discharge capacity of the $LiFePO_4$/C composites reached 125mAh/g and 160mAh/g at C/15 and C/20 discharge rates, respectively. Shiraishi et al[62]. used LiOH, $FeSO_4$ and $(NH_4)_3PO_4$ as raw materials, synthesized the $LiFePO_4$at 170^oCwiththe hydrothermal method. The capacity of the as-prepared powders was only 65mAh/g. Raman spectroscopy analysis revealed there were impurities phase of α-Fe_2O_3 on the surface of $LiFePO_4$ particles, resulting in two discharge plateaus of 3.5 V and 2.5 V. Then Shiraishi did the follow-up heat treatment of the $LiFePO_4$ synthesized by hydrothermal method and studied the difference of the electrochemical performance of the material before and after heat treatment. They found that the follow-up heat treatment is indispensible which increased capacity from 65mAh/g to 150mAh/g.

Hydrothermal methods can directly synthesize $LiFePO_4$ without inert gas protection. The $LiFePO_4$ powder have uniform phase and particle size is generally very small. Follow-up heat treatment is indispensible to obtain good electrochemical performance. The method is only suitable for a small amount of powder preparation. Design and manufacture large-scale thermo-stable high-pressure reactor is very difficult. Hence, the method is not feasible for industrial production.

2.5 Carbon-Thermal Reduction Method

Carbon-thermal reduction method is a solid state reaction. The iron source is mainly divalent iron ferrous oxalate or iron acetate, which is very expensive. Therefore, some researchers used low-cost ferric iron as the iron source by high temperature reduction method and successfully prepared carbon coated $LiFePO_4$ composite material. Barker et al[63]. used Fe_2O_3, LiH_2PO_4 as raw materials and carbon as the reductant and carbon source. Through the carbon-thermal reduction method pure phase $LiFePO_4$ and magnesium doped$LiFePO_4$ were successfully synthesized at the temperature of 650°C.The discharge capacity reached 156mAh/g. Mi et al[64]. used $FePO_4.4H_2O$ as the iron source, and homogeneously mixed with $LiOH.H_2O$ with addition of certain amount of polypropylene. Under nitrogen atmosphere at the temperature between500^oC and 800^oC heat treatment for 10 hours carbon coated material was obtained. The author believed that hydrogen generated from polypropylene pyrolysisacted as the reductant. The discharge capacity reached 164mAh/g at 0.1C rate and 150mAh/g at 0.5C rate. Liao et al[65]. used iron phosphate as iron source, iron powder as reductant, lithium phosphate as lithium source, and sucrose as carbon source. The raw materials were firstly ball-milled with high energy for 24 hours then heat-treated for 30 minutes at the temperature of 600°C to obtain the $LiFePO_4$/C composite material. At 1C rate the discharge capacity reached 138mAh/g. At 5C rate, discharge capacity reached 109mAh/g.

The carbon-thermal reduction method is a cost effective and simple in operation to synthesize $LiFePO_4$/C, and hence, readily implement in industrial production. This method is suitable for adopting low-cost the Fe^{3+} precursors as the raw material. The carbon additives will generate the reducing atmosphere during the sintering process, reducing Fe^{3+} to Fe^{2+} and simultaneously preventing the oxidation of ferrous iron by the residual oxygen. The surplus

carbon in the raw materials may play the roles of dispersant and conductive agent, preventing the agglomeration of $LiFePO_4$ particles. This method provides a new and cheap method for the$LiFePO_4$/C nano-composite commercial processing. However, it is still challenging to fully reduce the Fe^{3+}in the raw materials and to avoid the impurities in the product. The presence of impurities will affect the electrochemical performances of $LiFePO_4$.

2.6 Co-precipitation Method

Co-precipitation method is a liquid state method to synthesize ultrafine powder. In the presence of precipitator, each ingredient in the solution usually containing two or more metal ions will be homogeneously precipitated. In most cases, Fe^{2+}, Li^{+} and PO_4^{3-} soluble salts were used as raw materials and dissolved in the aqueous solution under N_2 protection. At the appropriate PH value, the precursors precipitate. After filtering, washing, drying, and sintering, $LiFePO_4$ powder can be obtained. Arnold et al[66]. added the LiOH solution into the mixed solution of $(NH4)_2Fe(SO_4)_2$and H_3PO_4. Under N_2 protection, controlled PH value and intensively stirring the $Fe_3(PO_4)_2$ and Li_3PO_4 mixed precipitate was obtained. The precipitate was sintered at the temperature between 650°C and800°C to obtain the $LiFePO_4$ powder. The material had a discharge capacity of 160mAh/gat C/20 rate. At C/2 rate discharge capacity reached145mAh/g. Park et al[67]. used the same precursors and obtained a mixture of green-color suspension solution after stirring for 10 minutes. The deposit was separated from the solution by a centrifugal separator, then washed with de-ionized water, and dried in a vacuum oven at 60°C for 5h. The deposit was then mixed with 3wt.%high surface area carbon black. The sintering took place between 550°C and 800°C under N_2 +1 vol.% of H_2 gas protection. When the discharge rate increased from C/10 to 1C, the discharge capacity just decreased 13% from 125mAh/g to 110mAh/g.

Co-precipitation method can mix raw materials evenly. As a result, the synthesis temperature is lowered. The process is simple and easy to implement in mass production. The samples prepared by this method usually have small particle sizes with uniform size distribution. The main problem lies in the different precipitation rate of each component and equilibrium solubility product, which may lead to deviation of the composition and the loss of uniformity.

2.7 Sol-gel Method

Sol is referred to a colloidal system that has the characteristics of liquid in which the dispersed particles can be either solid or macromolecules with the sizes in the range of 1-1000nm. Gel is referred to a colloidal system that has the characteristics of solid in which the dispersed substances form a continuous network skeleton and the skeleton gaps are filled with liquid or gas. The content of disperse phase in gel is very low, normally between 1% -3%. In the sol-gel synthesis method, the compounds with high chemical activity are usually selected as precursors. These raw materials are homogeneously mixed in the liquid solution. With the occurrence of hydrolysis and condensation reactions, stable transparent sol system will be formed in the solution. The sol particles will slowly polymerizing the liquid phase and gradually age into in the three-dimensional network. Eventually, the fluidity is lost and the three-dimensional network structured gel will be generated. The solid gel will be transformed nano-scale level materials after drying, sintering and solidification processes. The sol-gel synthesis method has the following advantages:

1. Good chemical homogeneity(up to molecular level). For multi-component materials, sol prepared by the metal salts solution can result in uniform distribution of each component achieves at the atomic level. When sol prepared by metal alkoxide can achieve the molecular level distribution;

2. Easy to control reaction process and can render evenly doping elements at the atomic/molecular level of mixing;

3. Nano-particles can be prepared with narrow size distribution and high chemical purity;

4. High specific surface area of the precursors result in relatively low sintering temperature, The low sintering temperature will reduce energy consumption, alleviate components volatilization, reducing air pollution, and avoid phase separation etc;

5. Simple equipment and ready for mass production

Compared with the various other synthesis methods depicted in the previous sections, the sol-gel method is considered as one of the most promising methods towards synthesis of nanomaterials as well as nanocomposites.

Croce et al[68]. firstly reported using sol-gel method to synthesize $LiFePO_4$. Firstly, ascorbic acid, serving as a reductant to reduce Fe^{3+} to Fe^{2+} , was added to the LiOH and $Fe(NO_3)_2$ solution followed by addition of H_3PO_4. Secondly, ammonia was added to adjust the PH value. Thirdly, metal powder (copper or silver, respectively, 0.1um average particle size, 1wt%) was added to the solution. The solution was then heated at 60°C to obtain the gel. This gel was further heated at350°C for 12h followed by sintering at 800°C for 24h under N_2 protection. The Cu-added $LiFePO_4$ reached the capacity of 140mAh/g at C/5 rate. The metal dispersion did not affect the structure of the $LiFePO_4$ but it benefited to the growth of small size particle, reduction of the interparticle resistance and enhancement of the bulk conductivity.

K. Hsu et al[69]. used citric acid as the chelating agent as well as a carbon source which can prevent the oxidation of Fe^{2+} and provide the network structure of carbon for electron conduction.

$FeC_2O_4.2H_2O$ and $LiNO_3$ were dissolved in nitric acid solution, followed by the addition of citric acid to the solution. Saturated $NH_4H_2PO_4$ was added to the solution after continuously stirring for 20 min. The solution was heated with continuously stirring for 4h to vaporize the excess water. After gelation in a circulation oven for a week at 60°C, the dried precursor was sintered in a furnace at 400-950°C in nitrogen atmosphere protection for 2h (10°C/min). Changing the sintering temperature from 450°C to 950°C, the growth of particles was insignificant because the carbon network prevented the growth of the particles. When the sintering temperature was at 850°C, the particle size was around20-30nm. The conductivity of the $LiFePO_4$/C composites reached $2.46x10^{-3}$S/cm at room temperature. The discharge capacity at 0.1C rate was 150mAh/g(see Fig.6).

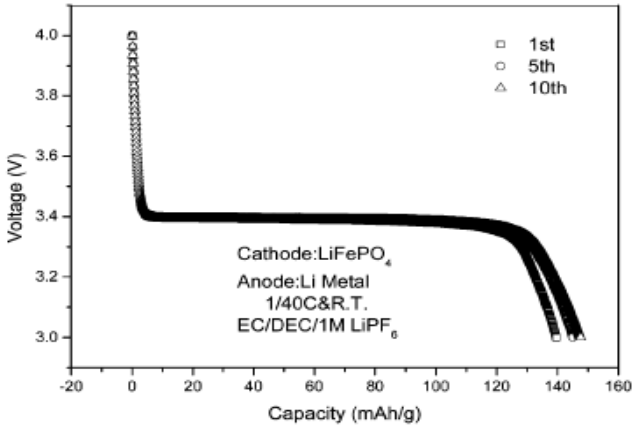

Fig. 6 Discharge profiles of $LiFePO_4$/C sintered at 850°C for 2h

Hu et al[70]. did a series studies on the preparation parameters of the sol-gel method and compared with the solid-state synthesis method. Their solid-state preparation method was similar to the method used by Yamada et al. For sol-gel samples, the raw materials were $Fe(NO_3)_3.9H_2O$, $Li(CH_3COO).2H_2O$, H_3PO_4 and $HOCH_2COOH$. The metal compounds were firstly dissolved in phosphoric acid and de-ionized water. The mixture was continuously stirred until homogeneous

solution. The glycolic acid was added with the molar ratio of glycolic acid to metal ions was 2:1. Ammonium water was added to adjust the PH value between 8.5 and 9.5. The solution was heated at 70-80°C under N_2 until gel formed. Later, the gel was placed in an alumina boat and sintered at 500°Cfor 10h under flowing N_2. The resultant powders were grounded and heated at 2°C/min to 600°C or 700°C under N_2 for various length of time between 5-15h to obtain the $LiFePO_4$ powders. All the particle size of samples was below 200nm. It was confirmed that the particle size of all the samples prepared by sol-gel method were significantly smaller than the samples prepared by traditional solid-state method. Initially, the reversible capacity of the products obtained by sol-gel was only110mAh/g lower than that of the solid-state specimen (120mAh/g). After organic carbon source was added during the grounding process for the formation of carbon coating, discharge capacity reached around 140mAh/g, higher than the solid-state method which was 120mAh/gat high discharge current of 0.055mA/cm^{-2}.

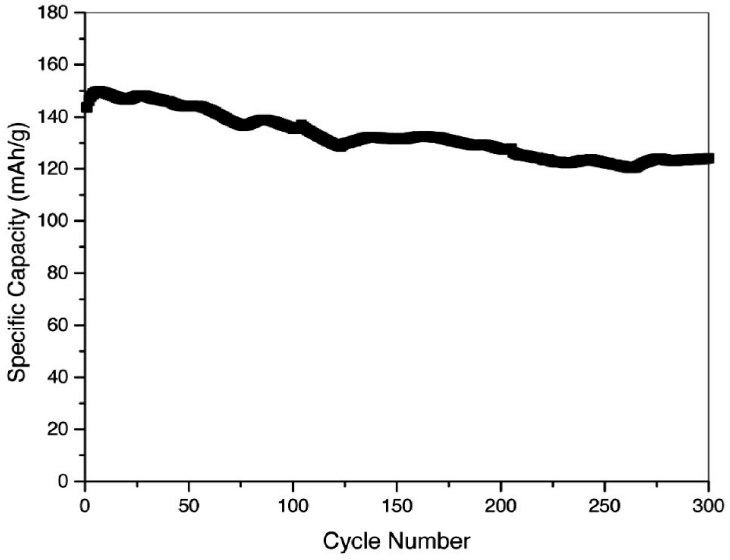

Fig. 7 Cycle performance of $LiFePO_4$ obtained from 0.75M gel at 2C rate

Yang et al[71]. used non-aqueous sol-gel method to synthesize $LiFePO_4$/C. They firstly dissolved $Li(CH_3COO).2H_2O$, $Fe(CH_3COO)_2$ and H_3PO_4 in ethylene glycol instead of water. The

sol was continuously stirred under N_2 flow until the gel formed. The gel was then sintered under N_2 at 700^oC for 12h to obtain carbon coated $LiFePO_4$. EDS analysis showed that the carbon content of product was 1.8 wt% and the carbons were finely distributed on the surface of the particles. The particle size was around 200-300nm. The discharge capacity at C/100 was 165mAh/g. Under C/5 rate, the initial discharge capacity was150mAh/g. After 100 cycles, the capacity decreased to 140mAh/g. Under 2C rate, the discharge capacity changes from 148mAh/g to 125mAh/g after 300 cycles (Fig.7).

Choi et al[72]. used $CH_3CO_2Li.2H_2O$, $FeCl_2.4H_2O$ and P_2O_5 as raw materials. Each raw material was dissolved in ethanol to yield a 1M solution. Equal molar ratio of lauric acid surfactant was added to the solution after 3h stir. The precursors were sintered at 500^oC for 5h to obtain uniformly distributed $LiFePO_4$/C (100-300nm). The discharge capacity at 10C rate was 123mAh/g. At all discharge rates, the reduction of capacity was only 0.083% within first 33 cycles (Fig.8).

The $LiFePO_4$ powders synthesized by the sol-gel method have small particle size and uniform distribution. Large drying shrinkage occurs in sol-gel method. In comparison with other methods, relatively long synthesis period and the accurate processing conditions are demanded for sol-gel method. Therefore, systematic studies and deep understanding of the influences of the key parameters (species of chelating agent, PH value of solution etc.) on the microstructure and performances of materials have significant values for both scientific research and practical application.

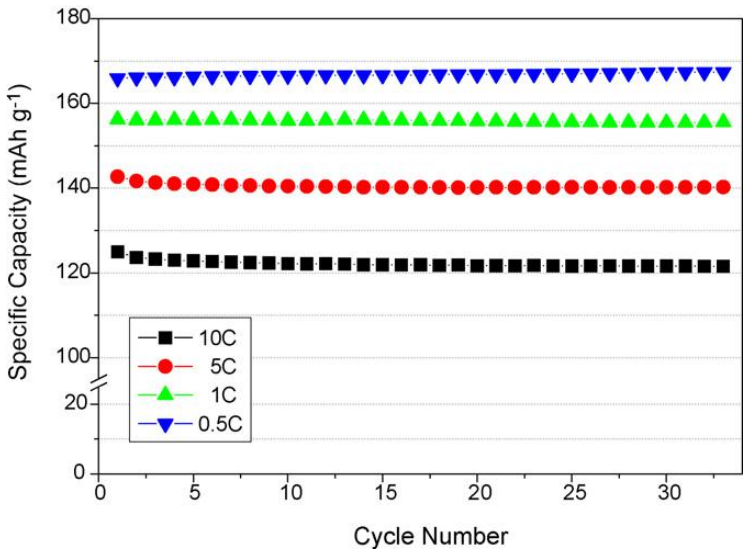

Fig. 8 Cycle performance of $LiFePO_4$ synthesized with lauric acid at 500^{o}C between 10C and C/2 rates for up to 33 cycles

Table 3 Comparison of processing parameters and electrochemical performances for different synthesis methods

Synthesis method	**Processing parameters**	**Electrochemical performance**	**Reference**
Solid-state	Precursors: Fe_2O_3, $NH_4H_2PO_4$, Li_2CO_3. Finely ground precursors. 1st heating 200-300°C. 2nd heating 850°C 24h	116mAh/g ($0.05mA/cm^2$)	Padhi[23]
Solid-state	Precursors: Li_2CO_3, $FeC_2O_4.2H_2O$, $(NH_4)_2HPO_4$. 1st heating 300°C. 2nd heating 450°C 10h. 3rd heating 800°C36h.	120mAh/g	Andersson[53]
mechanochemical	Precursors: Li_2CO_3, $(NH_4)_2HPO_4$,FeC2O4.2H2O. Ball-milling 3h. Sintering 700°C 10h	145mAh/g (0.1C)	Shin[57]
mechanochemical	Precursors: $Fe_3(PO_4)_2.5H_2O$, Li_3PO_4.Ball-milling 24h. Sintering 550°C 15min	150mAh/g (C/50)	S.Franger[58]
Microwave	Precursors: Li_2CO_3, $Fe(CH_3COO)_2$, $NH_4H_2PO_4$. Microwave heating 5-20min (500W, 2.45GHz)	125mAh/g (60°C)	Higuchi[59]
Microwave	Precursors: $(NH_4)_2Fe(SO_4)_2.6H_2O$, H_3PO_4. Microwave heating few minutes (650W)	151mAh/g (C/10)	Park[60]
Hydro-thermal	Precursors: $FeSO_4$, LiOH, H_3PO_4. Reacted in autoclave 120°C 5h.	100mAh/g ($0.14mA/cm^{-2}$)	Yang[61]
Hydro-thermal	Precursors: $Fe_3(PO_4)_2.5H_2O$, Li_3PO_4. Reacted in autoclave 220°C 1h (24MPa).	160mAh/g (C/20)	S.Franger[58]
Carbon-thermal	Precursors: $FePO_4.4H_2O$, $LiOH.H_2O$. Reductant: polypropylene. Ball-milling 2h. Sintering 500-800°C 10h with reductant.	150mAh/g (0.5C)	Mi [64]
Carbon-thermal	Precursors: $FePO_4.2H_2O$, $Li_3PO$and sucrose. Reductant: iron powder. Ball-milling 24h. Sintering 600°C 30min.	138mAh/g (1C)	Liao[65]
Co-precipitation	Precursors: LiOH, $(NH_4)_2Fe(SO_4)_2$, H_3PO_4. Control PH value, stir solution get precipitate. Sintering 650-800°C 12h	160mAh/g (C/20)	Arnold[66]
Co-precipitation	Precursors: LiOH, $(NH_4)_2Fe(SO_4)_2.6H_2O$, H_3PO_4. Control PH value, stir solution get precipitate. Sintering with 3wt% carbon black 550-800°C 12h	125mAh/g (C/10)	Park[67]

Synthesis method	Processing parameters	Electrochemical performance	Reference
Sol-gel	Precursors: LiOH, $Fe(NO_3)_3$, H_3PO_4. Chelating agent: ascorbic acid. Heating solution 60°C, control PH value, stir to get gel. Heating dried gel 250°C 12h. Sintering 800°C 24h.	140mAh/g (C/5)	Croce[68]
Sol-gel	Precursors: $FeC_2O_4.2H_2O$, $LiNO_3$, $NH_4H_2PO_4$. Chelating agent: citric acid. Heating solution, stir to 4h remove water. Dried 60°C 1 week. Sintering 400-950°C 2h.	150mAh/g (C/10)	Hsu[69]
Sol-gel	Precursors: $Fe(NO_3)_3.9H_2O$, $Li(CH_3COO).2H_2O$, H_3PO_4. Chelating agent: glycolic acid. Heating solution 70-80°C, control PH value, stir to form gel. 1st sintering 500°C 10h, 2nd sintering 600-700°C 5-15h.	140mAh/g ($0.055mA/cm^{-2}$)	Hu[70]
Sol-gel	Precursors: $Li(CH_3COO).2H_2O$, $Fe(CH_3COO)_2$, H_3PO_4. Chelating agent: ethylene glycol. Heating solution, stir to form gel. Sintering 700°C 12h	150mAh/g (C/5)	Yang[71]
Sol-gel	Precursors: $CH_3CO_2Li.2H_2O$, $FeCl_2.4H_2O$, P_2O_5. Chelating agent: lauric acid (surfactant). Stir solution to form gel. Sintering 500°C 5h	155mAh/g (1C)	Choi[72]
Sol-gel	Precursors: $LiOH.H_2O$, $FeC_2O_4.2H_2O$, $NH_4H_2PO_4$. Chelating agents: polyacrylic acid and citric acid. Heating solution 85°C, stir to form gel. Heating gel 500°C. Sintering 750°C	150mAh/g (C/8)	Wang[73]
Sol-gel	Precursors: $Fe(NO_3)_3 \cdot 9H_2O$, LiH_2PO_4, carbon nanospheres. Chelating agent: polyethylene glycol(PEG). Heating solution 50°C for 12h to form gel. Sintering 700°C 8h.	146mAh/g (0.1C)	Liu[74]
Sol-gel	Precursors: $FeC_2O_4.2H_2O$, $FeSO_4.7H_2O$, H_3PO_4. Chelating agents: citric acid, PEG400. Heating solution 70-80°C, stir to form gel. Microwave heating 18min(400W).	152mAh/g (0.2C)	Zhang[75]

Chapter 3 Experimental Aspects

3.1. Synthesis of $LiFePO_4$/C Powders

3.1.1 Raw materials

The raw materials used to synthesize $LiFePO_4$/C powders are listed in Table 4. For this research, $LiOH.H_2O$ was selected as the source of lithium. Since lithium salt may be lost during the sintering process, amount of lithium content added in the precursor was optimized. It is constantly reported that different iron source has significant impacts on the electrochemical performances of the $LiFePO_4$ products. The source of iron in most experiments was used $FeC_2O_4.2H_2O$. In a few experiments, $FeCl_2.4H_2O$ was used for comparison. H_3PO_4 and/or $NH_4H_2PO_4$ was used as the source of phosphate ions, which will affect the PH value of the sol. Basic complexing agents in this study are citric acid and ethylene glycol. Individual complexing agent as well as combination of the two with different ratios and their impacts on the product performances were investigated in this study. Detailed results and discussion can be found in chapters 4 and 5.

Table 4 Raw materials used to synthesis $LiFePO_4$/C Powders

name	Chemical formula	Vendor
lithium hydroxide	$LiOH.H_2O$	SIGMA-ADRICH
ammonium dihydrogen phosphate	$NH_4H_2PO_4$	Alfa Aesar
orthophosphoric acid	H_3PO_4	Alfa Aesar
iron oxalate	$FeC_2O_4.2H_2O$	ALDRICH
iron dichloride	$FeCl_2.4H_2O$	SIGMA-ALDRICH
Citric acid	$C_6H_8O_7$	SIGMA-ALDRICH
ethylene glycol	$C_2H_6O_2$	SIGMA-ALDRICH
ethanol	CH_3CH_2OH	PHARMCO-AAPER

3.1.2 Basic equipment utilized

The processing to synthesis $LiFePO_4/C$ powders includes sol-gel formation, drying, and high temperature sintering. Figures 9, 10 and 11 showed the actual setup pictures during sol-gel processing, drying, and high temperature sintering, respectively.

Fig. 9 Sol-Gel synthesize process

Fig. 10 Box furnace for dying the gel precursor

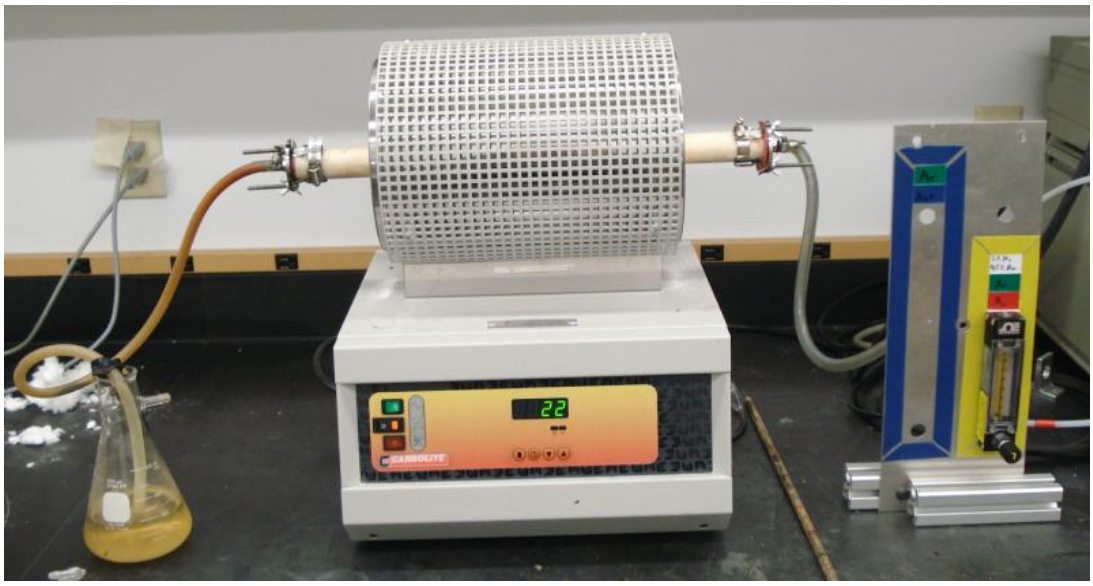

Fig. 11 Tube furnace for sintering the dried precursor

3.1.3 Synthesis of $LiFePO_4/C$ based on citric acid complexing agent

(1) Different sinter temperature.

In this set of experiment, all other parameters were fixed except the sintering temperature. The sources of Li, Fe and PO_4 were $LiOH.H_2O$, $FeC_2O_4.2H_2O$, H_3PO_4, respectively. The stoichiometric ratio among these three sources were fixed at stoichiometric value, i.e. 1:1:1. The molar ratio of citric acid to cations is 1:2.

First, 0.075mol citric acid was dissolved in 100mL distilled water at room temperature. Then 0.075mol $LiOH.H_2O$ and 0.075mol $FeC_2O_4.2H_2O$ were subsequently added to the citric acid solution. The mixture was stirred continuously for 30min. Afterwards, stoichiometric H_3PO_4 (0.075mol) was added and continuously stirred. After 1h mixing, temperature was raised from room temperature to 70°C. At 70^{o}C, the water gradually evaporated and a yellowish gel gradually formed. The gel was then transfer to the box furnace which was preheated at 120^{o}C and dried for about 12h. Afterwards, dry powder was removed from beaker and mortar grinded

into very fine powders. The gel powders was placed into alumina boat and sealed in the tube furnace. After purging 5 vol.%H_2 +N_2 inert atmosphere for about 15min, the temperature was ramped up to the setting point at the rate of 5^{o}C/min. The preset sintering temperatures were 500^{o}C, 600^{o}C, 700^{o}C and 800^{o}C and the sintering time was set for 10 hours. The powders were removed from the tube furnace after cooling down to room temperature. During the entire period of heating, sintering and cooling, the gas was continuously purged through the tube.

Table 5 Samples list

sample	temperature	water	Citric acid	$LiOH.H_2O$	$FeC_2O_4.2H_2O$	H_3PO_4
a	500°C	100mL	0.075mol	0.075mol	0.075mol	0.075mol
b	600°C	100mL	0.075mol	0.075mol	0.075mol	0.075mol
c	700°C	100mL	0.075mol	0.075mol	0.075mol	0.075mol
d	800°C	100mL	0.075mol	0.075mol	0.075mol	0.075mol

(2) Different sinter lithium amount.

In this set of experiment, all other parameters were fixed except the lithium amount. The lithium amount added to the sol precursor was 1, 1.1, 1.15, 1.2, 1.25 and 1.3 in molar ratio to iron source. Then sintering temperature was set at 700°C.

Table 6 Samples list

Sample	Temperature	water	$LiOH.H_2O$	Citric acid	$FeC_2O_4.2H_2O$	H_3PO_4
a	700°C	100mL	0.0825mol	0.075mol	0.075mol	0.075mol
b	700°C	100mL	0.08625mol	0.075mol	0.075mol	0.075mol
c	700°C	100mL	0.09mol	0.075mol	0.075mol	0.075mol
d	700°C	100mL	0.09375mol	0.075mol	0.075mol	0.075mol
e	700°C	100mL	0.0975mol	0.075mol	0.075mol	0.075mol

(3) Different citric acid amount

In this set of experiment, all other parameters were fixed except the citric acid amount. Li source with excessive 25mol% was selected and sintering temperature was still 700°C. In this study, the designed content of citric acid molar ratios to cations are 1/2 and 1/4.

Table 7 Samples list

Sample	Temperature	water	Citric acid	$LiOH.H_2O$	$FeC_2O_4.2H_2O$	H_3PO_4
a	700°C	100mL	0.075mol	0.09375mol	0.075mol	0.075mol
b	700°C	100mL	0.0375mol	0.09375mol	0.075mol	0.075mol

3.1.4 Use ethylene glycol as complexing agent and carbon source

After optimizing the general processing parameters, different complexing agent, i.e. ethylene glycol, was studied. In this setup of experiment, stoichiometric $NH_4H_2PO_4$ was used as the phosphate ion source. In addition, different iron sources, as well as PH values on the product performances were studied.

(1) Different iron source

Two different iron sources, i.e. $FeC_2O_4.2H_2O$ and $FeCl_2.4H_2O$ were studied. Firstly, designed content of EG was dissolved in 100ml distilled water at room temperature (designed content of ethylene glycol molar ratio of cations are fixed at: 1/2, 1/1, 3/2, 2/1, respectively). Then 0.05mol $LiOH.H_2O$ and 0.05mol $FeC_2O_4.2H_2O$ (or $FeCl_2.4H_2O$) were subsequently added to the EG solution. The mixture was stirred continuously for 30min. Afterwards, stoichiometric $NH_4H_2PO_4$ (0.05mol) was added and continuously stirred. After 1h mixing, temperature was raised from room temperature 70^{o}C. At 70^{o}C, the water gradually evaporated and a yellowish gel gradually formed. The gel was then transfer to the box furnace which was preheated at 120^{o}C

and dried for about 12h. Afterwards, dry powder was removed from beaker and mortar grinded into very fine powders. The gel powders was placed into alumina boat and sealed in the tube furnace. After purging 5 vol.%H_2 +N_2 inert atmosphere for about 15min, the temperature was ramped up to the setting point at the rate of 5^{o}C/min. The preset sintering temperatures was 700°C. And the sintering time was set for 10 hours. The powders were removed from the tube furnace after cooling down to room temperature. During the entire period of heating, sintering and cooling, the gas was continuously purged through the tube.

(2) Different EG amount

In this set of experiment, all other parameters were fixed except the EG amount. The designed content of EG molar ratio to cations are: 1/2, 1/1, 3/2, 2/1, respectively.

Table 8 Samples list

sample	water	EG	$LiOH.H_2O$	$FeC_2O_4.2H_2O$	$NH_4H_2PO_4$
a	100mL	0.05mol	0.05mol	0.05mol	0.05mol
b	100mL	0.1mol	0.05mol	0.05mol	0.05mol
c	100mL	0.15mol	0.05mol	0.05mol	0.05mol
d	100mL	0.2mol	0.05mol	0.05mol	0.05mol

(3) Different PH values

In this study, $LiOH.H_2O$ and stoichiometric $FeC_2O_4.2H_2O$ were added into ethylene glycol solution with the designed content of ethylene glycol molar ratio of cations is 1/2. The initial unadjusted PH value of the sol solution was 6.8. Then dilute hydrochloric acid or ammonia water was added to adjust the PH value of the solution (PH=0, 2, 4, 6 and 8).

3.2 Electrochemical Characterizations of the $LiFePO_4$/C powders

To assess the electrochemical performances, the synthesized $LiFePO_4$/C powders were mixed with electrical conducting graphite, polymer binders and coated on aluminum foil. The electrode membrane was then assembled in a swagelock cell and subjected to a series electrochemical characterizations. Basic chemicals and equipments for the experiments are listed in Table 9.

Table 9 Illustration of raw materials in experiments

name	Chemical formula	Vendor
1-Methyl-2-pyrrolidinone	C_5H_9NO	SIGMA-ALDRICH
PVDF	-	Alfa Aesar
graphite	-	ASBURY GRAPHITE MILLS, INC.
Aluminum foil	-	KWIK N FRESH
ethanol	CH_3CH_2OH	PHARMCO-AAPER
Electrolyte	$LiPF_6$/EC+DEC	ALDRICH
Lithium tablets	Li	ALDRICH
separator	-	ALDRICH
Swagelok cell	-	Self-made
Manual coater	-	GARDCO, CO.
Puncher	-	Maxis Max Puncher
Box oven	-	CARBDLITE
Glove box	-	VACUUM ATMOSPHERES CO.
Land cell testing station	-	武汉市金诺电子有限公司
Gamry	-	GAMRY INSTRUMENTS
Button cell set	-	MTI INTERNATIONAL
Button cell sealer	-	MTI INTERNATIONAL

3.2.1 Preparation of cathode electrode material

Using appropriate amount of 1-Methyl-2-pyrrolidinone (NMP) as solvent uniformly mixed the synthesized $LiFePO_4$/C active material, conductive agent (graphite) and binder (PVDF) as a certain mass ratio. Coat the mixer on an aluminum foil to make the cathode material coating with manual coater. Then oven dries the coating at 120°C for 12h. After drying, the electrode

membrane was punched into 3/8" diameter and pressed, and weighted before transfer into glove box.

3.2.2 Assembling of the cell

The assembly of the cell was done in the glove box. The glove box was full-filled with high purity argon gas, which controlled the oxygen and water contents lower than 0.5 ppm. In most studies, the swagelok cell was used in the experiment. Li tablet was used as the counter electrode. Electrolyte was 1M $LiPF_6$ (EC/DEC). The pre-cut cathode pellet was placed to the bottom of the cell container. Two layers of separator were stacked on top. Afterwards, a few drops of electrolyte were added. After Li pellet was placed on the top, a few more drops of electrolyte were added. The cell was then sealed and hand-tightened. Before transferring out of the glove box, voltage of the cell was checked using a multimeter.

For the cycle life testing, a button cell of 2032 was assembled in glove box and sealed in air. After the cathode, separator, electrolyte and Li foil were stacked subsequently in the cell cap, a spacer and a spring was placed on the top and the cell can was covered the entire assembly. The cell was then moved out of the glove box and quickly sealed with the help of button cell sealer.

3.3 Electrochemical performance testing

The electrochemical performance and analyses were conducted using the common techniques including: constant current charge-discharge testing, cyclic voltammetry (CV) and electrochemical impedance spectroscopy (EIS) analyses etc.

3.3.1Constant current charge-discharge testing

In this experiment, we assessed the charge and discharge capacities of the $LiFePO_4$/C specimens based on the followed standard charge/discharge conditions: 2.5-4.3V at constant

current of 50 μA. The cells were cycled at these conditions for 5 cycles. The measurement was performed on the Land battery tester, which can autimattically control the control and cutoff voltage. Table 10 presented the program used for the standard capacity characterizations. In addition to quantify the capacity of the materials, selected specimens were subjected to cycleability and rate capability evaluations. Tables 11 and 12 are the programs used to control the cycle numbers and different discharge current.

After the preset charge-discharge measurements were completed, the results were exported and saved in Microsoft Excel comptatible comfort. The data were then plotted using either Tecplot 360 or Origin 8.0 graphing softwares.

Table 10 Constant current charge-discharge program

stp	mode	End Cond1	GOTO
1	Rest	Time>=01:00	Next step
2	Charge CC: 50uA	Voltage>=4.3V	Next step
3	Discharge CC:50uA	Voltage<=2.5V	Next step
4	<IF>	Cycle<=5 times	2
5	<IF>		End_OK

Table 11 Long cycle life program

stp	mode	End Cond1	GOTO
1	Rest	Time>=01:00	Next step
2	Charge CC: 50uA	Voltage>=4.3V	Next step
3	Discharge CC:50uA	Voltage<=2.5V	Next step

4	<IF>	Cycle<=200 times	2
5	<IF>		End_OK

Table 12 Different discharge rate program

stp	Mode	End cond1	GOTO
1	Rest	Time>=01:00	Next step
2	Charge CC: 50uA	Voltage>=4.3V	Next step
3	Dishcarge CC: 20uA	Voltage<=2.5V	Next step
4	Charge CC: 50uA	Voltage>=4.3V	Next step
5	Dishcarge CC: 50uA	Voltage<=2.5V	Next step
6	Charge CC: 50uA	Voltage>=4.3V	Next step
7	Dishcarge CC: 100uA	Voltage<=2.5V	Next step
8	Charge CC: 50uA	Voltage>=4.3V	Next step
9	Dishcarge CC: 200uA	Voltage<=2.5V	Next step
10	Charge CC: 50uA	Voltage>=4.3V	Next step
11	Dishcarge CC: 500uA	Voltage<=2.5V	Next step
12	Charge CC: 50uA	Voltage>=4.3V	Next step
13	Dishcarge CC: 50uA	Voltage<=2.5V	Next step
14	Rest	Time>=01:00	End_OK

3.3.2 Cyclic voltammetric spectroscopy

Cyclic voltammetry (CV) method is to control the linearly changes with time of electrode potential within a certain range, meanwhile, measure the corresponding situation of current. Within the scanning potential range, a current peak occurs at a certain potential indicating an occurrence of an electrode reaction. If the electrode reaction is reversible, a peak will be observable in the reverse scanning direction. CV analysis technique can provide information of electrode process in a wide range of potential within a very short period of time.

CV profile can be correlated with galvanostatic charge-discharge measurement. The charge and discharge plateaus observed chrono-potentiometric profile corresponds to the redox peaks observed in the CV curves. The reversibility of the electrode reaction can be determined by the ratio of the redox electricity (peak area).

In the experiments, the initial scan voltage was set at 2.8V, scan to 4.0V then scan back from 4.0V to 2.8V. In order to get the relationship between the scan rate and polarization, samples were scanned at 0.02, 0.05, 0.075, 0.1, 0.2mV/S respectively.

3.3.3 EIS testing

Electrochemical impedance spectroscopy (EIS) analyses can provide electrolyte and electrode impedances under the AC stimulus. This method is to measure the current response passing through the electrode by imposing a sine-wave AC potential at under small amplitude. This analytical method is useful and important to study the electrode kinetics and the electrode surface phenomena. In this study, the EIS analyses were performed in Camry Reference 600 electrochemical measurement system. The frequency range was set from 0.1Hz to 10 KHz and AC amplitude at 5mV. Two-electrode cell system was used, in which $LiFePO_4$ as the working electrode and Li as the counter electrode and reference electrode. In order to study the EIS

evolution at the different charge/discharge status, EIS was recorded after very 30 min discharge at 50uA. The voltage before and after 30 discharge was recorded on land, The voltage before EIS was recorded on Gamry.

Chapter 4 Synthesis of $LiFePO_4/C$ based on citric acid complexing agent

Citric acid is a common complexing agent in sol-gel synthesis. It's a ternary organic acid, solid at room temperature. Its molecular formula is $C_6H_8O_7$ and the structural shows in figure 12. Citric acid complexing is based on the weak COOH acidic group chelating with metal ions. This results in metal cations uniformly embedded in a polymeric matrix, derived from citric acid complexing, forming a network-structured gel. Therefore, pyrolysis of the gel precursor can produce fine and uniform nanopowders.

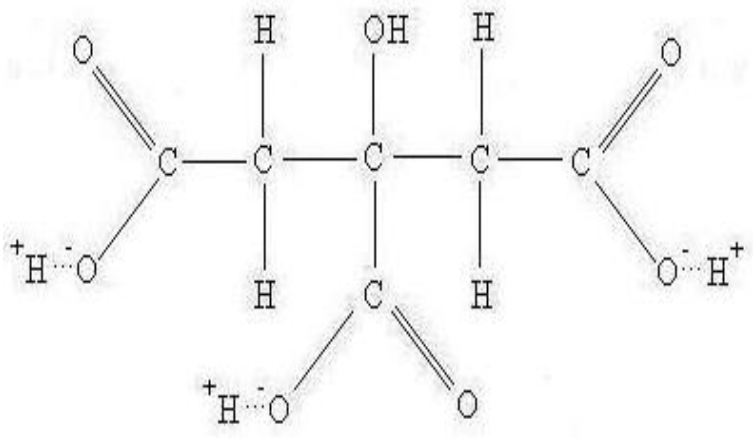

Fig. 12 Structure of citric acid

In the sol-gel synthesis of nanocomposite $LiFePO_4/C$, lithium and iron ions are evenly distributed in the sol solution and subsequent gel solid, in which the degree of ion dispersion at the atomic/molecular level. Using citric acid as complexing agent to synthesize $LiFePO_4/C$ cathode material was reported by several groups[76-77]. It was found that citric acid acted not only as a complexing agent but also a carbon source. As a result, the conductivity of the sample sintered under 850^{o}C is 10^{-3}S/cm, much higher than that of pure $LiFePO_4$. The reversible capacity of lithiation/delithiation reached 148mAh/g at room temperature under C/40 discharge/charge rate[69]. However, the influence of the processing conditions on the structure

and properties of the sol-gel synthesis $LiFePO_4$/C has not been systematically studied, which leads to the major objective in this study. In this chapter, the influences of sintering temperature, different amount of lithium source as well as citric acid on the electrochemical properties of the $LiFePO_4$/C samples were discussed in detail.

4.1 Sintering Temperature

Reaction temperature will directly determine the structure and properties of the product. In order to achieve olivine-structured $LiFePO_4$ from the sol-gel precursors, the optimal reaction temperature must be determined.

Thermal analysis can provide the thermal history and evolution of the materials as a function of temperature and hence, reaction mechanism of the raw materials. The lose of the weight during the increasing of the temperature directly correlate with the reactions at each temperature section.

Figure 13(a) shows the TG profiles obtained from the CA-based gel precursors, prepared from $FeC_2O_4.2H_2O$, $LiOH.H_2O$, H_3PO_4 and citric acid as raw materials. Figure 13(b) shows the TG profiles obtained from the EG-based gel precursor. The gel was prepared from $FeC_2O_4.2H_2O$, $LiOH.H_2O$, NH_2HPO_4 and ethylene glycol as raw materials via sol-gel approach. Detailed description can also be found in chapter 3.

As can be seen in the figure, materials have major mass loss from 150^{o}C to 250^{o}C. The whole sintering process can be divided into three stages: (1) As the temperature is increased to around 250^{o}C, the dramatic mass loss, up to 50% is mainly due to the evaporation of moisture in the gel as well as the decomposition of organic matters in the gel; (2) in the temperature range of 250-450^{o}C, the mass loss continues but much less significantly, which is associated with the

decomposition of remaining organic matters in the gel; (3) above 500°C, the mass of the reactants have maintain at 44.5% of the initial mass, suggesting that no more mass loss occurs and the powders start to crystallize into $LiFePO_4$ phase. The EG-based gel shows slightly difference in details from the CA-based gel in the TGA evolution profile. The EG-based gel experiences 40% mass loss in the temperature range of 150°C to 250°C. Afterwards, the gel slightly stabilizes and starts to decompose further between 350-550°C. Later there is no mass loss occurred above 500°C. The mass of the reactants maintained at 49% of the initial mass.

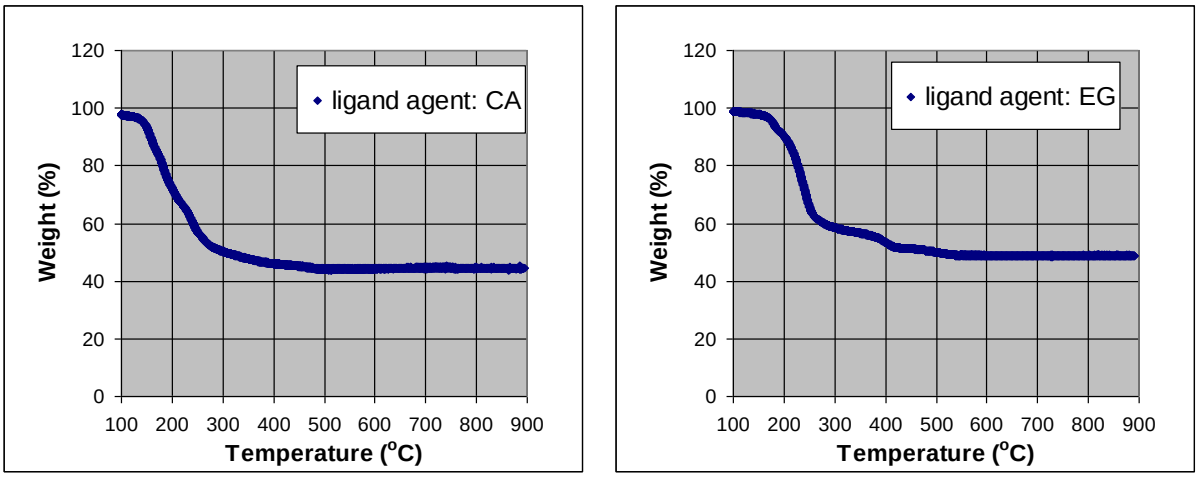

(a) (b)

Fig. 13 TGA curves of (a) CA-based gel precursor; and (b) EG-based gel precursor

Both TGA results suggest that no more mass loss occurs and the powders start to crystallize into $LiFePO_4$ phase above 500°C. As the temperature increases from 500°C to 900°C, the growth of the particles take place with the extra energy. Therefore, in this study, the sintering temperature was focused on the range of 500-800°C

4.1 .1 XRD analytical results

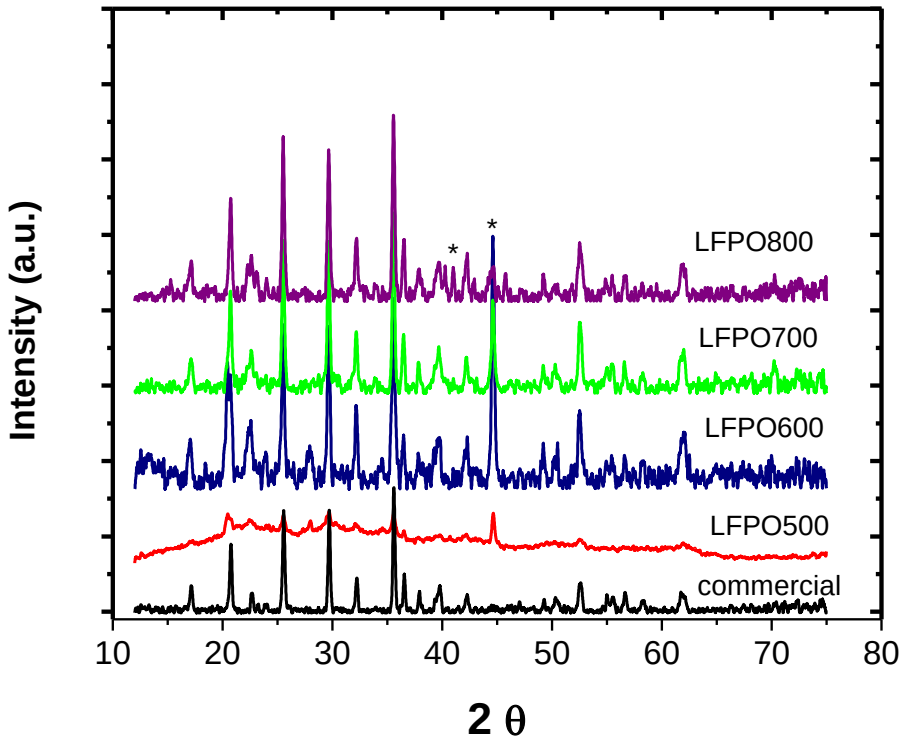

Fig. 14 XRD profiles of the products sintered at different temperatures in comparison with commercial $LiFePO_4$.

Figure 14 showed the X ray-diffraction profiles of the specimens after sintering at 500^{o}C, 600^{o}C, 700^{o}C and 800^{o}C. The results are compared with the standard XRD pattern obtained from commercial LiFePO4 products. It is clear that the specimen sintered at 500^{o}C just started to crystallize. However, the olivine structure has not been formed. When the sintering temperature increased to 600^{o}C, the amount of olivine-structure $LiFePO_4$ increased significantly, although there are still some peaks corresponding to the impurities as marked in the star symbol. Upon increasing the temperatures, the intensity of the peak gradually decreased indicating the reduction of the impurities. However, at sintering temperature of 800^{o}C, another phase of impurity was created with the appearance of diffraction peak at 41^{o}. The exact phases of the

impurities have not yet been identified at the moment. Comparing the XRD results obtained from the specimens sintered at the four temperatures, it is concluded the optimal sintering temperature is around 700^{o}C with the most desired olivine-structured $LiFePO_4$ and least impurities.

4.1.2 Electrochemical performances

Figure 15 shows the charge-discharge curves of samples listed in Table 5. The profiles were all obtained at discharge/charge current densities of 50uA/cm^2, equivalent to around 0.2C rate. The sample synthesized at 500^{o}C has only 18mAh/g. As the temperature increased to 600^{o}C, the capacity increased significantly to 73mAh/g. Discharge capacity of the sample sintered at 700^{o}C further increased to 120mAh/g. However, as the temperature reached 800^{o}C, the capacity reduced to 74mAh/g. Among the four sintering temperatures, 700^{o}C is optimal leading to the highest discharge capacity. Figure 16 summarizes the previous results and shows the reversible capacity as a function of sintering temperatures. It directly shows the optimal sintering temperature is in the vicinity of 700^{o}C when the max discharge capacity can be obtained. Obviously, the sintering temperature around 700^{o}C is optimal leading to the highest discharge capacity.

The electrochemical results corroborate very well with the XRD analyses. As stated in the previous section, the 500^{o}C sintered sample has yet fully crystallized and the crystalline portion contains the least $LiFePO_4$ phase. It is no doubt it shows the lowest capacity. Similarly, the crystallization and growth of olive-structure increased in the 600^{o}C sintered sample, thus the electrochemical performance is improved but far away from the theoretical capacity value due the large amount of impurities. The discharge capacity of 700^{o}C sintered sample at 0.2C rate is better than the other samples because it contains the most active $LiFePO_4$ phase. Further

increasing the temperature to 800°C introduced another phase of impurities, resulting the reduction of active $LiFePO_4$ phase and hence lowed electrochemical capacity of 800°C.

The series experiment indicated that the optimal sintering temperature is 700°C resulting in the most amount of LiFePO4 in the product and highest lithium storage capacity. Therefore, all the following samples in this chapter are prepared at 700°C sintering temperature.

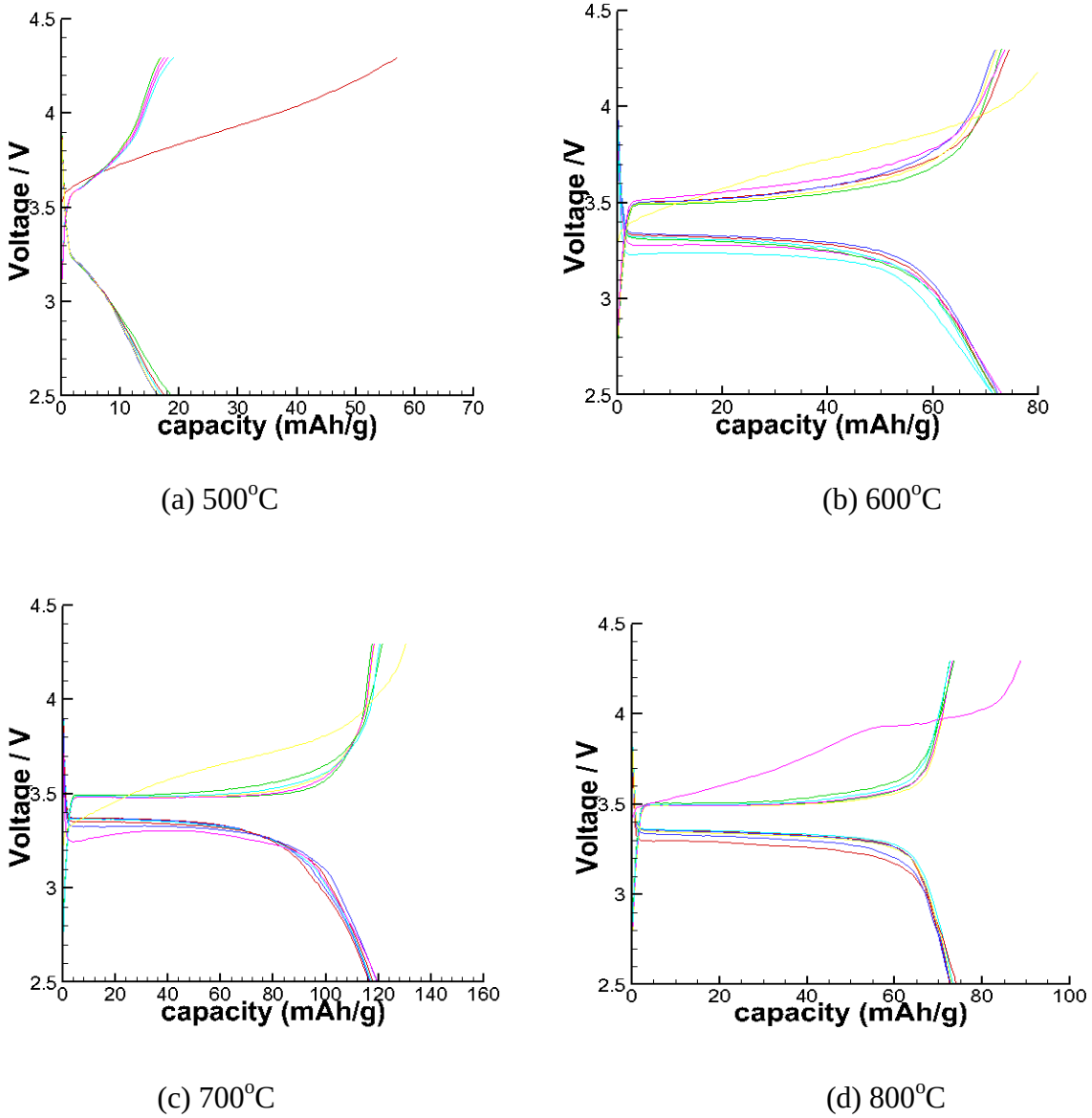

(a) 500°C (b) 600°C

(c) 700°C (d) 800°C

Fig. 15 Charge-discharge curves of $LiFePO_4$/C prepared at different temperatures

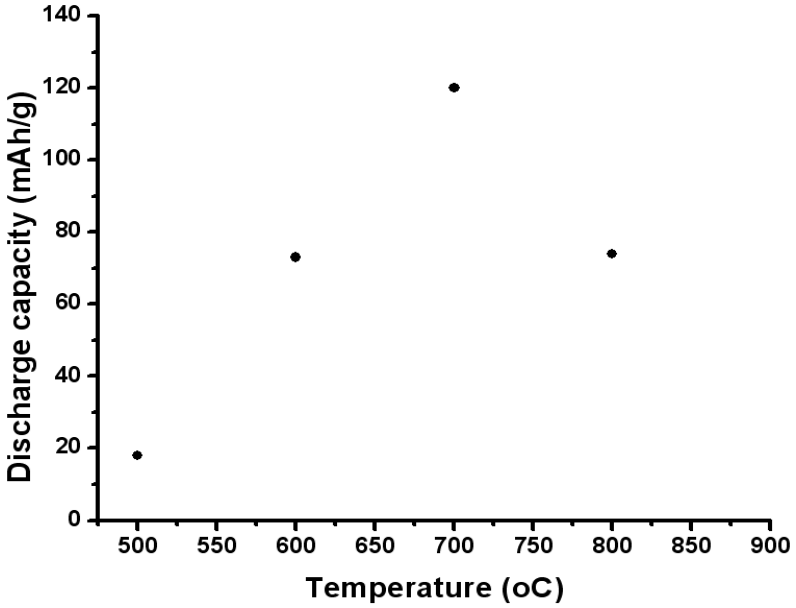

Fig. 16 Comparison of the discharge capacities of samples at different temperatures

4.2 Non-stoichiometric lithium source content

Lithium metal has the smallest atomic weight (6.94g/mol). When using lithium salts to synthesize cathode materials for Li-ion batteries, it is constantly observed the mass loss of lithium during the high temperature sintering step. Therefore, excessive lithium sources need to be added in the precursor to reach the stoichiometric $LiFePO_4$ product. In the following experiments, excessive amount of lithium from 10mol%, 15mol%, 20mol%, 25mol% to 30mol% $LiOH.H_2O$ were added in the preparation of sol-solution. This equivalent to the Li over Fe ratio is 1.1, 1.15, 1.2, 1.25 and 1.3, respectively.

Table 6 listed the actual amount of the raw materials used for the synthesis. Figure 17 shows the charge-discharge curves of these samples at 0.2C rate. The discharge capacity of above samples initially increases and then decreases with the increase of the lithium content. The discharge capacities of above samples are: 120mAh/g ($Li_{1.0}FePO_4$), 120mAh/g ($Li_{1.1}FePO_4$); 123mAh/g ($Li_{1.15}FePO_4$); 127mAh/g ($Li_{1.2}FePO_4$); 136mAh/g ($Li_{1.25}FePO_4$); 119mAh/g

($Li_{1.3}FePO_4$). Figure 18 shows the relationship between lithium contents and discharge capacities of above samples. The stoichiometric sample was also here as a reference. The samples with less excessive of lithium sources, e.g. 10 mol%, showed similar capacities of the stoichiometric sample. Increase the amount to lithium sources to 15 mol% and further 20mol% showed similar capacities gradually increased the capacity. The sample of lithium excessive 25mol% has the highest discharge capacity of 136mAh/g. While further increase the excessive lithium amount results in the decrease of the capacity, i.e. 119mAh/g at 30mol% excessive of lithium. Thus, the appropriate excessive lithium content is advantageous to the improvement of the electrochemical performance of $LiFePO_4$. Figure 4.6 shows the relationship between lithium contents and discharge capacities of above samples. It directly shows the discharge capacity of the lithium excessive 10mol% sample has no difference of the stoichiometric one, both theirs capacity is 120mAh/g. As the lithium content increase from Li excessive 10mol% to 25mol%, the discharge capacities increased from 120mAh/g to 136mAh/g. And the sample of lithium excessive 25 mol% researched the highest discharge capacity. Further increased the lithium content to excessive 30 mol%, the discharge capacity reduced to 120mAh/g.

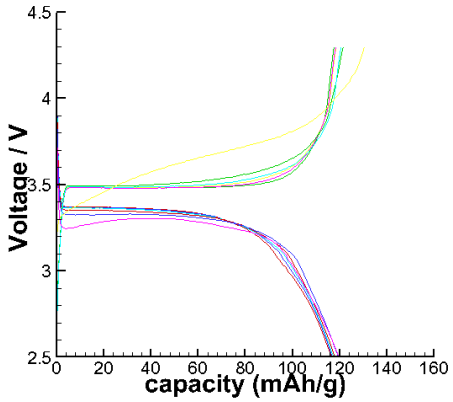

(a) $Li_{1.1}FePO_4/C$

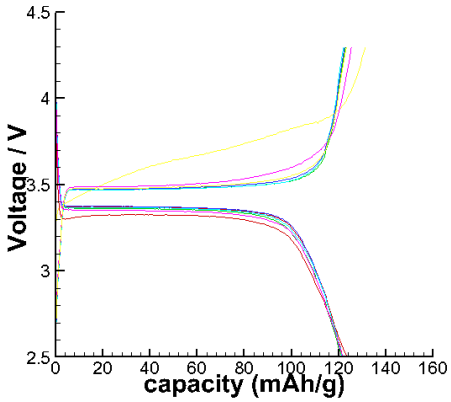

(b) $Li_{1.15}FePO_4/C$

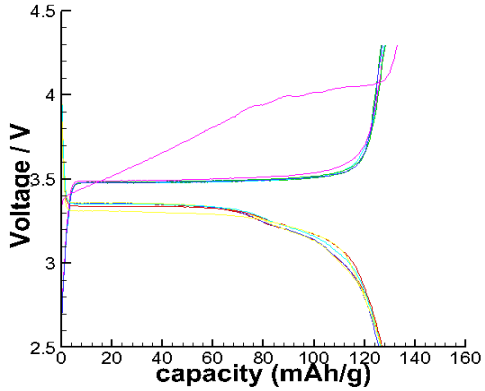

(c)$Li_{1.2}FePO_4/C$

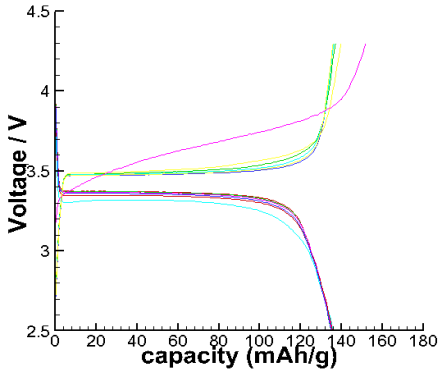

(d) $Li_{1.25}FePO_4/C$

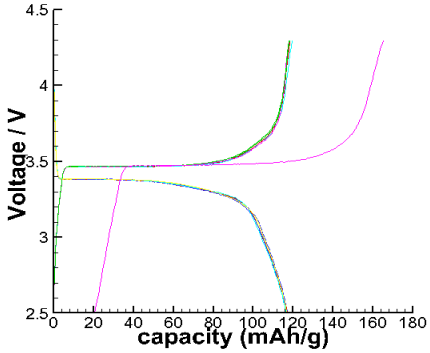

(e) $Li_{1.3}FePO_4/C$

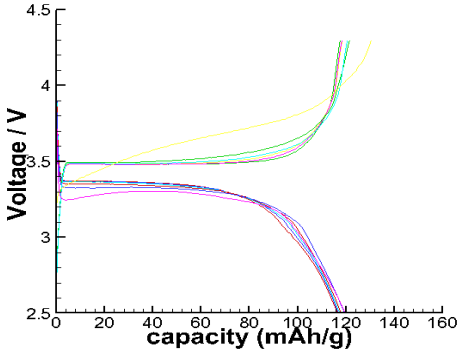

(f) $LiFePO_4/C$

Fig. 17 Charge-discharge curves of $LiFePO_4/C$ samples prepared at different lithium content

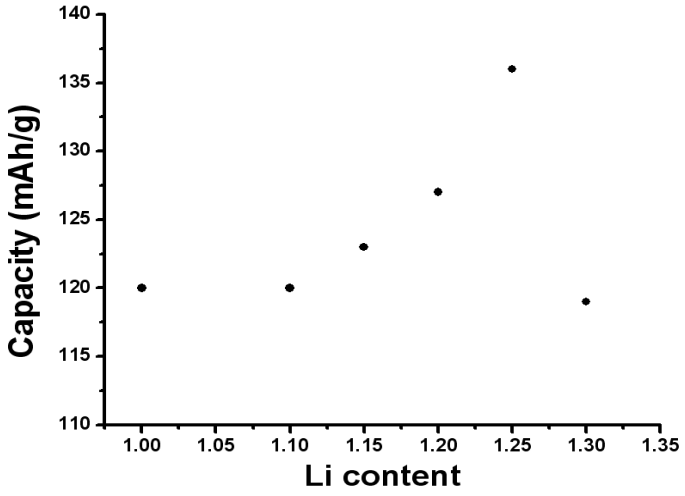

Fig. 18 Comparison of the discharge capacities of samples at different Li content

4.3 The influence of citric acid content on the electrochemical performance of $LiFePO_4/C$

During the sol-gel process, metal ions form complexes with the citric acid and eventually evenly distribute in the gel solid. The particle size and size distribution of products after sintering are directly relevant to the formation of complex gel. Complexing reactions may be different with changing the amount of the complexing agent, i.e. citric acid. Therefore, this section will present the results studying the influence of different content of citric acid on the structure and properties of $LiFePO_4$.

Figure 19 shows the charge-discharge curves of samples with two different molar ratio between citric acid and cations including both lithium and iron. The sample with citric acid molar ratio of 1/4 has the relative higher discharge capacity of 141mAh/g; the one with more citric acid with a molar ratio of 1/2 has a slightly lower discharge capacity of 136mAh/g. The large, uneven distribution of the particle size and more carbon content may cause the lower discharge capacity. As the carbon content of samples increase, the active material may decrease; result in the reduction of discharge capacity. The carbon content of the samples increase with the increase of the content of citric acid, and the agglomeration of the particles also increase with the increase of content of the citric acid, this may leading to the blockage of the diffusion channel of the Li ions, reduce the Li^+ diffusion rate, reduces the electrochemical performance of $LiFePO_4$. It is suggested that in the future research, systematically studies the influence of the carbon content (complex agent) on the performances of $LiFePO_4/C$ are necessary. The results will help us to understand the changing trend observed here in relation with citric acid amount.

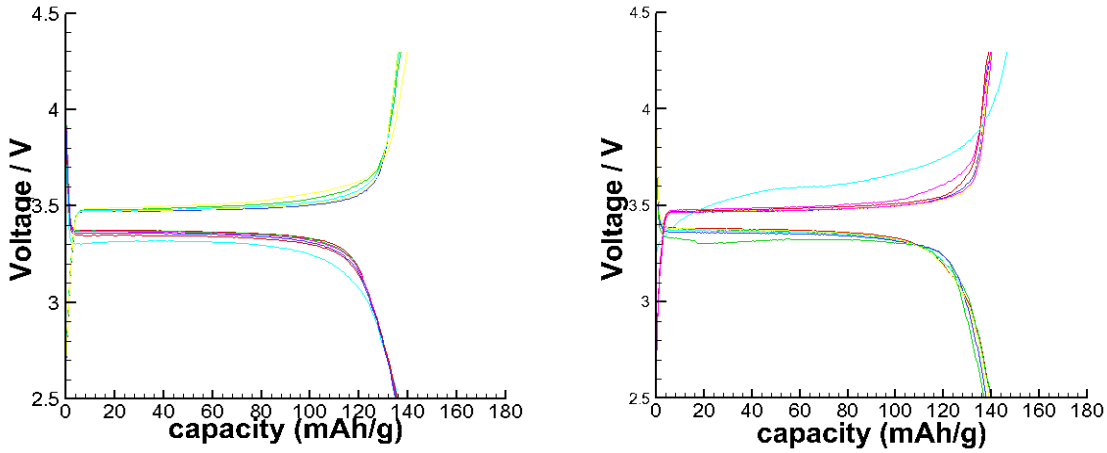

(a) 1/2 (b) 1/4

Fig. 19 charge-discharge curves of $Li_{1.25}FePO_4/C$ at 700°C with different content of citric acid molar ratio of cations (a: 1/2 b: 1/4)

4.4 Summary

This chapter presents the results on a few processing conditions used citric acid as cmplexing agent and carbon source in the sol-gle synthesis of $LiFePO_4C$ material. The influences of sintering temperature, the content of lithium source and the content of citirc acid on the eletrochemical performances of $LiFePO_4/C$ are presented. The findings can be summarized as the followings:

(1) Using $FeC_2O_4.2H_2O$, $LiOH.H_2O$, H_3PO_4 and citric acid as raw materials can result in the formation of LiFePO4/C composites.

(2) When molar ratio of Li to Fe sources is fized to 1: 1 and the citric acid to cations ratio is fixed to 1:2, the discharge capacity was found chaging with sintering temperatures. In the 500 to 800^oC, the highest discharge capacity of 120mAh/g was obtained at 700^oC. Therefore, it is concluded the optimal sintering temperature is in the vicinity of 700^oC at the experimental conditions.

(2) More lithium sources than the stoichiometric ratio in the product (Li:Fe = 1:1) need to be added in preparing the precursor. This will conpensate the mass loss of lithium during the sintering process. The highest discharge capacity is obtained on ($Li_{1.25}FePO_4$) with a value of 136 mAh/g, which is over 13% capacity increase in comparison with the precursors at the stoichiometric ratio.

(3) While other conditions are fixed, i.e. 700^oC and Li:Fe ratio 1.25:1, the citric acid molar ratio of cations between ¼ to ½ will have slightly different capacity results. The sample with less citric acid molar ration relative to cations has the relatively higher discharge capacity of

141mAh/g. This may be contributed to formation of less carbon on the surface of LiFePO4. More carbon will added the weight of inactive materials during the specific capacity calculation.

Chapter 5 Ethylene glycol as complexing agent for synthesis of $LiFePO_4/C$

In the previous chapter, $LiFePO_4$ was synthesized using citric acid as the complexing agent. The research results showed that different sintering temperatures have huge influences on the electrochemical performance of $LiFePO_4$ determined by the formation of the active olivine crystal structure. In addition , lithium content and amount of complexing agent have also some impacts on the electrochemical performances. The best reversible capacity using citric acid was 141mAh/g. In order to further improve the product quality and performances, different complexing agents were explored.

Ethylene glycol is a commonly used complexing agent in the sol-gel synthesis. It is a liquid at room temperature with molecular formula is $C_2H_6O_2$. The structural formula of ethylene glycol is HO-CH_2-CH_2-OH (see Figure 20). When it complexes with metal ions, generally use the adjacent hydroxyl oxygen atoms as the coordinating atoms to form complex compounds. EG has a lower specific surface tension than citric acid and hardly forms hydrogen bonds. Therefore, the synthetic materials from EG will have lower magnitude of agglomeration and uniform particle size. In this study, EG (ethylene glycol) was selected as the alternative complexing agent. The influences of different contents, PH values on the microstructure, charge-discharge performance by means of XRD, SEM. In addition selected specimens were subjected to EIS and CV analyses.

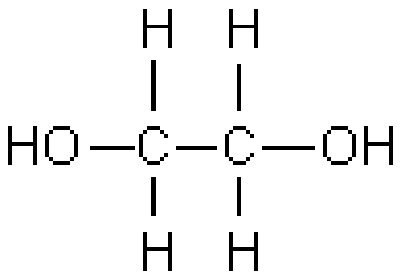

Fig. 20 Structure of EG

5.1 Different EG/cation molar ratio

5.1.1 Sample preparation

In this study, $LiOH.H_2O$ is used as Li source, $FeC_2O_4.2H_2O$ was used as the iron source, and $NH_4H_2PO_4$, is the source of phosphate ions. $LiOH.H_2O$ and $FeCl_2.4H_2O$ were subsequently added into the designed concentration of EG solution (distilled water as solvent). The molar ratio of EG over the total cations are varied from 1/2, 1/1, 3/2 and 2/1 (table 13). After mixing uniformly, stoichiometric $NH_4H_2PO_4$ was added and stirred for 1h at room temperature. Later, temperature was raised to 70 °C and until gel gradually formed resulting from the evaporation of water solvent. The gel was then dried in the box furnace at 120°C for 12h. After grinding the dry gel into fine powders, the gels were sintered under 5 vol. $\%H_2 + N_2$ inert atmosphere at 700°C for 10h. The obtained powders were then mixed with graphite and PVDF-NMP solution and coated on aluminum foil. After the coated film was dried at 120°C for 12h, the film was cut into the right and assembled into a testing for electrochemical characterization.

Table 13 Samples list

sample	water	EG	$LiOH.H_2O$	$FeC_2O_4.2H_2O$	$NH_4H_2PO_4$
a	**100mL**	**0.05mol**	**0.05mol**	**0.05mol**	**0.05mol**
b	**100mL**	**0.1mol**	**0.05mol**	**0.05mol**	**0.05mol**
c	**100mL**	**0.15mol**	**0.05mol**	**0.05mol**	**0.05mol**
d	**100mL**	**0.2mol**	**0.05mol**	**0.05mol**	**0.05mol**

5.1.2 Electrochemical performance

Figure 21 shows the charge-discharge curves of above samples at 700^{o}C under 0.2C rate. The discharge plateau potentials of those samples are all positioned around 3.4V. The sample with EG/cation molar ratio of 1/2 has the highest discharge capacity of 145mAh/g, which is 10% more than the specimen synthesized from citric acid complexing agent. When the EG/cation ratio change to 1/1, 3/2 and 2/1, the discharge capacities continuously decreased to 140mAh/g, 133mAh/g, and 116mAh/g, respectively. Figure 22 shows the relationship between EG contents and discharge capacities of above samples. It directly shows the discharge capacities decrease as the increase of the content of EG.

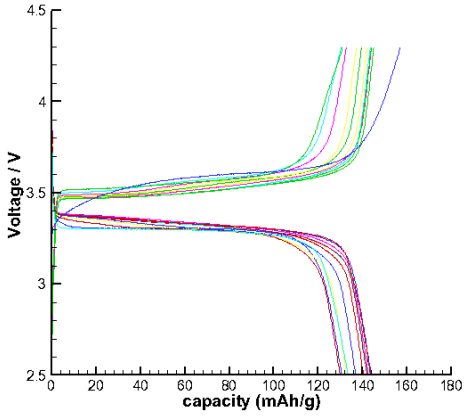

(a)

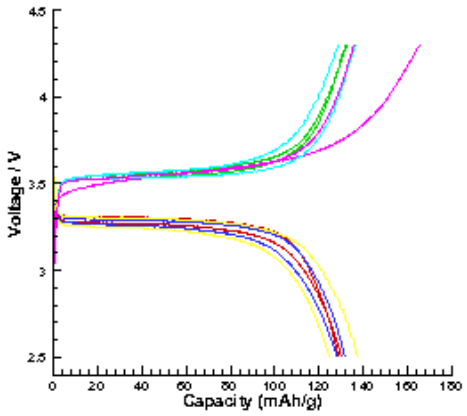

(b)

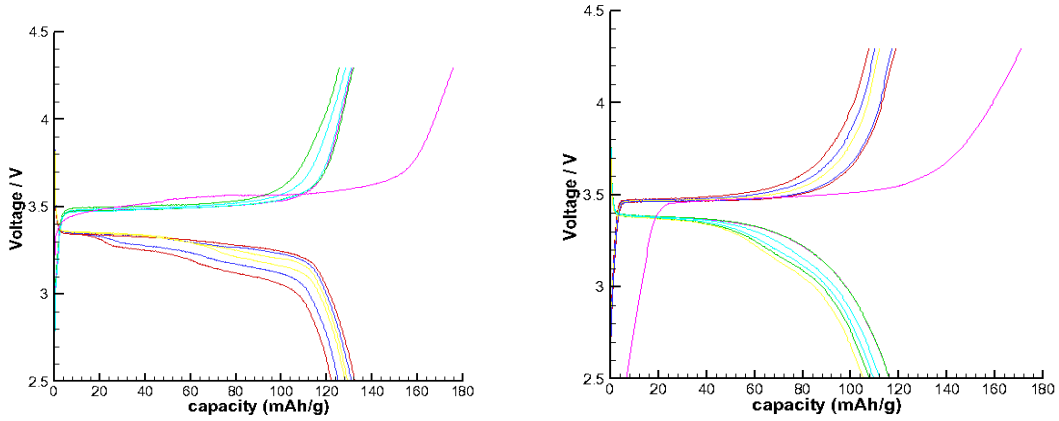

(c) (d)

Fig. 21 Charge-discharge curves of $LiFePO_4/C$ ($FeC_2O_4.2H_2O$ as iron source) at 700°C with different content of ethylene glycol molar ratio of cations (a: 1/2 b: 1/1 c: 3/2 d: 2/1)

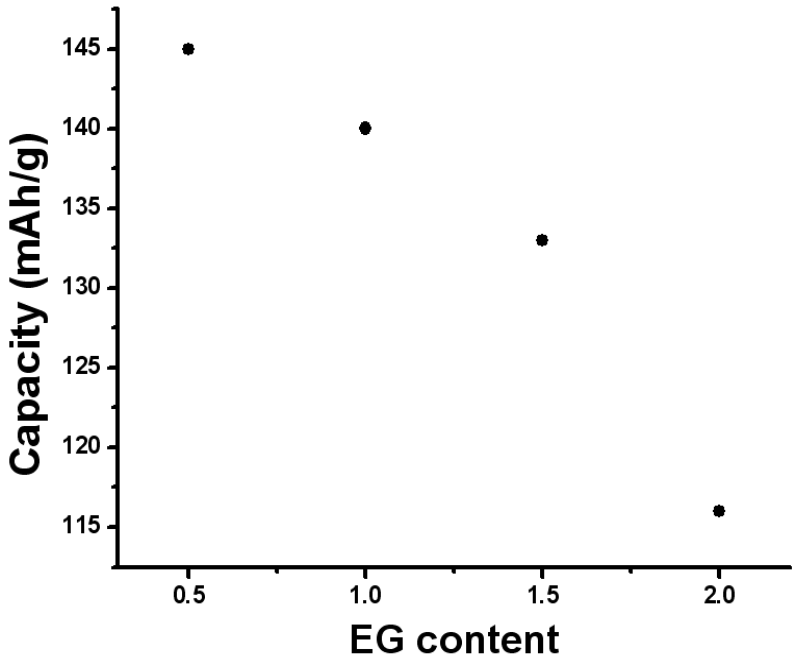

Fig. 22 Comparison of the discharge capacities of samples at different EG content

As the content of the ethylene glycol increase, the specific charge and discharge capacity decrease. This phenomenon may because of the samples contain different content of carbon. It is

known that the carbon content in the $LiFePO_4$/C product originates from the situ decomposition of complexing agent at high temperature sintering. Hence, it is reasonably to consider the carbon content of those samples will increase with the increase of the content of ethylene glycol. When there exit excess carbon in the $LiFePO_4$, the particle size and the magnitude of the agglomeration may increase along with the increase of the content of the ethylene glycol. The high carbon content may lead to the blockage of the diffusion channel of the Li ions, reduce the Li^+ diffusion rate, thus reduce the electrochemical performance of $LiFePO_4$. The sample with ethylene glycol molar ratio of cations of 2/1 has the lowest discharge capacity, which may be related with the highest carbon content. The moderate content of carbon may be able to inhibit the growth of the $LiFePO_4$ particle size. The carbon content of ethylene glycol molar ratio of cations of 1/2 may already enough to make the $LiFePO_4$ have relative fine and uniformly dispersed particles.

5.1.3 Phase analysis

Fig. 23 shows the XRD pattern of the sample with ethylene glycol molar ration of cations of 1/2. Compare the sample's XRD pattern with the standard pattern, the sample's XRD pattern doesn't show any impurity peaks, which means the sample is pure $LiFePO_4$ phase. From the figure we can tell the sample has sharp diffraction peaks, it can be indexed by the orthorhombic D_{2h}^{16}, Pmnb space grouping. Every diffraction peak of the sample is one-to-one correspond to the standard XRD pattern. Every peak of the sample has high intensity and half-peak breadth, which means the formed material has good crystallinity. There's no characteristic peak of carbon shows in the sample's XRD pattern, which means the ethylene glycol decompose to amorphous carbon or (and) carbon with low crystallinity during the sintering process. Further, compared with the XRD pattern obtained from the sample synthesized using citric acid, the peaks related

with impurity phase at 45^{o} was diminished. It is therefore submitted that EG complexing agent can result in better LiFePO4/C product, as manifested with the higher reversible capacity.

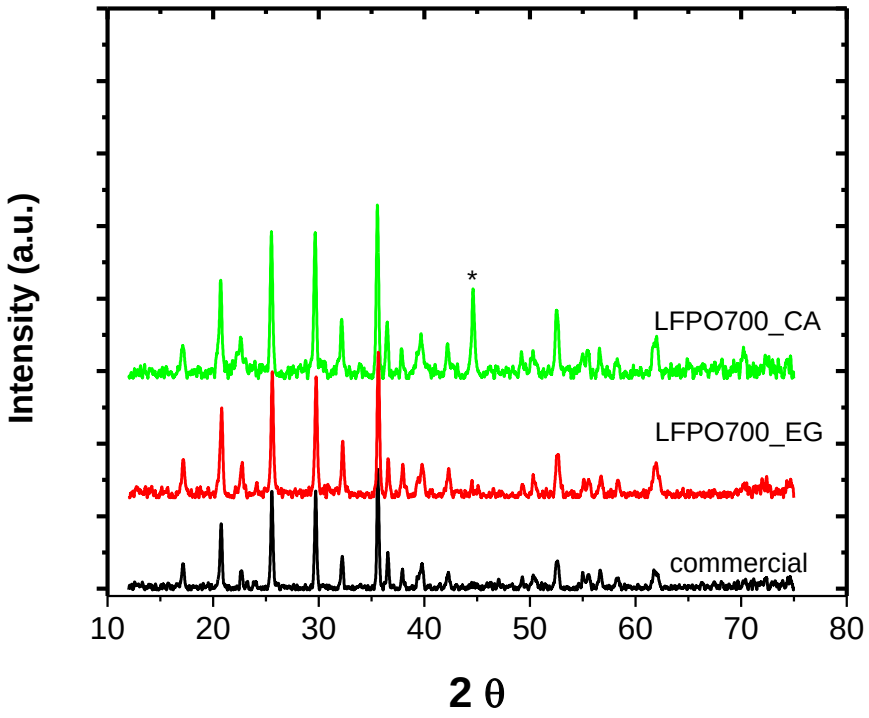

Fig. 23 XRD pattern of $LiFePO_4$/C the sample synthesized using EG complexing agent (EG/cation ratio is 1/2). For comparison, the XRD profiles of commercial standard $LiFePO_4$ and sampled synthesized using citric acid are also presented.

Citric acid and ethylene glycol have different complexation constants. Citric acid has a larger complexation constant when complexing with Fe^{2+}, the formed gel have stable structure. When the content of citric acid is high, the product contains large amounts of carbon. Excessive carbon on the surface of $LiFePO_4$ will block the diffusion of Li into the $LiFePO_4$ crystal structure, leading to the reduced lithium storage capacity and rate capability. In contrast, ethylene glycol has relative smaller complexation constant with Fe^{2+}, the structural stability of the formation gel is low; the carbon content of the sintered product may be lower. Therefore, choosing different

complexing agent in the precursor will alter the properties of the synthesized $LiFePO_4$. A more detailed mechanism discussion will be explained in the next chapter.

5.1.4 Morphology analysis

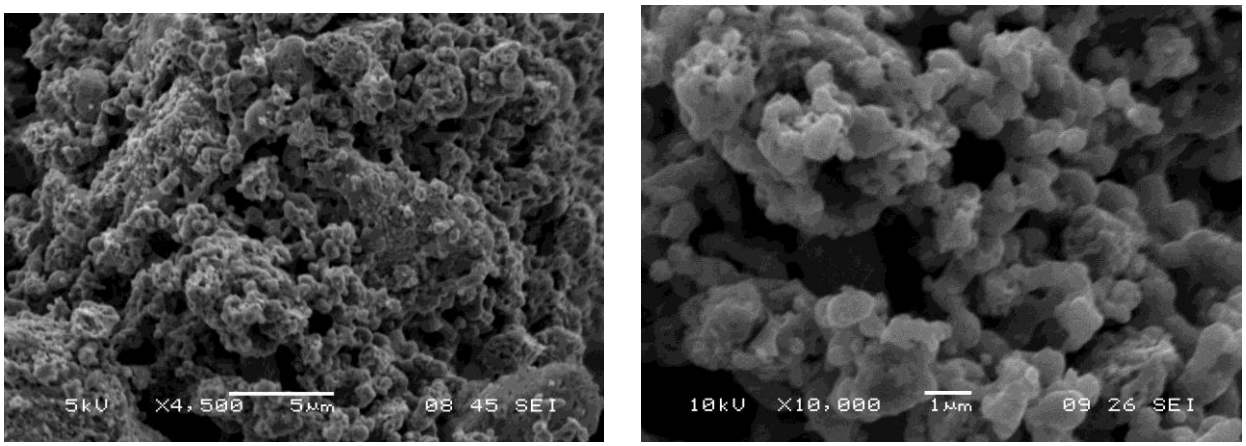

(a) (b)

Fig. 24 SEM images of $LiFePO_4$/C (the sample with EG/cation molar ration of 1/2)

Fig.24 are the SEM photographs of $LiFePO_4$/C with ethylene glycol molar ratio of cations of 1/2. From 24(a) we can see the have relative high magnitude of agglomerations. From the high magnification image as shown in figure 24 (b), we can tell that the material has uniformly distributed particles, the particle size less than 500nm. The particles are almost in spherical shape, which will significantly increase the specific surface area of the interface. The surface of particles is coated a thin carbon layer, coming from the in-situ decomposition of EG at high temperature. This carbon layer coated on the surface of $LiFePO_4$ can greatly improve the electrical contact between the particles. So that the electrolyte can penetrate into the active substances in order to facilitate the transportation of Li ions and electrons, to improve the utilization of $LiFePO_4$.

5.1.5 Rate Capability and cycling stability Evaluation

Figure 25 shows the discharge capacity profile of the best sample obtained at different discharge rates. From figure 25 it can be seen that all discharge plateaus are around 3.4V. With the increase of the C rate, there is no obvious reduction of the discharge plateaus. The capacities slightly decrease with the increase of the C rate. Figure 26 plot the capacity values as a function of the discharge rate. From 0.1C to 2C, the discharge capacities just decrease 7mAh/g. The decreasing amplitude is less than 5%.

For performance of the optimized sample was compared with the commercial product. From figures 27 and 28 we can see the commercial $LiFePO_4$ have discharge plateaus around 3.4V and initial capacity at 0.1C was 152mAh/g. However, the capacities decrease with the increase of the C rate. The discharge capacities decrease from 152mAh/g (0.1C) to 97mAh/g (2C) with a decreasing amplitude is 36%.

Figure 29 shows the cycle performance of the $LiFePO_4$/C (1/2 EG) sample at first 33 cycles. This sample shows a good cycle reversibility.

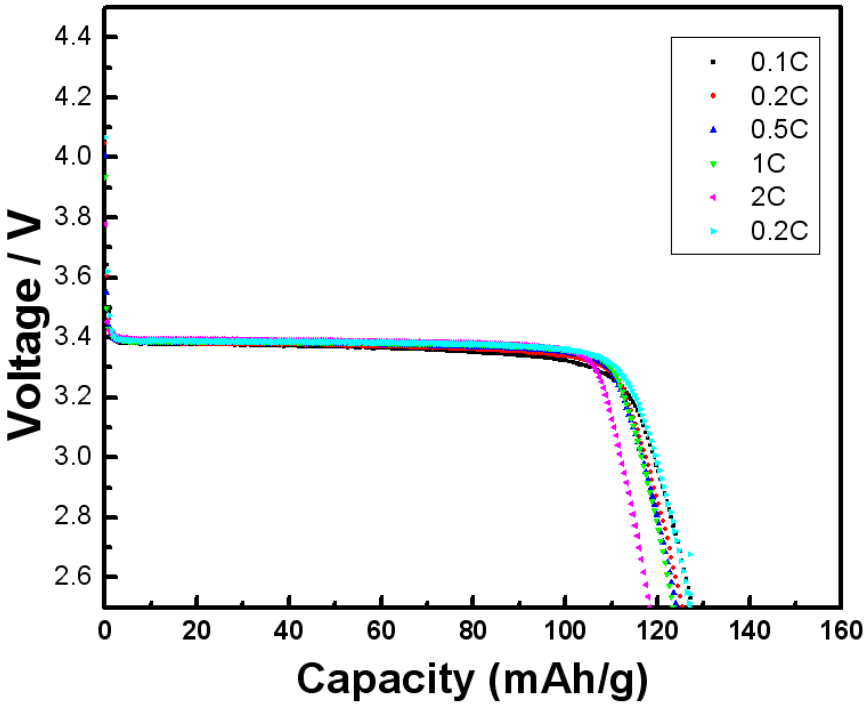

Fig. 25 Discharge curves of $LiFePO_4$/C (1/2 EG) at different C rates.

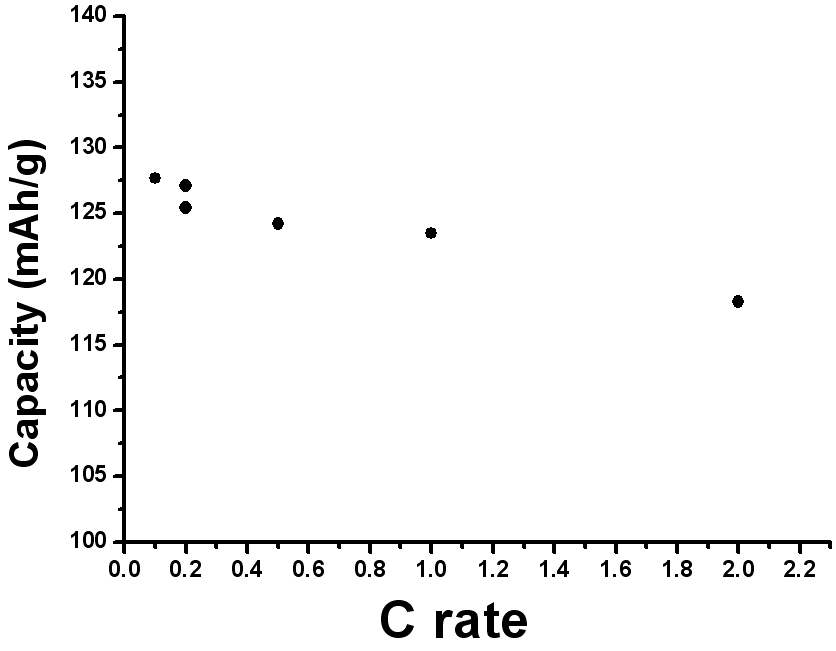

Fig. 26 Comparison of discharge capacities of $LiFePO_4$/C (1/2 EG) at different C rates.

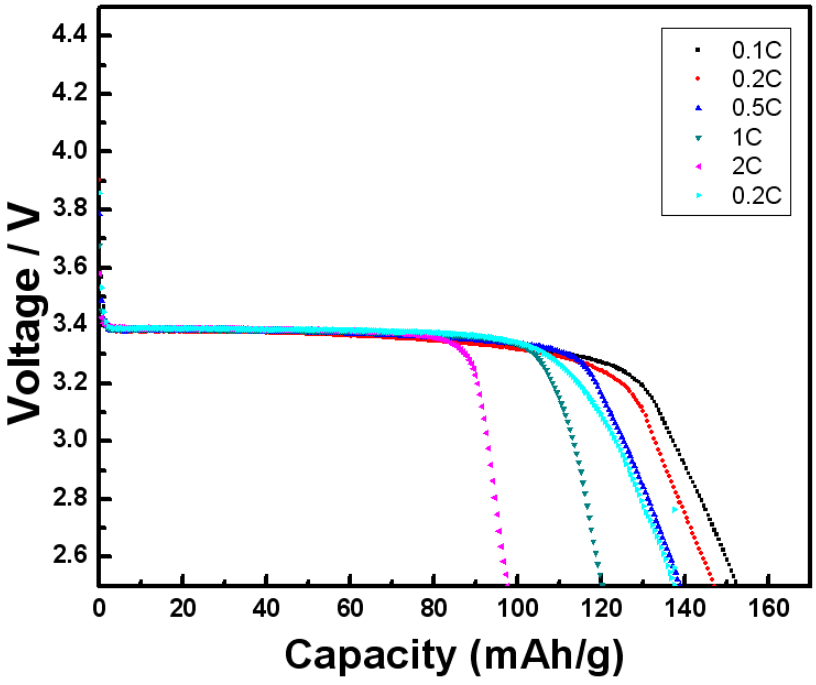

Fig. 27 Discharge curves of commercial $LiFePO_4$ at different C rates

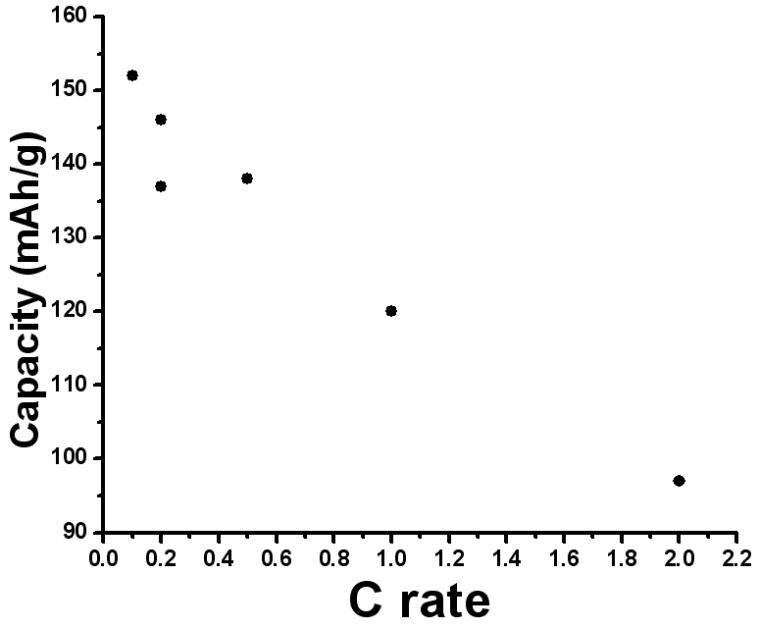

Fig. 28 Comparison of discharge capacities of commercial $LiFePO_4$ at different C rates

The decreased electrochemical performance of $LiFePO_4$ at higher C rate is related with the two-phase characteristics of this material during the lithiation/delithiation processes. This can be explained by the model of critical area proposed by Padhi et al[23]. For a $LiFePO_4$ particle, along with the lithiation process of Li^+, the $Li_xFePO_4/Li_{1-x}FePO_4$ interface will constantly move to the internal of the particle during the process of discharge. Therefore, the interfacial area will continuously shrinking. At a constant temperature, the transportation rate of Li^+ on unit interfacial area can be considered as a fixed value. So, when the discharge rate increased to a value that the sum of all the interfacial areas cannot support for the discharge current at that rate, the discharge process will become diffusion control. And this area is called critical area. The higher the discharge current, the larger the critical area and the number x of the available Li^+ that can lithiate into the particle will be smaller. This is why $LiFePO_4$ has low discharge capacities at high discharge rates. The above phenomenon shows that the carbon coating does not increase the bulk conductivity of $LiFePO_4$. While the carbon coating increase the surface conductivity and improve the kinetic properties of Fe^{3+}/Fe^{2+} redox processes.

Lithium ions have small free volume of movement, if the discharge current density is too large the discharge capacities will decrease. Theoretically, all the Li ions can delithiate, when the delithiation process complete, $LiFePO_4$ will becomes to $FePO_4$ and the cell volume will decrease from $0.2914nm^3$ to $0.2724nm^3$. However, practically during the delithiation process it will form $Li_xFePO_4/Li_{1-x}FePO_4$ two-phase interface. The channels for Li ions diffusion might become narrow along with the decrease of the cell volume during the delithiation process. It may block the Li transportation, so that the Li ions cannot get fully utilized. Some Li ions may not involve in the discharge processes.

The carbon content also has important influence on the discharge capacity of $LiFePO_4$. The carbon content too high will make the surface carbon thicker; it is easy to block the transportation of electrolyte and Li ions. Meanwhile, carbon is not active substance. The increment of the carbon content will reduce the volumetric energy density. Therefore, as long as it is enough to coat the active substances, the carbon content should be as little as possible.

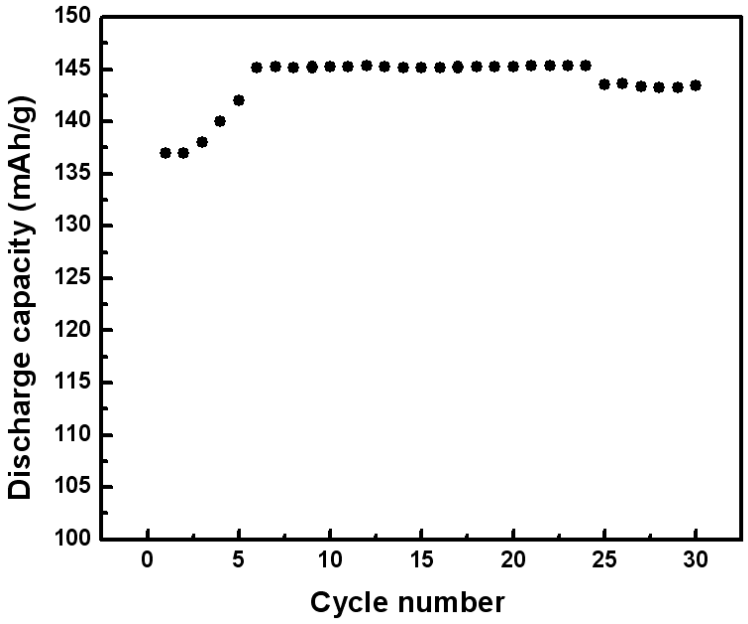

Fig. 29 Cycle performance of $LiFePO_4$/C (1/2 EG)

5.2 Using different iron source

5.2.1 Sample preparation

In this study, $FeCl_2.4H_2O$ is the iron source. All the other precursors, processing conditions are the same as those described in the section 5.2.

Table 14 Samples list

sample	Water	EG	$LiOH.H_2O$	$FeCl_2.4H_2O$	$NH_4H_2PO_4$
a	**100mL**	**0.05mol**	**0.05mol**	**0.05mol**	**0.05mol**
b	**100mL**	**0.1mol**	**0.05mol**	**0.05mol**	**0.05mol**
c	**100mL**	**0.15mol**	**0.05mol**	**0.05mol**	**0.05mol**
d	**100mL**	**0.2mol**	**0.05mol**	**0.05mol**	**0.05mol**

5.2.2 Electrochemical performances

Figure 30 shows the charge-discharge curves of above samples at 700^{o}C under 0.2C rate. All the samples have discharge capacities less than 100mAh/g. With the increase of the content of ethylene glycol, the discharge capacities have a tendency of reduction. Figure 31 shows the relationship between the EG contents and discharge capacities of above samples. It directly shows the discharge capacities decrease as the increase of the content of EG. At the EG of cations ratio of 1/2, the sample get the relative highest discharge capacity of 76mAh/g. As the EG content continually increased to 2/1, the discharge capacity reduced to 16mAh/g. Compare with Fig. 21, the discharge capacities of the samples synthesized by using $FeC_2O_4.2H_2O$ are all higher than the samples using $FeCl_2.4H_2O$ as the iron source. The sample with ethylene glycol molar ratio of cations of 2/1 has the lowest discharge capacity of 16mAh/g, which may be related with the highest carbon content. Except for the lowest capacity; this sample also has the lowest discharge platform potential. This means it has the highest polarization potential.

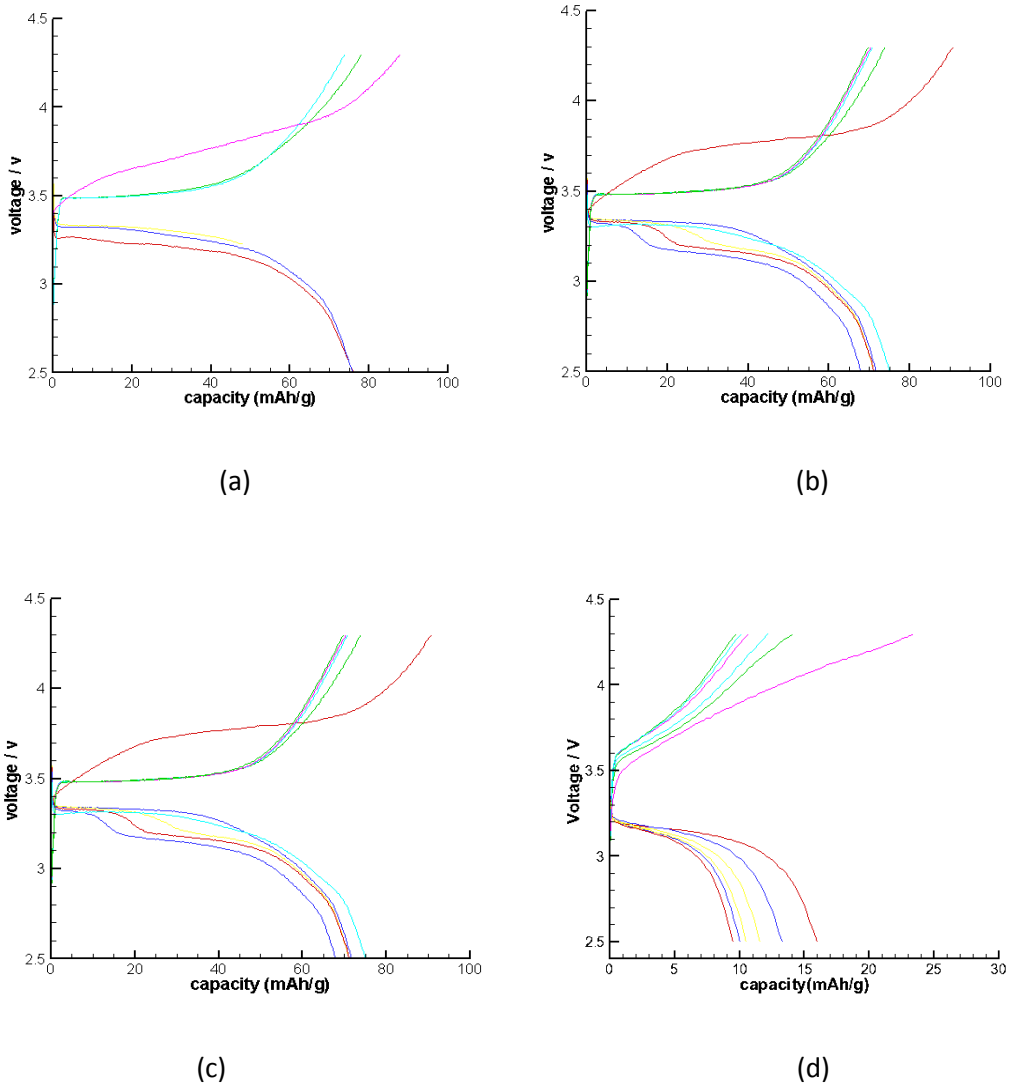

Fig. 30 Charge-discharge curves of $LiFePO_4/C$ ($FeCl_2.4H_2O$ as iron source) at 700°C with different content molar ratio of ethylene glycol to total cations (a: 1/2 b: 1/1 c: 3/2 d: 2/1)

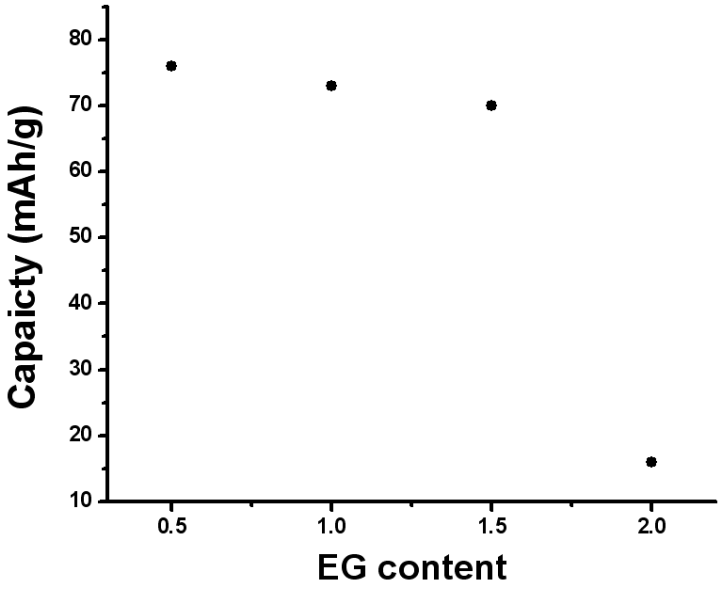

Fig. 31 Comparison of the discharge capacities of samples at different EG content

5.3 The influence of PH value

5.3.1 Sample preparation

In this study, $FeC_2O_4.2H_2O$, EG is the iron source and the ethylene glycol molar ratio to cations is 1/2. Dilute hydrochloric acid (HCl) and ammonia water to adjust the PH value to 0, 2, 4, 6 and 8. The initial unadjusted PH value of the sol solution is 6.8; the color of the solution is light green. When dropping dilute hydrochloric acid adjust the PH value around 2, the color of solution turns to yellow and the viscosity increase sharply. When dropping ammonia water to adjust the PH value around 8, the color the solution turns to kiwi-green and the viscosity decrease.

Table 15 Samples list

sample	water	PH value	EG	$LiOH.H_2O$	$FeC_2O_4.2H_2O$	$NH_4H_2PO_4$
a	**100mL**	**0**	**0.05mol**	**0.05mol**	**0.05mol**	**0.05mol**
b	**100mL**	**2**	**0.05mol**	**0.05mol**	**0.05mol**	**0.05mol**
c	**100mL**	**4**	**0.05mol**	**0.05mol**	**0.05mol**	**0.05mol**
d	**100mL**	**6**	**0.05mol**	**0.05mol**	**0.05mol**	**0.05mol**
e	**100mL**	**6.8**	**0.05mol**	**0.05mol**	**0.05mol**	**0.05mol**
f	**100mL**	**8**	**0.05mol**	**0.05mol**	**0.05mol**	**0.05mol**

5.3.2 Electrochemical performance

Figure 32 shows the charge-discharge curves of above samples at 700^{o}C under 0.2C rate. Sample e (PH=6.8), whose PH value is initial and unadjusted, has the highest discharge capacity of 145mAh/g. Sample a (PH=0) and sample f (PH=8) have lowest capacities, 41mAh/g and 82mAn/g respectively. Sample b (PH=2) has the discharge capacity of 112mAh/g, sample c (PH=4) has the discharge capacity of 118mAh/g and sample d (PH=6) has the discharge capacity of 130mAh/g. The discharge capacities of above samples first increase with the increase of the PH value of sol, when the PH value reach 6.8, the sample has the highest discharge capacity (145mAh/g), as the PH value of sol solution continuously increase, the discharge capacity has a tendency of reduction. When the PH value is 8, the discharge capacity of $LiFePO_4$ sharply decreases to 82mAh/g.

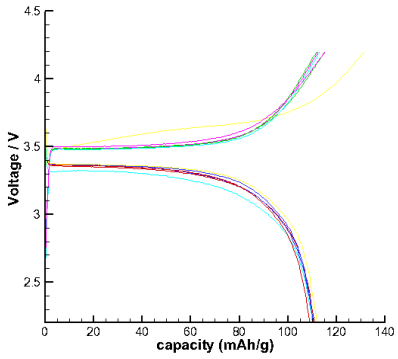

(a)

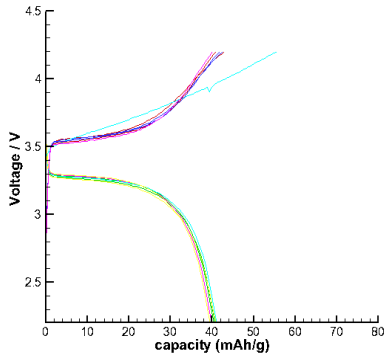

(b)

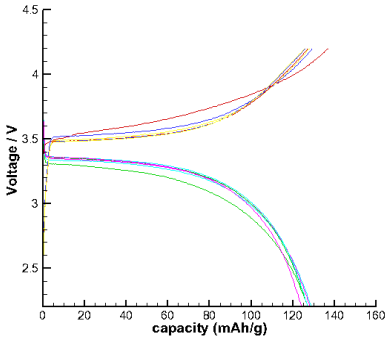

(c)

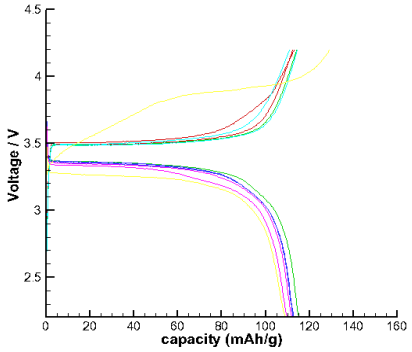

(d)

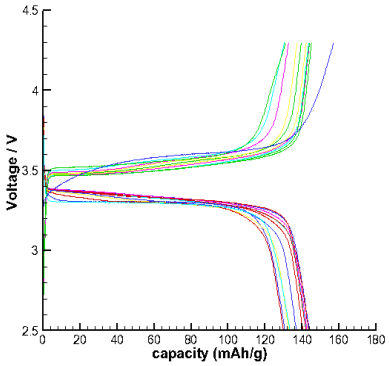

(e)

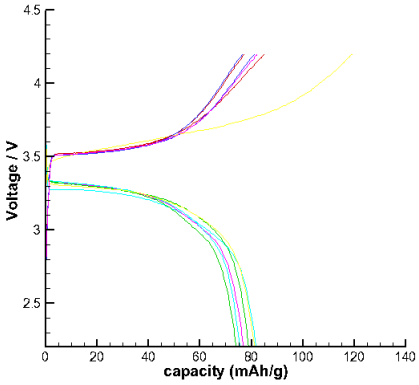

(f)

Fig. 32 Charge-discharge curves of $LiFePO_4/C$ of ethylene glycol molar ratio of cations 1/2 with different PH values (a: PH=0 b: PH=2 c: PH=4 d: PH=6 e: PH=6.8 f: PH=8)

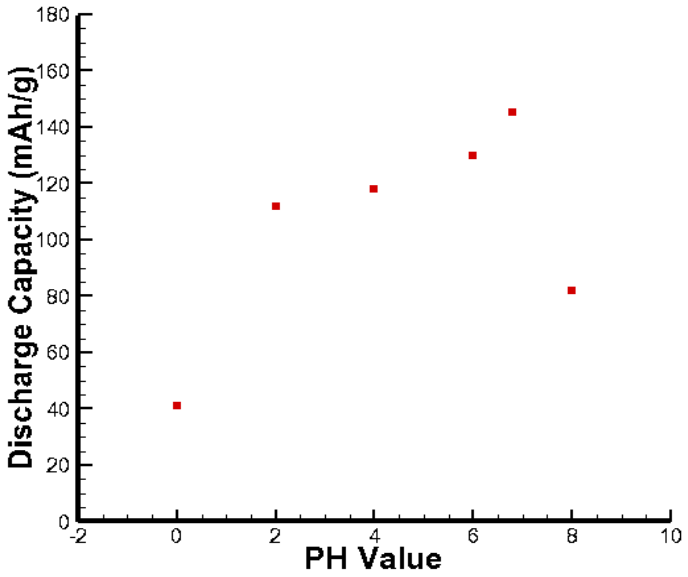

Fig. 33 Comparison of discharge capacities at different PH values

Figure 33 directly shows the relationship between PH values and discharge capacities of above samples. It shows the discharge capacities increase as the increase of the PH value. At the PH value of 6.8, the sample gets the highest discharge capacity of 145mAh/g. As the PH value continually increased to 8, the discharge capacity reduced to 82mAh/g. The main influence of the PH value of sol solution on the morphology of synthesized $LiFePO_4$ is at different PH value the uniformity of complexation between cations and ethylene glycol is different. Unifies the fore-mentioned viscosity change of the sol solution during the PH adjustment process, can be inferred, PH=2 is the transition point of the viscosity of sol solution increased significantly, sol quickly become gel, when the PH value continues to increase, the formed gel gradually dissolves. Therefore, maybe when PH is 2 Fe^{2+} and ethylene glycol have a good complexing and the cations distributed more uniformly than other PH values. Consequently, the dry gel can homogeneously nucleation and growth during the sintering process. The uniformly distributed

organic carbon network also can inhibit the growth of the agglomeration of $LiFePO_4$ particles, in order to obtain the products with small and well dispersed particles.

In summary, the PH value of sol-gel solution affects two main reactions of the sol-gel process: hydrolysis reaction and polymerization reaction, thereby affecting the complexation between cations and ethylene glycol. The adjustment of PH value change the complexation conditions between cations and ethylene glycol; suitable PH value is conducive to get uniform distribution of metal cations in organic substances and helpful to obtain $LiFePO_4$ powders with uniformly small size and well dispersed particles, in order to improve the material's electrochemical performance.

5.4 Combining CA and EG complexing agents

5.4.1 Sample preparation

In this study, a mixed solution of CA and EG with a molar ratio of 1:1 was used as the complexing agent, while all other experimental conditions were kept the same as before. It is also worth mentioning this gel was subjected to 2 days ball milling before sintering process.

Table 16 Sample list

sample	water	EG	CA	$LiOH.H_2O$	$FeC_2O_4.2H_2O$	$NH_4H_2PO_4$
	100mL	**0.025mol**	**0.025mol**	**0.05mol**	**0.05mol**	**0.05mol**

5.4.2 Electrochemical performance

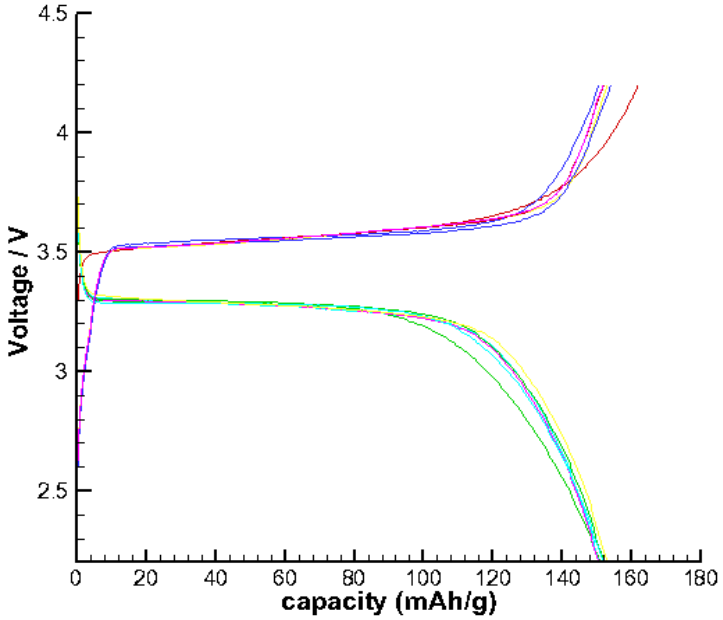

Fig. 34 Discharge curves of $LiFePO_4$/C (CA+EG)

Figure 34 shows the discharge curves of the $LiFePO_4$ (CA+EG) at 0.2C rate. At first cycle, the discharge capacity reached 150mAh/g. After 5 cycles, the discharge capacity increase to 152mAh/g. The high discharge capacity of the sample may because of the long time ball milling process. The ball milling process can reduce the particle size and break some partial agglomerations. This will help opening up the channels for the transportation of Li ions. Makes the lithiation/delithiation of Li ions more easily to occur. Ball milling process reduces the resistance for the transportation of Li ions, and improves the utilization efficiency of Li ions. Therefore, the discharge capacities have corresponding increment.

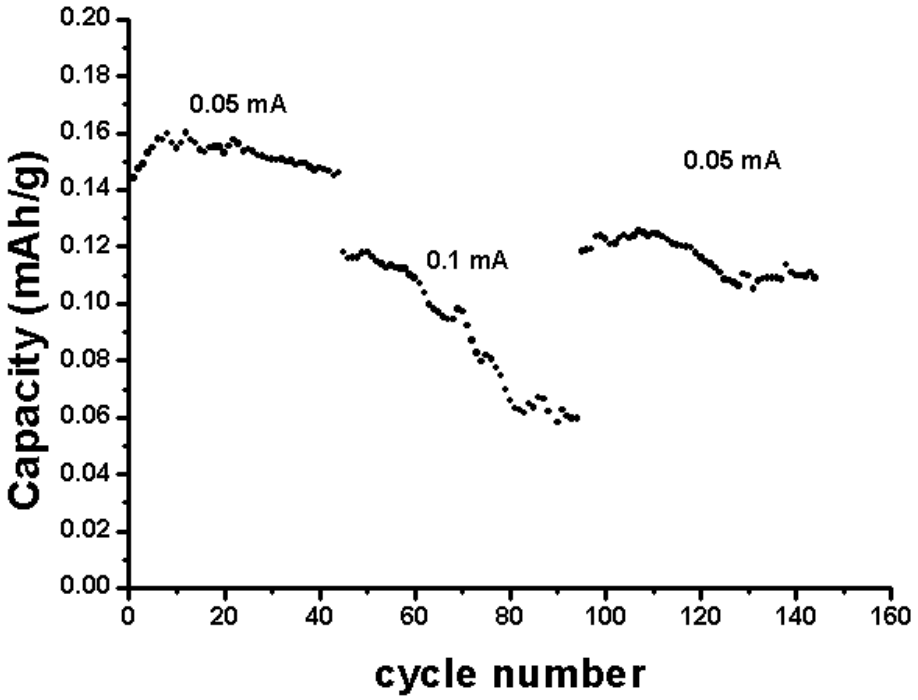

Fig. 35 Cycle life of $LiFePO_4$/C (CA+EG) at different discharge current density (button cell)

Figure 35 shows the cycle life of $LiFePO_4$/C (CA+EG) at different discharge current. For testing the cycle life we use the button cell instead of using the Swagelok cell. The button cell can be sealed more strictly than the Swagelok cell, so the active materials in the button cell can survive longer than in the Swagelok cell. Form the figure can be seen that the sample cycle at 0.05 and 0.1mA different discharge current. In the first couple cycles, the cell is in the activation status, after about 20 cycles the capacity increase from 0.14 to 0.16mAh/g. This means the kinetic property have an improvement, and the capacity get the corresponding increment. In $LiFePO_4$, the free volume is very small for the movement of Li ions. When the current density is too large the discharge process will become diffusion control from electrochemical reaction control, the transfer rate of Li ions is much slower than the conduction rate of the electrons. This is because $LiFePO_4$ its intrinsic conductivity is poor, so the capacity will reduce. The discharge current increase to 0.1mA, the discharge capacity starts to decrease. After 100 cycles the

discharge capacity reduced to 0.06mAh/g. Once the current density decreased, the capacity will increase back to the previous level. When the discharge current reduced from 0.1mA to 0.05mA, the capacity increased back to 0.13mAh/g. This indicates that the $LiFePO_4$ has a stable structure, the cell at 0.05mA cycled another 50 times, the discharge capacities still around 0.12mAh/g. This cell has a good cyclic performance and stability. The good cyclic performance on one hand is because the carbon coating improves the electrical conductivity of the material; on the other hand because of $LiFePO_4$ itself has a high stability structure. The phase $FePO_4$ formed after discharge is structural similar to $LiFePO_4$, the volume difference is just 6.81%.

5.5 Electrochemical Analyses

5.5.1 EIS analyses

Figure 36 shows the EIS curves of the sample $LiFePO_4$/C (1/2 EG) at different cycle numbers. "Fresh cycle" means directly test the electrochemical impedance of the cell without activation. From the figure it is seen that the cell's electrochemical impedance is relatively high before charge and discharge, was 1000Ω. After 5 cycles of activation, the impedance reduced to 320Ω, the impedance reduced to 180Ω after 11 cycles. Therefore, the process of activation has a very important impact on the properties of lithium ion batteries. The inside of the battery cells will have some minor changes during the subsequent charge-discharge processes, such as the change of the concentration of the electrolyte and the change of the anode Li. Those changes will increase the impedance. After 30 cycles, the impedance increased from 180Ω to 280Ω.

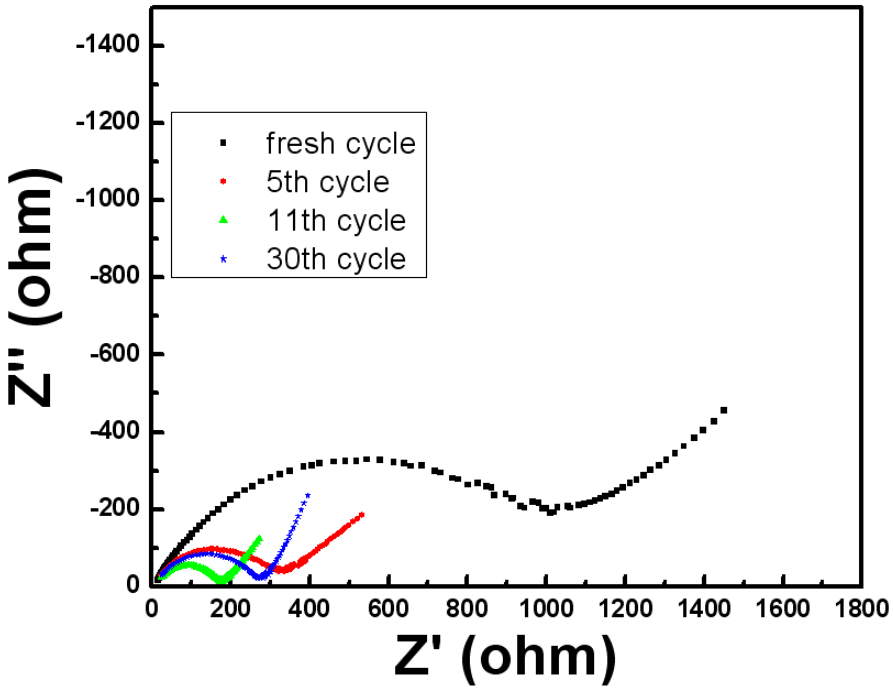

Fig. 36 EIS curves of $LiFePO_4$/C (1/2 EG)

An electrode process can be simply defined as the sum of a series of changes that occur on the electrode/liquid (electrolyte) interface. It generally has following steps: 1. Mass transfer in the liquid electrolyte phase. In this process, the reaction particles migrate in the liquid phase near the surface of electrode. 2. Electrochemical reaction process. In this process, the reactants have electrochemical reactions on the surface of electrodes or at the electrolyte/electrode interface. 3. The generation of new phase. In this process, the reactions will product new phase. The practical rate of the electrode process will be determined by the slowest step among above three steps.

In relation with lithiation process in $LiFePO_4$ during discharge: The first step is the transportation of Li ions in the electrolyte. The second step is charge transfer between lithium ion and electron together with lithium incorporation into the $LiFePO_4$ surface. The third step is Li ions diffusion or phase transformation into the solid electrode phase. The charging process is in principle the reverse process of lithiation process, i.e. delithiation process.

In this study, the electrode impedance changes at the different lithiation/delithiation stages were studies with the help of EIS. Figures 37 and 38 show the electrode impedance change during the charge-discharge processes.

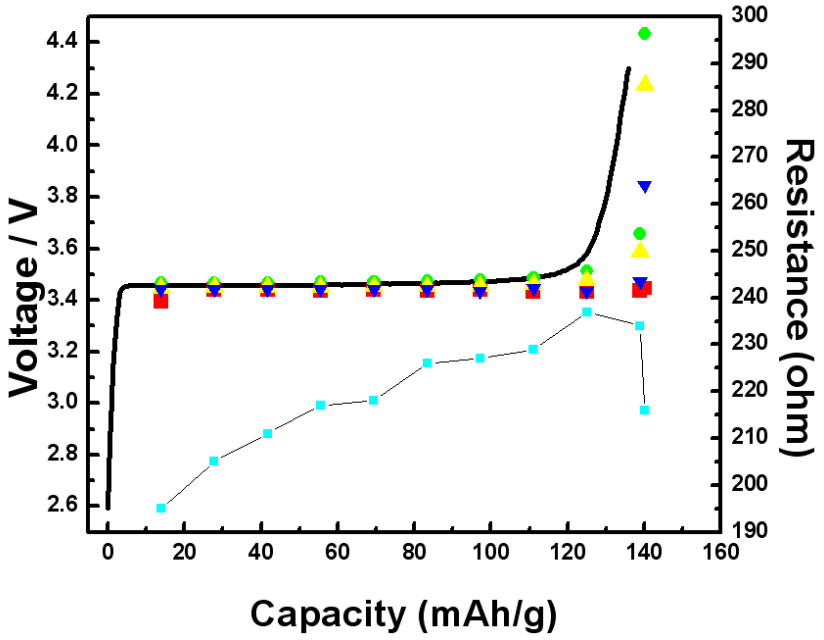

Fig. 37 Impedance change during the charge process for $LiFePO_4$/C (1/2 EG)

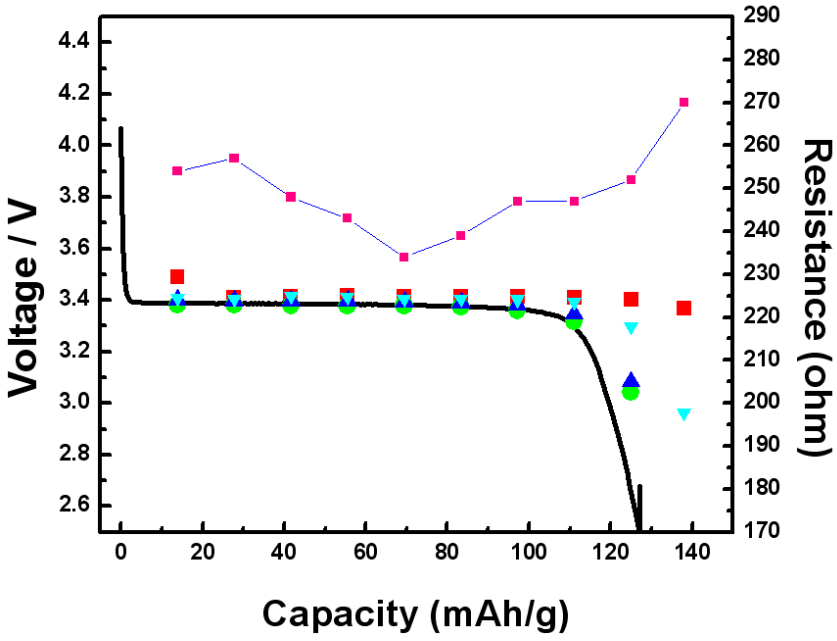

Fig. 38 Impedance change during the discharge process for $LiFePO_4$/C (1/2 EG)

The entire discharge process can be broadly divided into three stages. The first stage occurred in the early stage. The surface and shallow layer of particle contains a large number of Li ions, the mass transfer in the liquid phase is very fast and electrochemical reaction rate is relatively slow. So in this stage, the electrochemical reaction is the main controlling factor of the electrode process. When the Li ions on the surface or in shallow layer were being depleted, the Li ions needed for further reactions only can get from the deeper layer of the internal particles through diffusion. The intrinsic diffusion coefficient of Li ion is very low, $10^{-12}cm^2/S$ at room temperature. So, diffusion becomes the main controlling factor during this stage. And the intermediate stage between the above two stages is a hybrid control stage. It can be seen from the discharge curve of figure 34; the sample has very good kinetic properties. The entire discharge electrode reaction is mainly controlled by electrochemical controlling factor. Diffusion controlling factor just controlled a short period of time. Since the material has relative small particle size and uniform distribution, the diffusion length of the Li ions is relatively small so that the entire process is mainly controlled by the electrochemical controlling factors.

As can be seen in figure 38, the impedance is decrease in the initial electrochemical control stage. In the hybrid control stage, the impedance start to increase and in the end of the diffusion control stage the impedance is increased to the highest value of 270Ω. From the changes of the impedance, we can see the different stages of the discharge process more intuitively. It also shows the important influence of the activation on the kinetic properties of $LiFePO_4$.

The charging process shows in Figure 37 is just the opposite process of the discharge process. The impedance first increases, when the electrode behavior becomes electrochemical reaction control the impedance start to increase.

The electrochemical diffusion coefficient of Li ion D_{Li}, is a key parameter to characterize the kinetic performance of cathode materials for Li-ion batteries. It usually uses the following equation to define[78]: $D_{Li} = \pi f_T r^2/1.94$

Where f_T is the diffusion frequency of the electrode processes, r represents the average particle radius of the $LiFePO_4$ getting from the electron microscopy. The order of magnitudes of D_{Li} calculated by this equation at different charge-discharge rate is all ~$10^{-12}m^2/S$. But the value is smaller than the diffusion coefficient of Li ion in other cathode materials such as $LiMn_2O_4$ and $LiCoO_2$ (10^{-8}~$10^{-11}m^2/S$)[79]. The small value of D_{Li} also indicates that the electrochemical behavior of $LiFePO_4$ have a great relationship with the current density. In order to overcome the kinetic limitation at high current density, two methods are commonly used. One is to use relatively high operating temperature which can increase the D_{Li} value. The other one is by appropriate ion doping to replace Li sites to improve the ionic/electron conductivities of $LiFePO_4$.

5.5.2 CV analyses

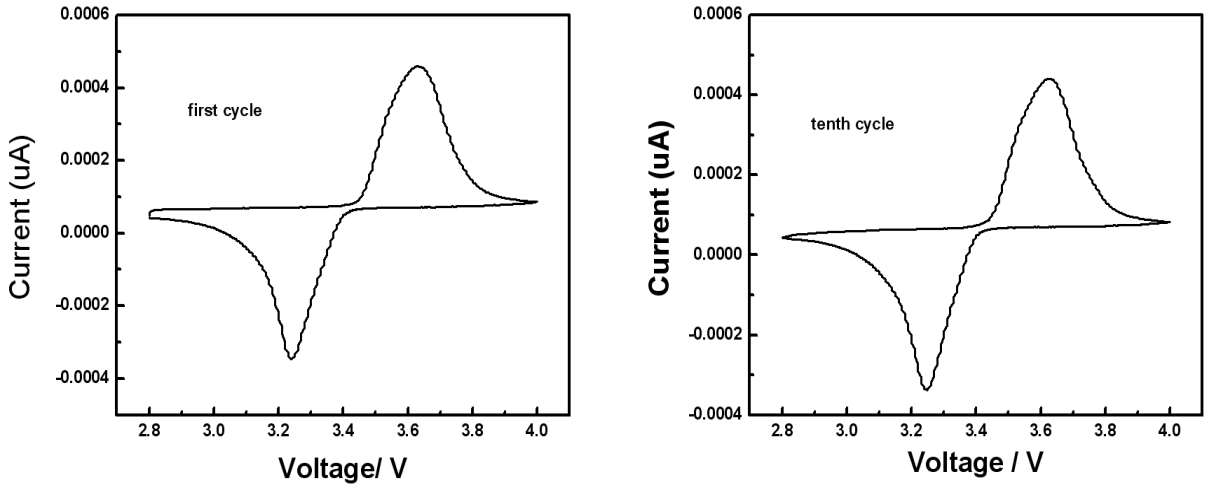

(a) (b)

Fig. 39 CV curves of $LiFePO_4$/C (1/2 EG): (a) first cycle (b) tenth cycle

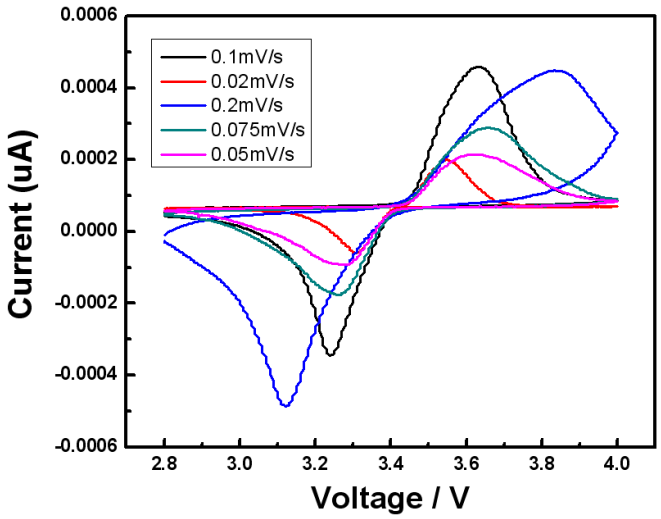

Fig. 40 CV curves of $LiFePO_4$/C (1/2 EG) at different scan rates (from inner to outer: 0.02, 0.05, 0.075, 0.1, 0.2mV/S)

Figure 39 show the CV curves of $LiFePO_4$/C (1/2 EG) sample at different cycles. The cell was cycled at 0.1mV/S scan rate. The area of the curve qualitatively refers to the charge and discharge capacity of battery. The upper half peak is the oxidation peak, corresponding to the charging process. The lower half peak is the reduction peak, corresponding to the discharging process. The voltage increase from 2.8V to 4.0V, the battery is in the charging status. Li ions delithate from the $LiFePO_4$ structure, part of the $LiFePO_4$ become $FePO_4$, the voltage corresponding to oxidation peak is 3.7V. The voltage scan back from 4.0V to 2.8V, the battery is in the discharging status. Li ions lithiate back into the $LiFePO_4$ structure, the voltage corresponding to reduction peak is 3.23V. The spacing between the oxidation peak and reduction peak reflects the polarization between the electrodes. The larger the spacing the higher the polarization, the deviation of the actual potential from the equilibrium potential will be larger. In opposite, the smaller the spacing the smaller the polarization, the deviation of the actual potential from the equilibrium potential will be smaller. From figure (a) we can see that the oxidation peak and reduction peak are similar in shape, and have good symmetry. The ratio of the oxidation peak and reduction peak is close to 1, which means this material has good lithiation/delithiation

reversible ability. After 10 cycles, the shapes of its oxidation peak and reduction peak barely changed. This indicates that the material has good cyclic reversibility.

Figure 40 is the CV curves of $LiFePO_4$ (1/2 EG) at different scan rates. It can be seen from the figure, the redox peak currents will increase with the increase of the scan rate. And the potential difference between the oxidation peak and reduction peak increase along with the increase of the scan rate too. Which means the polarization of this material becomes larger with the increase of scan rate. When increasing the scan rate, the polarization during the process of charge transfer will make the oxidation peak move to high potential, while reduction peak move to low potential.

Conclusions:

1. When using $FeCl_2.4H_2O$ as iron source and EG as complexing agent to synthesis the $LiFePO_4$. the samples have poor discharge capacities. The discharge capacities decrease with the increase of the EG content. The sample prepared with the EG/cations molar ratio of 1/2 sample has the highest discharge capacity of 76mAh/g.

2. When $FeC_2O_4.2H_2O$ was selected as the iron source, the electrode performances are much better than that prepared from $FeCl_2.4H_2O$. XRD analyses confirmed the pure olivine-strucutred LiFePO4 phase. SEM morphological images show the particles are in spherical shape and the particle size is less than 500nm. The dark-black colored product suggested that there is a thin amorphous carbon layer coated on the surface of the sample, which will be confirmed using TEM analysis. Samples synthesized $FeC_2O_4.2H_2O$ show the same tendency as $FeCl_2.4H_2O$ in terms of correlation with the EG content. The discharge capacity decreases with the increase of the EG content. The sample prepared with EG/cation molar ratio of 1/2 sample has the highest discharge capacity of 145mAh/g. The sample has a good kinetic property and cyclic reversibility. The high rate performance of this sample is even better than the commercial $LiFePO_4$. Samples synthesized both by $FeCl_2.4H_2O$ and $FeC_2O_4.2H_2O$ has the same tendency of discharge process. Which is the discharge capacity will decrease with the increase of the EG content.

3. When combined CA and EG with molar ratio of 1:1 was used as the complexing agent, the sample has a discharge capacity of 152mAh/g. It is unclear at the moment if the combination contributes to the high capacity. Since long-term ball milling process was applied to the gel before sintering, the ball milling process can reduce the particle size and block some partial agglomeration, thus will improve the discharge capacity. The sample has a good cyclic performance, after 150 times cycles, the capacity still maintains around 0.12mAh/g.

4. After varying the PH values of the precursor, it is found that the un-adjusted PH sample (PH=6.8) has the highest discharge capacity of 145mAh/g. The discharge capacity first increase with the increase of the PH value and reaches the maximum value at the PH=6.8. Continually increase the PH value to 8 the discharge capacity reduced.

5. The CV curves of the EG-based LiFePO4/C at different cycle numbers has barely changed, which means the sample has a good Li reversibility and cycle reversibility. The CV curves of the sample at different scan rates shows the polarization will increase with the increase of the scan rate.

Chapter 6 Understanding the complexing mechanism and impacts on the sol-gel precursors on the performances of $LiFePO_4$

From this research, it has been found that different chelating agents have significant impacts on the performances of $LiFePO_4$ when all the other experimental factors are controlled to the same conditions. In general, EG is better than CA. Combination of EG and CA is also better than single CA. On the other hand, researchers have submitted that different valence of iron sources plays an important impact on the electrochemical performances, carbon content and morphology of $LiFePO_4$ no matter what kinds of chelating agent is utilized. We hypothesized that other parameters such as PH value in the sol precursor will may vary the ferrous ions contents during the sol-gel preparation, although the starting raw material is ferric oxalate, which eventually affects the properties of the $LiFePO_4$. During the sol-gel processing, the iron ions react with the chelating agent and form complex compounds. There are three states in the whole process, i.e. sol → gel → sintered product. The particle size and uniformity of the sintered product LiFePO4 will determines its electrochemical performances. The sol was dispersed in the solution; it can keep good uniformity by continually stirring. The gel will be different when different iron sources and complexing agents exist in the sol precursor. So, the formation of the middle state-gel is very important, it will directly determine the properties of the sintered product. In this chapter, we intend to understand the possible sol-gel mechanism on the impacts of iron sources and complexing agents as well as iron valency state on the eventual product of $LiFePO_4$. Firstly, basic concepts about complxing reaction in coordination chemistry will be introduced. Secondly, the influence of using different iron sources and complexing agents on the properties of $LiFePO_4$ will be interpreted according to these coordination theories.

6.1. Complexing Reaction and Complexing Equilibrium

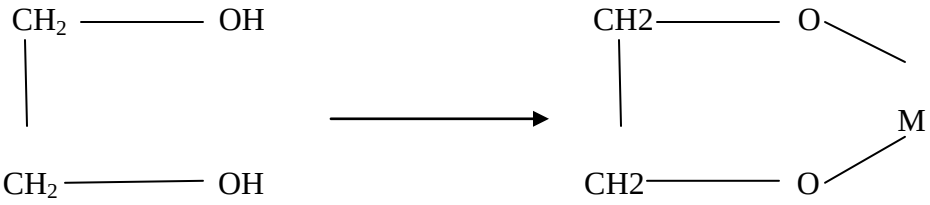

Fig. 41 Structure of the complex compound formed by EG

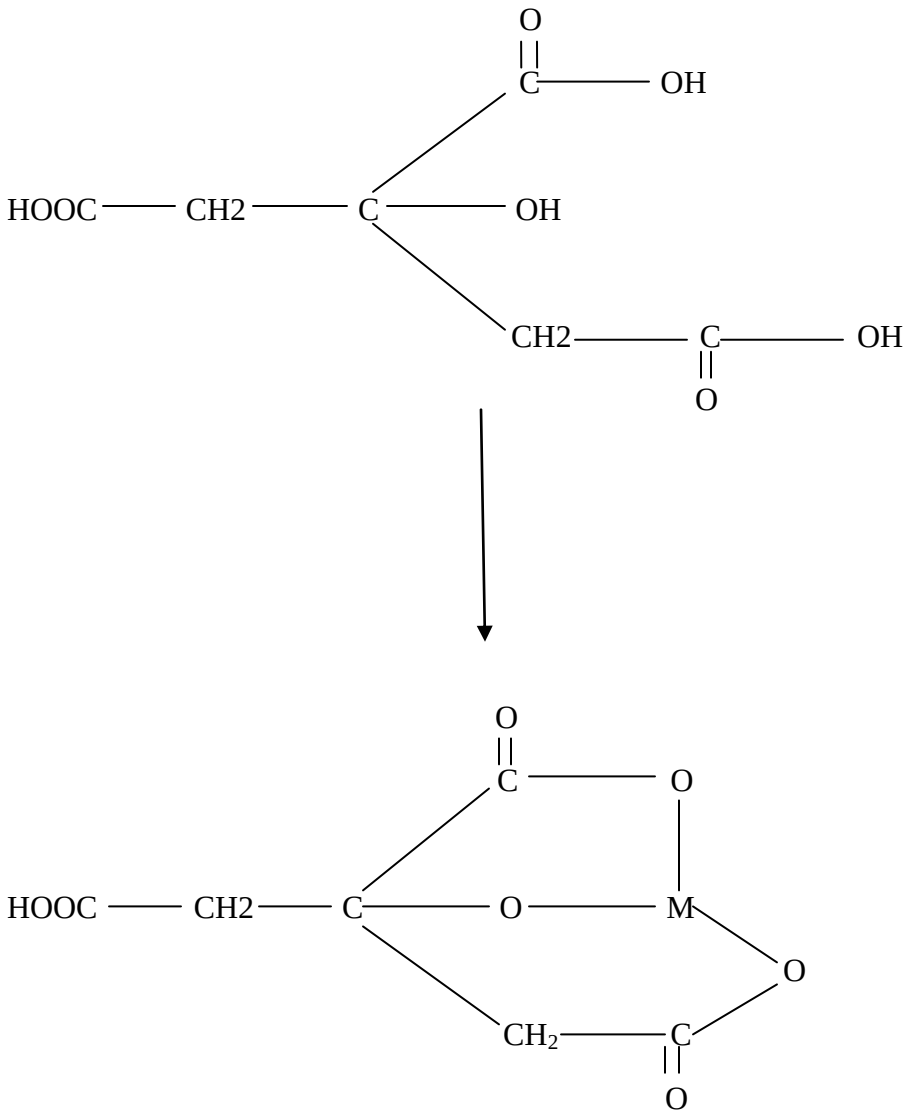

Fig. 42. Structure complex compound formed by CA

One metallic ion/atom can be combined with several same of different ions/molecules, which is collectively referred as complex group (or coordination ions) and the corresponding process is complex reaction. For example, $[Fe(CN)_6]^{4-}$, $[Co(NH_3)_6]^{3+}$ belong to coordination ions[80-81]. In the complex group, the metallic ion is surrounded by the coordination ligands. In most cases, the coordination ligands provide free electrons to share with the central ion, forming covalent bonds. The ligand contains only one coordination atom is known as monodentate ligand and the group is considered as simple ligand complexs. When the ligand contains 2 or more coordination like bezene rings, the groups is usually referred to as chelate complex.

Both EG and CA complexing agents, used in this study, act as simple complexing agents. When EG complexes with metal ion, it normally uses two adjacent hydroxyl oxygens as the coordination atoms and the coordination hydroxyl can be neutralized. The structure of the formation complex compound is shown in Figure 41. CA is a ternary hydroxyl carboxylic acid, the structure of the chelat compound formed by its acid radical and the metal ions may like the figure shown in Fig. 42.

When the reaction rate of formation of the complex equals to the dissociation reaction rate, the complex reaction reaches equilibrium. There are various complex equilibrium constants in correlation with the detailed reaction processes., where M represents metal ion, L represents complexing ligand:

(1) The stability constant of complex compound

For simple one step complexing reaction,

$$M + L \Leftrightarrow ML \qquad K_{ML} = \frac{[ML]}{[M]\times[L]}$$

where M represents metal ion, L represents complexing ligand. [M], [L] and [ML] are the concentration of metal ion, complex agent and complex compound respectively. Then K_{ML} is the equilibrium constant of the complex compound determined by the concentration of each item.

For some ML_n type complex compounds, their formation and dissociation in the solution are step by step. They present a series of equilibriums in the solution, and have corresponding equilibrium constant for each level.

$M + L \Leftrightarrow ML$ $\quad$ 1^{st} order $K_1 = \frac{[ML]}{[M]\times[L]}$

$ML + L \Leftrightarrow ML_2$ $\quad$ 2^{nd} order $K_2 = \frac{[ML_2]}{[ML]\times[L]}$

…….

$ML_{n-1} + L \Leftrightarrow ML_n$ $\quad$ n^{th} order $K_n = \frac{[ML_n]}{[ML_{n-1}]\times[L]}$

The cumulative equilibrium constant, $\beta_{i.,}$ is the product of the stepwise value. The n^{th} order of cumulative stability constant also known as the total stability constant.

1^{st} order: $\beta_1=K_1$, $\log \beta_1= \log K_1$

2^{nd} order: $\beta_2=K_1K_2$ $\log \beta_2 =\log K_1+\log K_2$

……..

n^{th} order: $\beta_n=K_1K_2\cdots\cdots K_n$ $\log \beta_n= \log K_1+\log K_2+\cdots\cdots+\log K_n$

It is well known that the larger the complex equilibrium constant, the more stable the complex compound. Therefore, the complex equilibrium constant directly correlates with the stability of the complex, which depends mainly on the natures of the central ion and ligand. The relationships between the stability of complex compound and the central ion as well as ligand are[82]:

Rule 1: The transition metal ions are more easily to form ligand than the main group metal ions. In the main group, alkali metal ions are the weakest;

Rule 2: The same metal ion in two oxidation states with the same ligand to form two complex compounds with the same coordination number, usually the high valance metal ions will form higher stability complex compound;

Rule 3: The ligand is as an electron donor has reaction with metal ions and form complex compounds. So the stronger the alkality it has, the more stable the complex compound.

Rule 4: The stability of the chelate usually higher than the non-chelate with similar composition and structure

Rule 5: The chelat with five-membered ring or six-membered ring is very stable.

Rule 6: The more the rings chelate has, the more it will stable.

Table 17 lists, from reference, the cumulative equilibrium constant values of some common complex agents and the two different valency ions. It can be seen from the table the stability of complex compounds formed from Fe^{2+} are all small than it formed from Fe^{3+} with the same complex agent. Moreover, it also can be seen the complex agents such as citric acid and EDTA they form five or six-membered rings during the complex process, so the corresponding

stability constants of the formed complex compounds are all relatively larger. In comparison, the stability constants of the complex compounds formed from oxalic acid or COOH group acid are relatively smaller.

Table 17 The cumulative stability constants between some common complex agents and Fe^{2+} and Fe^{3+}

Complex agent		$Log\beta_1$	$Log\beta_2$	$Log\beta_3$	$Log\beta_4$
Citric acid	Fe^{2+}	15.5			
	Fe^{3+}	25			
Hydroxyl Group/COOH	Fe^{2+}	5.56	9.77	9.67	8.58
	Fe^{3+}	11.87	21.17	29.67	
Oxalic acid	Fe^{2+}	2.9	4.52	5.22	
	Fe^{3+}	9.4	16.2	20.2	
EDTA	Fe^{2+}	14.33			
	Fe^{3+}	24.23			
Ethylene glycol	Fe^{2+}	9.67			
	Fe^{3+}	29.67			

6.2 Understanding the influences of iron sources and complex agents on products of $LiFePO_4$

Apparently, the types of central ion (metal ion) and complex agent (ligand) have decisive influences on the stability of the formed complex compounds. Different metal ions react with different complexing agents will form the complex compounds with different stabilities. In the

following we will discuss the relationship between the stability of the complex compounds formed by sol-gel preparation and the performances of the final sintered $LiFePO_4$.

During the sol-gel preparation $LiFePO_4$ process, complex agent will have complex reaction with the Li ions and iron ions. According to Rule 1, the complex ability between iron ions and complex agents is stronger. Therefore, the iron source is important than the Li source during sol-gel formation. Based on Rule 2: the stability of complex compound formed by Fe^{3+} is higher than it formed by Fe^{2+} when they use the same complex agent. Based on rule 3 and 4, CA which has high alkalinity and formaing higher number of chelate than oxalic group (from precursor) and EG, the complex compound is stronger.

Additionally, citric acid is a ternary acid, has three carboxyl functional groups. The complex compounds formed from citric acid have two types: three ligands L^{3-} and two ligands HL^{2-}. Table 18 shows the stability constants of the complex compounds formed from citric acid with Fe^{2+} or Fe^{3+} ion. It can be seen from the table, the iron ions with three ligands L^{3-} from CA is more stable. Therefore, in the following discussion we consider CA uses three ligands to proceed complex reaction with iron ions. I contrast, EG is dihydric alcohol. Hence EG use the two hydroxyl groups to coordinate with the metal ions.

Table 18 Stability constants of complex compounds formed from citric acid with Fe^{2+} or Fe^{3+} ions

Complex agent		$Log\beta_1$
Citric acid (L^{3-} ligands)	Fe^{2+}	15.5
	Fe^{3+}	25
Citric acid (HL^{2-} ligands)	Fe^{2+}	3.08
	Fe^{3+}	12.5

Table 19 Comparison of discharge capacity as well as carbon content in LiFePO4 product and stability of the different complex compounds

Complex agent		Discharge capacity(mAh/g)	Carbon content (wt.%)	Logβ
Citric acid (L^{3-} ligand)	Fe^{2+}	120	6.0	15.5
	Fe^{3+}	95	10.1	25
Ethylene glycol	Fe^{2+}	145	3.3	9.67
	Fe^{3+}	75	6.4	29.67

In terms of performances, here we focus on the standard discharge capacity at 0.2C rate (Dc) obtained from this study as well as and the carbon content (Cc) obtained from literatures[83]. Table 19 listed theses results in comparison with the stability constants of the complex compounds formed from Fe^{2+} or Fe^{3+} with CA and EG respectively.

From Table 19, the following trend is observed:

$$\beta(Fe^{2+}, EG) < \beta(Fe^{2+}, CA) < \beta(Fe^{3+}, CA) < \beta(Fe^{3+}, EG)$$

$$Dc(Fe^{2+}, EG) > Dc(Fe^{2+}, CA) > Dc(Fe^{3+}, CA) > Dc(Fe^{3+}, EG)$$

$$Cc(Fe^{2+}, EG) < Cc(Fe^{2+}, CA) < Cc(Fe^{3+}, EG) < Cc(Fe^{3+}, CA)$$

It is interesting to note the consistant trend among the capacity, carbon content and complex stability. The capacities of $LiFePO_4$ sintered from the above 4 complex compounds are inversely proportional to the stability constants of their corresponding complex compounds. While the carbon content and the stability constants of the complex compounds are corroborative. This relationship indicates that the smaller the complex constant the complex compounds will be beneficial to achieve better electrochemical performances $LiFePO_4$.

According to the theory of coordination of chemistry, the larger the complex constant the more stable the complex product. Therefore, the complex compounds will more difficult be decomposed during the sintering process, so the proportion of the carbon retained in the final phase is greater. The formed phase can be largely retained in the presence of multiple interwoven ring structure, so the crystallinity will be relatively poor, resulting in sintered product $LiFePO_4$ with low discharge capacities. While the complex compound with small complex constant is less stable itself, it's relatively easy to be decomposed at the same sintering condition. As a result, a large part of the carbon contained in the complex agent will be released in the form of CO_2 during the sintering process. The carbon content left in the main phase will be relatively low. Small amounts of carbon still can play the function of improving the electrical conductivity of the composite phase, at the same time it won't have too much impact on the volume energy density of active substances. On the other hand, the formed main phase of $LiFePO_4$ mostly exists in the form of small particles resulting from the smaller gel accumulation. The small particle size will help to reduce the diffusion path of Li ions in the active substance, conduce to improve the discharge ability of materials. Small amounts of carbon still can play the function of improving the electrical conductivity of the composite phase, at the same time it won't have too much impact on the volume energy density of active substances.

Compared to Fe^{3+}, the complex compounds formed from Fe^{2+} will have lower stability, resulting in the main phase of the sintered $LiFePO_4$ will have good crystallinity. The materials are in the form of particles, contain less carbon and have good electrochemical performance.

For the choice of the same precursor (the same metal ion), the different complex agents will have a great impact on the performance of the prepared $LiFePO_4$. From the previous summarize can be seen that select the complex agent with low complex constant, the formed

complex compounds with the metal ions will have low stability because of the simple structure (simple ring or no ring). The complex compounds are easy to be decomposed during the sintering process, conducive to obtain the materials with good discharge abilities. In the condition of using the same metal ions, the stability of the complex compounds formed from EG is lower than that formed from CA, and the synthesized LiFePO4 by former have better performances. And this conclusion is consistent with the real experiments (chapter 4). This indicates that the $LiFePO_4$ will have different discharge abilities under the same conditions with different complex agents.

Concluding Remarks

The theory of complex equilibrium determines that the larger the complex constant, the more stable the complex compounds. There are well established rules to correlated with the properties cations and ligands with the stabilities of the formed complex compounds.

When metal ions in two oxidation states are coordinated with the same kind of ligand, in general, the coordination complex formed by the higher valence metal ion has higher stability. The complex compounds formed by Fe^{2+} and complex agents have small stability constants compared with Fe^{3+}. Therefore, Fe^{2+}-containing complex is easily decomposed during sintering process. Consequently, the formed $LiFePO_4$ exists in the form of small particles, contains less carbon content originated from the ligand, and hence, exhibit good discharge ability. In consideration of the complex agents, stability constants of the complex compounds formed by EG or CA are different under the condition of using the same metal ion. The complex compounds formed by EG have small stability relative to CA. Similarly, the gel complex is decomposed faster during sintering process leading to less carbon content and high discharge ability. Therefore, two suggestions are proposed, based on the study and discussion through out this master thesis research, in the aspects f selecting iron sources and complex agents for the sol-gel preparation of $LiFePO_4$:

(1) For the iron source: select salt composed of Fe^{2+} as much as possible, such as $FeC_2O_4.H_2O$, $Fe(CH_3COO)_2$ etc.

(2) For the complex agents: select the complex agents contain less number of carbon atoms with small molecules. The formed complex compounds will have small stability constants, such as ethylene glycol, oxalic acid etc.

The selection of precursors and complex agents also have some reference values for the preparation of the $LiMPO_4$ (M=Mn, Ni, Co etc.) series of cathode materials, or other cathode and nano-functinoal materials.

Chapter 7 Conclusions and Future Work

This research, on the basis of a comprehensive review of the researches on various synthesis approaches and intrinsic properties of the state-of-the-art lithium-ion battery cathode – olivine-structured $LiFePO_4$, is directed to investigate key processing factors in sol-gel synthesis of $LiFePO_4$/C nanocomposite and their impacts on the structure and electrochemical performances. Studies are focused on the key factors including sintering temperatures, different Li contents, iron sources, different complexing agents, PH values on the structure and electrochemical performances of $LiFePO_4$. The results can be summarized as the following:

1. Gel Evaluation with increasing temperatures. When $FeC_2O_4.2H_2O$, $LiOH.H_2O$, H_3PO_4 are used raw materials and citric acid (CA) or ethyl glycol (EG) as complexing agent, the gel experiences three stages upon increasing temperature. (1) As the temperature is increased to around 250^{o}C, the dramatic mass loss, up to 50% is mainly due to the evaporation of moisture in the gel as well as the decomposition of organic matters in the gel; (2) in the temperature range of 250-450^{o}C, the mass loss continues but much less significantly, which is associated with the decomposition of remaining organic matters in the gel; (3) above 500^{o}C, the mass of the reactants have maintain at 44.5% of the initial mass, suggesting that no more mass loss occurs and the powders start to crystallize.

2. Sintering temperatures. The specimen sintered at 500^{o}C just started to crystallize but with major amorphous components. Only a very small amount of olivine-structured $LiFePO_4$ is formed. When the sintering temperature increased to 600^{o}C, the amount of olivine-structure $LiFePO_4$ increased significantly, although there are still some peaks corresponding to the impurities. Further increasing the temperatures results in the reduction of the impurities. However, at sintering temperature of 800^{o}C, another phase of impurity was created. It is

concluded the optimal sintering temperature is around 700^{o}C with the most desired olivine-structured $LiFePO_4$ and least impurities.

Consequently, the 500^{o}C sample barely has discharge capacity. The discharge capacities increase with the increase of the sintering temperature and reach the highest value of 127mAh/g at 700^{o}C. As the sintering temperature is continuously increased to 800^{o}C, the discharge capacity decreases to 74mAh/g. The electrochemical results corroborated well with the crystal structure analyses. Therefore, the optimal sintering temperature is determined around 700^{o}C.

3. The amount of lithium. When using lithium salts to synthesize cathode materials for Li-ion batteries, it is constantly observed the mass loss of lithium during the high temperature sintering step. Therefore, excessive lithium sources need to be added in the precursor to reach the stoichiometric LiFePO4 product. Using $LiOH.H_2O$, $FeC_2O_4.2H_2O$, H_3PO_4 and citric acid in the raw materials, electrochemical capacity is also correlated with the amount of lithium source added in the precursor. As the lithium source increase from 100% to 130%, the discharge capacity increases from 127mAh/g to 136mAh/g and then decreases to 125mAh/g. The lithium sources with excessive 25 mol% provides the best electrochemical performance.

4. The amount of complexing agent. During the sol-gel process, metal ions form complexes with the citric acid and eventually evenly distribute in the gel solid. The particle size and size distribution of products after sintering are directly relevant to the formation of complex gel. In addition, the citric acid is the source of carbon. As the carbon content of samples increase, the active material may decrease; result in the reduction of discharge capacity. The agglomeration of the particles also increase with content of the citric acid, leading to the blockage of the diffusion

channel of the Li ions, reduce the Li^+ diffusion rate, reduces the electrochemical performance of $LiFePO_4$.

The experimental results confirmed that the amount of citric acid affects the electrochemical different contents. The sample synthesized with less citric acid shows high discharge capacity. For instance, the sample prepared with citric acid to cation molar ration of 1/4 has higher discharge capacity (141mAh/g) than the one prepared CA/cation ratio of 1/2 whose capacity is 136mAh/g. The large, uneven distribution of the particle size and more carbon content may cause the slight reduction of the discharge capacity.

Similarly, the sample prepared with EG/cation molar ratio of 1/2 has the highest discharge capacity of 145mAh/g, which is 10% more than the specimen synthesized from citric acid complexing agent. When the EG/cation ratio change to 1/1, 3/2 and 2/1, the discharge capacities continuously decreased to 140mAh/g, 133mAh/g, and 116mAh/g, respectively.

5. Different iron sources. In this research, two different iron sources, i.e. $FeCl_2.4H_2O$ and $FeC_2O_4.2H_2O$, are compared when all other processing parameters are fixed. In this study $NH_4H_2PO_4$ is the source of phosphate ions and EG as complexing agent. All the samples from $FeCl_2.4H_2O$ with different EG contents have very poor discharge capacities. The sample prepared with the optimal EG/cation molar ratio of 1/2 has the relatively highest discharge capacity of 76mAh/g. The discharge capacities decrease with the increase of the EG content.

6. Different PH values. PH value of sol-gel solution affects two main reactions of the sol-gel process: hydrolysis reaction and polymerization reaction, thereby affecting the complexation between cations and ethylene glycol. The adjustment of PH value will change the complexation conditions between cations and complexing agent. Appropriate PH value of the sol solution is

beneficial to obtain uniform distribution of metal cations in organic substances and helpful to obtain $LiFePO_4$ powders with uniformly small size and well dispersed particles, in order to improve the material's electrochemical performance.

In this study, dilute hydrochloric acid (HCl) or ammonia solution was used to adjust the PH values to 0, 2, 4, 6 and 8. It observed that the discharge capacities increase as the increase of the PH value below PH of 7. At the PH value of 6.8, the sample gets the relative highest discharge capacity of 145mAh/g. As the PH value continually increased to the basic region with a PH value of 8, the discharge capacity reduced to 82mAh/g.

7. Different complexing agents. With the same molar ratio of complexing agent to total cations, the samples prepared using EG has a capacity of 145mAh/g, which is 10% more than the specimen synthesized from citric acid complexing agent (127mAh/g). The results indicate EG is a better complexing agent then CA.

XRD analyses show the product prepared from EG has insignificant impurity. The particles are uniform, spherical with an average size less than 500 nm. In addition to the improved discharge capacity, the sample showed excellent rate capability with only 5% reduction when the discharge rate was increased from 0.2C to 2C, much better than one commercial product. The better rate capability may be attributed to the higher content of carbon, which increases the electronic conductivity and reduces the particle agglomeration.

Using combined CA/EG mixture with a molar ratio of 1:1, together with a long-term ball milling process of the gel before sintering, the final product shows a capacity of 152mA/g. At the moment, it is unconcluded if the combined CA/EG complexing works better than EG. The ball milling process can reduce the particle size and block some partial agglomeration, thus

improving the discharge capacity. The sample has a good cyclic performance, after 150 times cycles, the capacity still maintains above 75% of its initial value. The good cycle performance is due to the carbon coating on the $LiFePO_4$ surface and its stable structure.

8. Within this research scope, the optimal condition is determined to be: 1) good raw materials are LiOH as lithium source, $FeC_2O_4.2H_2O$ as iron source, $NH_4H_2PO_4$ as the source of phosphate ions, and EG as complexing agent; 2) excessive lithium may be necessary to compensate the evaporation loss during the sintering process; 3) sintering temperature is around 700^oC the sintering environment is 5 vol. $\%H_2 + N_2$ reducing/inert atmosphere; 4) ball-milling the dried gel before sintering process may be beneficial to achieve high reversible capacity.

9. The influences of complexing agents and iron sources on the sol-gel preparation of $LiFePO_4$ can be interpreted based on the principle of complexing reaction and complexing equilibrium in the coordination chemistry. When the complex compounds formed by Fe^{2+} and complex agents having small stability constants, the gel is easily decomposed during sintering process, resulting in the product with small particles and less carbon content. Therefore, high capacity is achieved. This is the case when EG is used as the complexing agent.

Accordingly, CA and Fe^{3+} sources are unfavorable for their large stability constants, which will eventually produce large particles. When CA is used as the complexing agent, the gel may exist in the form of cross-linked network, rendering high carbon content and low capacity.

As a cathode material for Lithium-ion batteries, $LiFePO_4$ shows relative high capacities, good cyclic performance and rate performances. The iron source and complex agents are closely related to the electrochemical performance of the synthesized $LiFePO_4$, establish a certain contact through the coordination chemistry theory. However, there are many work needed to be

expanded. On the basis of the studies in the thesis, the following research may be worth to explore in depth in the near future:

***1. Choice of suitable complexing agent and precursor materials*.** It has been concluded that the Fe^{2+} iron source and complexing agents with small stability constant are better choices based on the coordination chemistry theory. While lithium source and phosphorus source selection work can also be started and fundamental coordination chemistry may be studied. Meanwhile, the impact of the anion group in iron sources is yet unclear. Relationship between the complex stability of the complexing agents and the carbon content is worth to quantify, providing the guidance of the carbon content influence on the electrochemical capacity, cycle life, and rate capability. Ultimately, optimal electrochemical performances of $LiFePO_4$ can be achieved.

2. Further refinement the particle size of the $LiFePO_4$. In addition, appropriate surfactant can be added in the sol-gel synthesis process. Surfactants are compounds that can lower the surface tension of a liquid, the interfacial tension between two liquids, or that between a liquid and solid. It is normally used to synthesize nano powder materials[84]. In the solution, the surfactant can encapsulate the colloid particles and form a polymer protectively layer on the surface of colloid particles, play a role in spatial steric effect, inhibit the growth of particles and thus reduce the agglomeration. Therefore, with the help of surfactant the $LiFePO_4$ will have smaller particle size and better distribution of the particles. The uniformly distributed particles will improve the utilization of the $LiFePO_4$ thus increase the electrochemical performance.

3. Combination of other methods that can improve the electrode performances. Side et al[85]. used Sol-Gel template method synthesized LiFePO4/C material and achieved an outstanding discharge capacity of 165mAh/g at 3C rate. The superior electrochemical

performance was ascribed to the unique nano-fiber morphology of $LiFePO_4$, which greatly reduce diffusion path of the Lithium ions. In the meantime, the carbon coating overcomes the low intrinsic conductivity of $LiFePO_4$. It is suggested to develop sol-gel approach combined with some advanced technology.

4. Combination of the microscopic mathematical model with the macrostructure model. The present development in $LiFePO_4$ encounters a certain bottleneck. The poor discharge capacity at large current density hinders its prospect for industrial applications. In order to achieve a breakthrough, not only the experiments but the theoretical prediction is as also needed. The micro-theory and macro-model simulation can not only save experiment time, provide improvement measures for experiments, but also can verify the assumptions base on the experiments[86].

The first principle theory is widely used in Lithium-ion battery materials. The theoretical calculation can show the lattice parameters of the electrode material, the average potential, discharge curves, phase stability, the diffusion properties of Li-ions and so on. So far, there are many researchers used the first principle theory studied the LiFePO4 and its related materials[87-88]. The studies show that they consider $LiFePO_4$ as semiconductor or semimetal, and the Lithium ions are in the form of one-dimensional diffuse in the $LiFePO_4$ structure. If can combine the quantum chemistry calculation with the mathematical models, start from both the micro macro perspectives, use the results to guide the experiments. This may be a desirable method for the final settlement of the problem of the poor intrinsic conductivity of $LiFePO_4$, which is also applicable for the improvement the electrochemical performances of other electrode materials for Lithium-ion batteries.

References

[1] Nazri, holam-Abbas, and ianfranco Pistoia. Lithium Batteries, Science And Technology. New York, N.Y.: Springer Verlag, 2009. 1-708.

[2] Yoshio, asaki, R. J. Brodd, and Akiya Kozawa. Lithium-ion Batteries, Science And Technologies. New York ; London : Springer Verlag, 2009. 1-452. Print.

[3] M. Winter, and Brodd R.J. "what are batteries, fuel cells,and supercapacitors? ." Chemical Reviews. 104.10 (2004): 4245-4269.

[4] K Mizushima, P.C. Jones, P.J. Wiseman, and J.B. Goodenough. "LixCoO2 (0<x<-1): anew cathode material for batteries of high energy density." Mater. Res. Bull.,1980, 15(6): 783-789

[5] Wakihara M., Yamamoto O. Lithium ion batteries fundamentals and performance. Tokyo: Kodansha Ltd., 1998:1-125

[6] Thackeray, M.M., "structural considerations of layered and spinel lithiated oxides for lithium ion battery." [J].J. Eletrochem. Soc. 142.8 (1995): 2558-2563

[7] Ohzuku, T., M. Kitagawa, and T. Hiral. "Electrochemistry of manganese dioxide in lithium nonaqueous cell." [J].J. Eletrochem. Soc.. 137.3 (1990): 769-775

[8] Yamada, A., M. Hosoya, and S C, Chung. "Olivine-type cathodes Achievements and problems."[J].J.Pow Sources.. 119 (2003): 232-238

[9] Takeuchi, E.S., H. Gan, M. Palazzo., et al. "Anode passivation and electrolyte solvent disproportionation:mechanism of ester exchange reaction in lithium-ion batteries." [J].J. Eletrochem. Soc.. 144.6 (1997): 1944-1948

[10] Smart, M.C., B.V. Ratnakumar, S. Surampudi, et al. "Irreversible capacities of graphite in low temperature electrolytes for lithium-ion batteries." [J].J. Eletrochem. Soc.. 146.11 (1999): 3963-3969

[11] Murphy, D.W., Broadhead J.and Steele B.C.H. "Materials for advanced batteries." [M].New York : Plenum Press, 1980:145

[12] A. Deb, U. bergmann, S.P. Cramer, et al. "structural investigations of LiFePO4 electrodes and in situ studies by Fe-ray absorption spectroscopy."[J]. Electrochem. Acta,. 50 (2005): 5200-5207

[13] Whittingham, M S. "lithium batteries and cathode material." Chem. Rev.. 104 (2004): 4271-4301

[14] P, Arora, RE White, and M. Doyle. "Capacity fade mechanisms and side reactions in Lithium-ion batteries." [J].J. Eletrochem. Soc.. 145.10 (1998): 3647-3667

[15] AG, Ritchie, Giwa Co, Lee JC, et al. "Future cathode materials for lithium rechargeable batteries." J Power Sources. 80.1 (1999): 98-102.

[16] D, Larcher. "Electrochemical active LiCoO2 and LiNiO2 mabe bycationic exchange under hydrothermal conditions ." J Electrochem Soc. 144.2 (1997): 408-417

[17] M, Broussely, Biensan p, and Simon B. "Lithium insertion into best materials: the key to success for Li ion batteries." Electrochhimica Acta. 45. (1999): 7-12.

[18] N, kunagai, Fukiwara T, and Tamno K. "Physical and electrochemical characterization of Li-Mn-V-O spinel as as positive materials for rechargeable lithium betteries ." J Electrochem Soc. 142.3 (1996): 1007-1013.

[19] M, Wakihara. "Recent developments in lithium ion batteries." J Materials Science and engineering. R33. (2001): 109-134.

[20] H, Kawai, nagata M, Kageyama M, et al. "5V lithium cathodes based on spinel solid solutions Li2Co1+xMn3-xO8(-1<x<1)." Electrochhimica Acta. 45.1-2 (1999): 315-327.

[21] X, Wu. "Improvement of electrochemical properties of LiNi0.5Co1.5O2 spinel." J Power Sources. 109. (2000): 53-57.

[22] B J, hwang. "Effect of Al substitution on the stability of LiMn2O4 spinel synthesized by citric acid sol-gel method." J Power Sources. 102. (2001): 326-331.

[23] A K, Padhi, nanjundaswamy K S, and Goodenough J B . "Phospho-olivines as positive-electrode materials for rechargeable lithium batteries." J Electrochem Soc. 144.4 (1997): 1188-1194.

[24] A K, Padhi, nanjundaswamy K S, and Goodenough J B . "structure on the Fe3 /Fe2 redox couple in iron phosphates." J Electrochem Soc. 45.5 (1997): 1609-1613.

[25] K S, Nanjundaswamy, Padhi A K, Goodenough J B , et al. "Synthesis, redox potential evaluation and electrochemical characteristics of NASICON-related-3D framework compounds." J Solid State Ionics. 92.1-2 (1996): 1-10.

[26] C Y , Ouyang, Wang D Y, et al. "First principles study on NaxLi1-xFePO4 as cathode material for rechargeable lithium battereis ." J Chiese Phys. Lett. 23.1 (2006): 61-64.

[27] Ni, J F , H Zhou, J T Chen, et al. "LiFePO4 doped with ions prepared by co-precipitation method." J Mater. Lett. 59.28 (2005): 2361-2365.

[28] A S , Andersson, and Thomas J O. "The source of first-cycle capacity loss in LiFePO4." J Power Sources." 97-98. (2001): 498-502

[29] M, Takahashi, Tobishima S, Takei K, et al. "Characterization of LiFePO4 as the cathode material for rechargeable lithium batteries." J Power Sources. 98.1 (2001): 508-501.

[30] A, Deb, Bergman U, E J Cairns, and S P cramer. "Structural investigations of LiFePO4 electrodes by Fe X-ray absorption spectroscopy." J Physical Chemistry B. 180.22 (2004): 7046-7049.

[31] H S. Kim, Cho B W , et al. "cycling performance of LiFePO4 cathode material for lithium secondary battereis." J Power Sources. 132.1-2 (2004): 235-239.

[32] A S Andersson, Thomas J O, kalska B, et al. "Thermal stability of LiFePo4-based cathodes ."Electrochem Solid-state Lett. 3.2 (2000): 66-68.

[33] A, Yamada, Hosoya M, Chung S C , et al. "olivine-type cathodes achievements and problems." J Power Sources. 119.1 (2003): 232-238.

[34] D, Morgan, Van der Ven A, and Ceder G. "Li conductivity in LixFePO4(M=Mn,Fe,Co,Ni) olivine materials."Electrochem Solid-state Lett. 7.2 (2004): A30-A32

[35] J M, tarcsscpm, and Armand M. "Issues and challenges facing rechargeable lithium battereis." Nature. 414.6861 (2001): 359-367.

[36] M, Takahashi, Tobishima S, and Takei K. "Reaction behavior of LiFePO4 as a cathode material for rechargeable lithium batteries." Solide state ionics . 148.3-4 (2002): 283-289.

[37] F, Croce, Epifanio A D, hassoun J, et al. "A novel concept for the synthesis of an improved LiFePO4 lithium battery cathode ." Electrochem Solid-state Lett. 5.3 (2002): A47-A50.

[38] Chuang, S.Y., J.T. Bloking, and Y.M. Chiang. "Electronically conductive phospho-olivines as lithium storage electrodes.." *Nature Materials*. 1.2 (2002): 123-128.

[39] S, Shi, Liu l, ouyang C, et al. "Enhancement of electronic conductivity of LiFePO4 by Cr doping and its identification by first-principles calculations." J Phys.Rev.B. 68. (2003): 195108.

[40] P S .Herle, Ellis B W , Coombs N, et al. "Nano-network electronic conduction in iron and nickel olivine phosphates ." J Nat. Mater.3. (2004): 147-152.

[41] Y B , Xu, Lu Y J, Yan L, and Yang RD . "synthesis and effect of forming Fe2P phase on the physics and electrochemical properties of LiFePO4/C materials." J Power Sources. 160.1 (2006): 570-576.

[42] C W, Kim, Park J S, and Lee K S. "Effect of Fe2P on the electron conductivity and electorchemical performance of LiFePO4 synthesized by mechanical alloying using Fe3 raw material." J Power Sources. 163.1 (2006): 144-150.

[43] Y H, Rho, Nazar L F, Perry L, and Ryan D. "Surface chemistry of LiFePO4 studied by mossabur and x-ray photoelectron spectroscopy and its effect on electrochemical properties." J Electrochem Soc. 154.4 (2007): A283-A289.

[44] J, Molenda, Ojczyk W, Liu R S , et al. "Diffusional mechanism of deintercalation in LiFe1-yMnyPO4 cathode material." Solide state ionics . 177.26-32 (2006): 2617-2624.

[45] J, Molenda. "Electronic limitations of lithium diffusibility rom layered and spinel toward novel olivine type cathode materials ." Solide state ionics . 176. (2005): 1687-1694.

[46] M S, Whittingham, Song Y N , Zavalij N A, et al. "Some transition metal (oxy)phosphates and vanadium oxides for lithium battereis." J materials Chemistry. 15.33 (2005): 3362-3379.

[46] N, Ravet, Goodenough J B, Hovington P, et al.electrochemical Society of Japan Meeting Abstract. 99.2 (1999): abstract 127.

[47] N, Ravet, Chouinard Y, Armand M, et al. "Electroactivity of natural and synthetic triphylite ." J Power Sources. 97.8 (2001): 503-507

[48] M, Gaberscek, Dominko R, and Jamnik J. "Is small particle size more important than carbon coating? An example study on LiFePO4 cathodes ."Electrochemistry Communications. 9.12 (2007): 2778-2783.

[49] M M, Doeff, Wilcox J D, Kostecki R, and Lau G. "optimization of carbon coating on LiFePO4." J Power Sources. 163.1 (2006): 180-184.

[50] Y G, Xia, Yoshio M, and Noguchi H. "Improved electrochemical performance of LiFePO4 by increasing its specific surface area."Electrochhimica Acta. 52.1 (2006): 240-245.

[51] J L, Allen, Jow T R, and Wolfenstine J. "Kinetic study of the electrochemical FePO4 to LiFePO4 phase transition ." Chemistry of materials. 19.8 (2007): 2108-2111

[52] A, Yamada, Chum S C, and Hinokuma K. "optimized LiFePO4 for lithium battery cathodes ." J Electrochem Soc. 148.3 (2001): 224-229.

[53] A S , Andersson, Kalska B, and Thomas O. "lithium extraction/insertion in LiFePO4: an X-ray Diffraction and Mossbauer Spectroscopy Study ."Solide state ionics . 130. (2000): 41-52.

[54] M, Herstedt, Stjerndahl M, Nyten A, et al. "Surface chemistry of carbon-treated LiFePO4 particles for LI-ion battery cathode studies by PES."Electrochem Solid-state Lett. 6.9 (2003): A202-A206.

[55] S, Franger, Le Cras F, Bourbon C, and Rouault H. "Comparison between different LiFePO4 synthesis routes and their influence on its physico-chemical properties." J Power Sources. 119. (2003): 252-257.

[56] X Z , Liao, Ma Z F, He Y S, Jiang Y , et al. "Electrochemical behavior of LiFePO4/C cathode material for rechargeable lithium batteries." J Electrochem Soc. 152.10 (2005): A1969-A1973.

[57] H C, Shin, Cho W L, and Jang H. "electrochemical properties of the carbon-coated LiFePO4 as a cathode material for lithium-ion secondary batteries." J Power Sources. 159.2 (2006): 1383-1388.

[58] S, Franger, Cras Le, Bourbon B, et al. "LiFePO4 synthesis routes for enhanced electrochemical performance."J Electrochem Soc. 5.10 (2002): A231-A233.

[59] M, Higuchi, katayama K, Azuma Y, et al. "Synthesis of LiFePO4 cathode material by microwave processing ." J Power Sources. 119.1 (2003): 258-261.

[60] K S, Park. "Synthesis LiFePO4 by coprecipitation and microwave heating ." Electrochemistry Communications. 5.20 (2003): 839-842.

[61] S, Yang, Zavalij P Y, and Whittingham M S. "Hydrothermal synthesis of lithium iron phosphate cathodes."Electrochemistry Communications. 1. (2001): 505-508.

[62] K, Shiraishi, Dokko K, and Kanamura K. "Formation of impurities on phospho-olivine LiFePO4 during hydrothermal synthesis." J Power Sources. 146. (2005): 55-558.

[63] J, Barker, saidi M Y, and Swoyer J L. "Lithium iron phosphor-olivines prepared by a novel carbonthermal reduction method ." Electrochem Solid-state Lett. 6.3 (2003): 53-55.

[64] C H, Mi, Zhao XB, Cao G S, et al. "In situ synthesis and properties of carbon-coated LiFePO4 as Li-ion battery cathodes." J Electrochem Soc. 152.3 (2005): 483-487.

[65] X Z , Liao, Ma Z F, Wang L, et al. "A novel synthesis route for LiFePO4/C cathode materials for lithium-ion batteries." Electrochem Solid-state Lett. 7.12 (2004): 522-525.

[66] G, Arnold, Garche J, Hemmer R, et al. "Fine-particle lithium iron phosphate LiFePO4 synthesis by a new low-cost aqueous precipitation technique ." J Power Sources. 119-121. (2003): 247-251.

[67] K S, Park, Kang K T, Lee S B, et al. "synthesis of LiFePO4 with fine particle by co-precipitation method ." J Mater. Res. Bull.. 39. (2004): 1803-1810.

[68] F, Croce, Epifanio A D, hassoun J, et al. "A novel concept for the synthesis of an improved LiFePO4 lithium battery cathode ." Electrochemistry Communications. 4. (2002): 239-244.

[69] Hsu, Kuei-Feng, Sun-Yuan Tsay, and Bing-Joe Huwang. "Synthesis and characterization of nano-sized LiFePO4 cathode material prepared by a citric aicd-based sol-gel route." J materials Chemistry. 14. (2004): 2690-2695.

[70] Y, Hu, Doeff M M, Kostercki R, and Finones R. "electrochemical performance of sol-gel synthesized LiFePO4 in lithium batteries ." J Electrochem Soc. 151.8 (2004): A1279-A1285.

[71] Jingsi, Yang, and Jun John Xu. "Nonaqueous sol-gel synthesis of high-performance LiFePO4." Electrochem Solid-state Lett. 7.12 (2004): A515-A518.

[72] D, Choi, and Kumta P N. "Surfactant based sol-gel approach to nanostructured LiFePO4 for high rate Li-ion batteries." J Power Sources. 163.2 (2007): 1064-1069.

[73] GX, Wang, Bewlay Steve, Jane Yao, H K Liu, et al. "Characterization of LiMxFe1-xPO4(M=Mg,Zr,Ti) cathode materials prepared by the sol-gel method ."Electrochem Solid-state Lett. 7.12 (2004): A503-A506.

[74] Liu , Youyong, Chuanbao Cao, and Jing Li. "Enhanced electrochemical performance of carbon nanospheres-LiFePO4 composite by PEG based sol-gel synthesis." Electrochhimica Acta. 55. (2010): 3921-3926.

[75] zhang. Yong, Hui Feng, Xingbing Wu, Minghao Liu et al. "One-step microwave synthesis and characterization of carbon-modified nanocrystalline LiFePO4." Electrochhimica Acta. 54. (2009): 3206-3210.

[76] A, Hemandez, fabela S, Toffes-Gonzalez LC, and Sannchez E. "Preparation and electrochemical behavior of sol-gel LiNi0.3Co0.7-xMxO2 (M=Mn,Al).." Ceramics International. 34.1 (2008): 225-229.

[77] PZ, Shen, Jia DZ, Huang YD, Liu L, and Guo ZP. "LiMn2O4 cathode materials synthesized by the cellulose-citric acid method for lithium ion batteries."J Power Sources. 158.1 (2006): 608-613.

[78] C G, barral, Diard JP, Gorrec B Le, and Montella C. "Determination of the diffusion coefficient of an inserted species by impedance Spectroscopy application to the H/HxNb2O5 system." J Appl Electrochem.. 23. (1993): 93-97.

[79] J, Barker, Pynenburg R, Koksbang R, and saidi MY. "An electrochemical investigation into the lithium insertion properties of LixCoO2.." *Electrochhimica Acta*. 41. (1996): 2481-2488.

[80] Davies, J. A. (1996). Synthetic coordination chemistry: Principles and practice. Singapore: World Scientific.

[81] Martell, Arthur E. Coordination Chemistry. New York: Van Nostrand Reinhold, 1971.

[82] A Dean, John. Lange's Handbook of Chemistry . 15th. mcgraw-Gill Professional Publishing

[83] Z, Chen, and Dahn J R. "Reducing carbon in LiFePO4/C composite electrodes to maximize specific energy, volumetric energy, and tap density." J Electrochem Soc. 149. (2002): A1184.

[84] Myers, D. (2006). Surfactant science and technology. Hoboken, N.J: J. Wiley.

[85] CR, Sides, Croce F, Young VY, Martin CR, and Scrosati B. "A high-rate, nanocomposite LiFePO4 carbon cathode." J Electrochem Soc. 8. (2005): A484

[86] G, Ceder, Doyle M, Arora P, and Fuentes Y. "Computational modeling and simulation for rechargeable batteries." MRS Bull. 8. (2002): 619.

[87] F, Zhou, Kang k, Maxisch T, Ceder G, and Morgan D. "The electronic structure and band gap of LiFePO4 and LiMnPO4." Solid State Commun.. 132. (2004): 181.

[88] YN, Xu, Chung SY, Blocking JT, Chinag YM, and Chiang WY. "Electronic structure and electrical conductivity if undoped LiFePO4." Electrochem Solid-state Lett. 7. (2004): A131.